

Legacy of Polymer-Coated Fertilizer in Agroecosystems

By

Cameron Beaupre

Thesis submitted in partial fulfillment of the requirements for the degree of

Master of Science

Environmental and Life Science

Brandon University

© Cameron Beaupre

2024

i. Abstract

Polymer coatings, designed to encapsulate granular urea fertilizer, have emerged as a solution in agriculture to mitigate nitrogen losses. Polymer coatings of polymer-coated urea have exhibited notable persistence in Manitoba soils. The persistence of these polymer coatings may potentially influence crop development, yield, and food safety. Moreover, their persistence in the environment could impact both micro and macroscopic inhabitants of local ecosystems. An incubation study was conducted in a controlled greenhouse environment to assess the degradation of polymer coatings in two different soil types. Linear, negative exponential and spherical shell degradation models were used to assess the degradation of the polymer coatings, and degradation models revealed a full degradation within two years, as anticipated. Additionally, repeated soil sampling in farm fields where polymer-coated urea was applied provided additional insight into the persistence of polymer coating within agroecosystems in Manitoba. Polymer coatings were observed eight years after fertilizer application and the spherical shell degradation model extrapolated a full degradation within 67 years in the natural agroecosystem. Furthermore, the persistence and distribution of polymer coatings were assessed over time across landscape positions following a single polymer coated urea application at a field site near South Tobacco Creek. Polymer coating concentration increased with decreasing elevation (i.e., lower landscape positions) over time and was observed leaving the field via surface runoff during the spring snowmelt. These findings demonstrate that agroecosystems can be sources of polymers (i.e., microplastics) to surrounding ecosystems. These observations highlight the need for further investigation of the impact of polymer coatings across various ecosystems.

ii. Acknowledgements

I greatly acknowledge and appreciate support from Agriculture and Agri-Foods Canada (AAFC) for access to equipment and project materials for acquiring the field data. Additionally, thanks are extended to Clayton Jackson, who contributed to implementation of experimental designs, Jeff Griffith and the farm department who contributed resource information and fertilizer application details at the Brandon Research and Development Centre (BRDC) field sites, Henry Wilson for hydrological data and model critiques, and Dale Steppeler who contributed sampling area within the South Tobacco Creek watershed to research.

Secondly, I greatly acknowledge and appreciate support from Brandon University (BU) for access to equipment, project materials, and greenhouse resources for acquiring the incubation data. Additionally, thanks are extended to Bernadette Ardelli, who contributed to the extraction procedure for polymers, Tadesse Mengistu and the chemistry department who contributed resources to use in the incubation study, and both Terrence McGonigle and Pamela Rutherford at the Brandon University for allocating space for the incubation study within the greenhouse.

We respect the treaties that were made on these lands and acknowledge that both BU's main campus and BRDC are within Treaty Two territory. On behalf of both BRDC and BU, we acknowledge that we are on shared traditional homelands of the Dakota Oyate, Anishinaabeg, Oji-Cree, Cree, Dene, and the Red River Metis peoples.

iii. Table of Contents

i.	Abstract.....	2
ii.	Acknowledgements	3
iii.	Table of Contents.....	4
iv.	List of Figures	8
v.	List of Tables.....	12
vi.	List of Equations	14
vii.	List of Abbreviations	15
1	Introduction.....	16
1.1	Degradation of Plastics and Polymers	21
1.2	Mobility of Plastics and Polymers in Agroecosystems	28
1.3	Impacts of Plastics and Polymers on Ecological and Human Health.....	33
1.4	Purpose and Objectives.....	40
2	Methods	42
2.1	Polymer Persistence in Manitoban Field Sites.....	42
2.2	Assessment of Polymer Coating Degradation.....	48
2.2.1	Field Site Sampling Methodology	48
2.2.2	Greenhouse Equipment and Setup.....	50
2.2.3	Sampling Scheme.....	51

2.3	Polymer Coating Degradation	53
2.4	Tracking Polymer Coatings from Accumulation to Redistribution to Loss.....	57
2.4.1	Accumulation of Polymer Coatings	57
2.4.2	Redistribution of Polymer Coatings.....	58
2.4.3	Loss of Polymer Coatings via Surface Runoff	59
2.5	Statistical Analyses	61
3	Results	63
3.1	Polymer Coating Degradation.....	63
3.1.1	Comparison of Manitoban Soils Degradation	63
3.1.2	Extrapolating Polymer Coating Degradation	64
3.1.3	Field and Greenhouse Degradation Comparison	65
3.2	Tracking Polymer Coatings from Accumulation to Redistribution to Loss.....	68
3.2.1	Accumulation and Redistribution of Polymer Coatings	68
3.2.2	Loss of Polymer Coatings via Surface Runoff	74
4	Discussion.....	76
4.1	Polymer Coating Degradation	76
4.1.1	Slow Degradation Rate Implications	81
4.1.2	Limitations of Polymer Coating Degradation	83
4.2	Tracking Polymer Coatings Redistribution and Loss	85
4.2.1	Redistribution and Loss Implications	87

4.2.2	Limitations of Redistribution and Loss.....	88
4.3	Future Steps.....	90
5	Conclusion	92
5.1	Polymer Coating Degradation.....	92
5.2	Tracking Polymer Coatings Mobility	93
6	References	95
7 Appendix A:	Assessment of soil sampling methods for the quantification of polymer coatings	117
7.1	Sampling Methodologies	117
7.1.1	Bulk Density Sampling Methodology.....	117
7.1.2	Surface Area Monolith Sampling Methodology.....	118
7.2	Assessment of Sampling Methodologies	118
7.2.1	Recovery Rate of Polymer Coatings	118
7.2.2	Visual Assessment of Methodologies	119
7.2.3	Wilcoxon Rank Sum	121
7.2.4	Methodology Selection	122
8 Appendix B:	Soil Temperature and Water Content in the Field and Greenhouse Studies	124
9 Appendix C:	Model Comparison	132
9.1	Negative Exponential Function Derivation	132
9.2	Mass as a Function of Time	133

9.3	Complete Degradation Time	134
10	Appendix D: Release Rate of Urea	136
11	Appendix E: Soil Organic Carbon and Nitrogen	139

iv. List of Figures

Figure 2-1: Geolocation of the Brandon Research and Development Center (BRDC) and South Tobacco Creek (STC) using rnaturalearth software package in R (Massicotte P, South A (2024) rnaturalearth: World Map Data from Natural Earth, version 1. 0. 1. 9000).	42
Figure 2-2: Brandon Research and Development Center field sites, MB Canada using Google Earth Pro 9.3.6.9796. (January 14, 2024). 49°50'59.06" N, 99°57'53.27" W, eye alt 20.70 km. .	43
Figure 2-3: Brandon Research and Development Center field two, MB Canada using Google Earth Pro 9.3.6.9796. (January 14, 2024). 49°52'33.48" N, 99°58'31.33" W, eye alt 2.34 km.	45
Figure 2-4: South Tobacco Creek twin watersheds field site, MB Canada using Google Earth Pro 9.3.6.9796. (January 14, 2024). 49°20'16.25" N, 98°21'57.96" W, eye alt 1.93 km. White dots represent soil sampling positions across the field site, and the red diamonds represent the two edge-of-field weirs.	47
Figure 2-5: Embedded polymer capsule in a 5-mm diameter soil aggregate.	49
Figure 2-6: Fertilizer applied to the soil base (A), and the spatial placement of all replicates within the Brandon University greenhouse (B).	51
Figure 2-7: Weir filter set against the v-notch of the east weir, with water flow moving downslope (moving towards the top of the image).	59
Figure 3-1: No statistical difference between polymer mass and time during the incubation study for two Manitoban soils. Polymer degradation was measured in a controlled greenhouse using 58 Stockton-Wheatland (BRDC) and 77 Dezwood (STC) soils. Statistics performed by ANOVA, comparing the degradation rate between the two soils, error bars indicate standard deviation of polymer coating mass **** p < 0.001.	63

Figure 3-2: Extrapolation of linear regression, negative exponential and spherical shell models measure different full degradation times within the incubation study. (A) The three models were fitted to the incubation data, (B) extrapolated to determine full degradation. All three models projected a full degradation within the four-year biodegradability standard.	64
Figure 3-3: Extrapolation of linear regression, negative exponential and spherical shell models measure different full degradation times within the field study. (A) The three models were fitted to the field data, (B) extrapolated to determine full degradation. The three models projected different full degradations with linear regression in 8986 days, spherical shell in 24524 days, and negative exponential in 34232 days.	65
Figure 3-4: Visualization of the statistical difference between incubation and field studies using the linear, negative exponential and spherical shell models. Statistics performed by ANOVA, comparing the degradation rate between the two studies, error bars indicate standard deviation of polymer coating mass **** p < 0.001.	68
Figure 3-5: Statistical difference in polymer coating concentration at STC and polymer coating mass at BRDC Field 2 when comparing sampling depth of 0-5 cm and 5-10 cm over time, error bars indicate standard deviation. (A) Polymer coating concentration measured across BRDC Field 1, BRDC Field 2, and STC field sites, (B) polymer coating mass measured across BRDC Field 1, BRDC Field 2, and STC field sites. Statistics are performed by a one-way ANOVA, comparing the polymer coating concentration at BRDC Field 1, BRDC Field 2, and STC **** p = 0.921, p = 0.376, p = 0.0008, and comparing polymer mass across sampling depths at BRDC Field 1, BRDC Field 2, and STC **** p = 0.257, p = 0.008, p = 0.918.....	70
Figure 3-6: Polymer coating concentration increased with descending elevations, and polymer mass was lower in the riparian compared to field elevations at STC, error bars indicate standard	

deviation. (A) Polymer coating concentration measured across STC elevations, (B) polymer coating mass measured across STC elevations. Statistics are performed by a one-way ANOVA, comparing the polymer coating concentration across upper, middle, lower, and riparian elevations at STC **** p = 0.0341, and comparing polymer mass across upper, middle, lower, and riparian elevations at STC **** p = 0.02292.....	72
Figure 3-7: Polymer coating concentration decreased over time, and polymer coatings were observed within the riparian at STC, error bars indicate standard deviation. (A) Overall decline of polymer coating concentration at STC, (B) observance of polymer coating mass within the riparian area, and (C) polymer coating concentration across field elevations over time. Statistics are performed by a one-way ANOVA, comparing the polymer coating concentration over time across upper, middle, lower, and riparian elevations at STC **** p < 0.0001.	74
Figure 4-1: Backup of ice on the weir filter.....	89
Figure 7-1: Polymer capsules recovered using the bulk density methodology.	117
Figure 7-2: Carved excavated surface area monolith.....	118
Figure 7-3: Polymer coating concentration was bimodal using bulk density and was normal using surface area monolith methodologies. Statistics are performed by Wilcoxon Rank sum, comparing the polymer coating concentration between methodologies at BRDC Field 1, BRDC Field 2, and STC **** p = 0.09158, p = 0.02642, p= 0.25710.	119
Figure 7-4: Banded fertilizer application resulted in a difference between bulk density and surface area monolith sampling methodologies and broadcast fertilizer application resulted in no difference between methodologies. The difference in polymer coating concentration was normal for BRDC and STC. Statistics are performed by Wilcoxon Rank sum, comparing the polymer coating concentration between methodologies **** p = 0.00065.....	120

Figure 8-1: Mean soil temperature of soil replicates were equivalent between BRDC and STC soils during the incubation study.....	126
Figure 8-2: Mean soil moisture of soil replicates were equivalent between BRDC and STC soils during the incubation study.....	128
Figure 8-3: Seasonal variability in soil moisture visualized across BRDC and STC field sites during the thesis. Frozen soil in Manitoba resulted in lowered soil moisture readings between 2022 and 2024.....	129
Figure 8-4: Seasonal variability in soil temperature visualized across BRDC and STC field sites during the thesis. The mean soil temperature of BRDC and STC was 5° between 2022 and 2024.	130
Figure 10-1: The incubation data is characterized by two phases that include the present of urea and the absence of urea. The first 104 days represent PCU fertilizer containing urea and subsequent days represent the absence of urea.....	137
Figure 10-2: The first phase of the incubation data is primarily characterized by the loss of urea. The mass of the first 104 days is represented by polymer coatings with urea and the mass of urea is much larger than the mass of the polymer coating.....	138

v. List of Tables

Table 1: Comparison of polymer coating full degradation projections using linear regression, spherical shell, and negative exponential models. The three models were applied to both the incubation and field data to determine the persistence of polymer coatings and compare the difference in degradation between the two studies.	66
Table 2: Fitted values for the negative exponential model for the degradation of polymer coating capsules. The initial conditions (A) are based on the starting mass and number of polymers, the decay rate (S) based on the polymer type/composition/molecular weight, temperature, moisture, size, shape, and mean capsule mass (K).....	66
Table 3: Field data comparison of linear regression analysis applied to Wheatland/Stockton (BRDC) and Dezwood (STC) soils. The estimated marginal means of linear trends upper limit for both soils contained zero.....	67
Table 4: The Akaike Information Criterion (AIC) values using linear regression, spherical shell, and negative exponential models. No statistical difference measured between the linear regression, spherical shell, and negative exponential models.	67
Table 5: Estimated and recovered number ± standard error of polymer coating capsules at the field sites over time. Fall 2022 and Spring 2023 were sampled to a depth of 5cm and Fall 2023 to a depth of 10cm. ND = no data.....	69
Table 6: The mean polymer coating capsule mass and standard error across 0-5 cm, 5-10 cm, and 0-10 cm soil depths spanning BRDC Field 1, BRDC Field 2, and STC. A statistical differences between mean polymer coating capsules across 0-5 cm, 5-10 cm soil depths occurred at BRDC Field 2.....	71

Table 7: The mean polymer coating capsule mass and standard error across 0-5 cm, 5-10 cm, and 0-10 cm soil depths spanning upper, middle, lower, and riparian elevations at South Tobacco Creek. No statistical differences between polymer coating capsule mass between 0-5 cm and 5-10 cm soil depths. No polymer coating capsules were observed within the riparian 5-10 cm soil depth.....	71
Table 8: The recovered number of polymer coating capsules ± standard error across 0-5 cm, 5-10 cm, and 0-10 cm soil depths spanning upper, middle, lower, and riparian elevations at South Tobacco Creek 16- months after ESN application. A statistical difference in polymer coating concentration occurred across hillslope elevations. ND = not detected.....	73
Table 9: Comparison of the amount of polymer coating capsules transported during the surface runoff event at STC during the spring of 2023 between the west and east weir. The amount of polymer coating capsules recovered was dependent on the accumulated volume through the weir.	
.....	75
Table 10: Comparison of mean polymer coatings between bulk density and surface area monolith sampling methods using Wilcoxon Rank-Sum analysis. A statistical difference between bulk density and surface area monolith sampling methods occurred at BRDC Field 2.	122
Table 11: Comparison of polymer coating degradation using linear regression between field and incubation for soil temperature above 20 °C.	131
Table 12: Soil organic carbon and nitrogen percentage across BRDC Field 1, BRDC Field 2, and STC field sites and elevations.....	139

vi. List of Equations

Equation 2-1: The mean mass of a polymer coating for each elevation defined as the summation of cumulative mass divided by the cumulative count then divided by number of soil samples taken at that elevation.....	53
Equation 2-2: Polymer degradation rate defined as the differential mass loss per unit time.	54
Equation 2-3: Linear regression mean polymer coating mass.....	54
Equation 2-4: A negative exponential model fit defining the decomposition of the polymer coating.	54
Equation 2-5: Specific surface degradation rate constant defined as the polymer degradation rate divided by the surface characteristics (density and surface area) of the polymer coating.	54
Equation 2-6: Applied negative exponential fit defined using a spherical shell.....	55
Equation 2-7: Mass as a function of time defined by decreasing radius and surface area over time.....	55
Equation 2-8: Complete degradation time defined by decreasing radius and surface area over time.....	55
Equation 2-9: Input of polymer coating capsules defined by the application rate, number of applications, and polymer coating mass percentage divided by the mean polymer mass.	57
Equation 2-10: Flow rate calculation defined by water depth through a v-notch weir.	60
Equation 2-11: Estimated MPs removed defined by a runoff event ratio multiplied across the cumulative runoff.....	61
Equation 9-1: Spherical degradation Model.	133
Equation 9-2: Complete Degradation for decreasing radii and surface area of a sphere.	134

vii. List of Abbreviations

AAFC	Agriculture and Agri-Food Canada
ASTM	American Society for Testing and Materials
BP	Biodegradable Polymer
BRDC	Brandon Research and Development Center
CH ₄	Methane
CO ₂	Carbon dioxide
GHG	Greenhouse gases
K	Potassium
MP	Microplastic
N	Nitrogen
NH ₃	Ammonia
N ₂ O	Nitrous Oxide
NP	Nanoplastics
O ₂	Oxygen
P	Phosphorus
PCU	Polymer-Coated Urea
STC	South Tobacco Creek

1 Introduction

The global community's concerns and focus on addressing plastic pollution underscores the urgency of mitigating its environmental impact. Microplastics of size less than 5 mm are being recognized as one of the greatest threats to the environment and mankind (Laskar & Kumar, 2019). The Canadian government has recognized microplastics as a threat and has taken proactive measures. Canada's commitment to a zero plastic waste objective, as outlined in the Zero Plastic Waste document (2021), demonstrates a clear recognition of the need to safeguard the environment for future generations. This commitment is reinforced by regulation aimed at banning single-use plastics in the Single-use Plastics Prohibition Regulations (2023). The pervasive presence of plastics in our environment leaves a lasting imprint on both local ecosystems and the planet at large. By collectively reducing the influx of plastic waste into our surroundings, we uphold our responsibility to nurture a healthy and sustainable environment for current and future generations.

The world is shifting towards sustainable agricultural practices driven by an expanding awareness of environmental challenges. Within the agricultural sector, plastics have been used to transform standard practices by embracing innovative technologies to meet the demand of a growing population. Plastic products such as mulch films, and fertilizer coatings are applications of plastics that enhances water use efficiency yield, and agricultural productivity (Huang et al., 2024; Sofyane et al., 2024). For example, fertilizer coatings have been developed to provide a timed-release, or slow-release of nutrients which have increased efficiency by reducing environmental losses (Majaron et al., 2020). However, the challenge to recover plastics increases with duration since application, and how many instances of plastic used (Z. Y. Zhao et al., 2023). Agricultural plastics can often be single-use and through repeated applications have slower

degradation resulting in their accumulation (Tian et al., 2022). There are no efficient and distinguished strategies to eliminate microplastics from soil (Seo et al., 2024). The importance of monitoring plastic degradation is further exemplified as plastics become smaller in size.

Plastic materials eventually degrade into microplastics which are less easily recovered, and small-scale fragments will be observed more frequently as pieces degrade within soil over time. For example, plastics mulches cover wide areas of soil. Plastic mulches are a form of biodegradable plastics used in agriculture to suppress weed growth, conserve moisture and regulate soil temperature (Brodhagen et al., 2015; Sintim & Flury, 2017). However, fragments of plastics can be harmful to plants and soil health. Additionally, fragmented plastic abundance increases over time as the plastic degrades. Effects of degrading biodegradable plastic can negatively affect plant rhizospheres and soil properties (Cui et al., 2024; Qi et al., 2020; Yu et al., 2021). Further, the proliferation of single-use plastics on a larger scale could contaminate soils, waterways, and other ecosystems. Therefore, the effects of polymer coatings within the soil should be monitored.

Within the industrial sector, efforts are underway to offer sustainable alternatives to single-use plastics. Multiple companies have developed unique polymer coatings for fertilizers such as Nutrien, ICL, Simplot, and Harrell's. The current polymer-coated fertilizer market size in 2024 was estimated at 1.22 billion USD in the United States alone (Mordor Intelligence, 2024). Nutrien has developed an innovative solution to previous polymer coating in the form of Environmentally Smart Nitrogen (ESN), employing a biodegradable polymer coating to encapsulate urea. The permeable membrane of the polymer coating allows water to permeate its surface, facilitating controlled release of N into the soil. The protective semi-permeable coating controls water penetration and thus the rate of dissolution, and ideally synchronizes nutrient

release with plant requirements (Trenkel, 2010). This slow-release process not only enhances N use efficiency by reducing loss to the environment but could also boost crop yields (Taysom et al., 2023).

Polymer-coated fertilizers aim to reduce N losses to the environment. Reducing soil N losses is an important part of mitigating nitrous oxide (N_2O) emissions. N_2O has a global warming potential 273 times that of CO_2 for a 100-year timescale as outlined by the United States Environmental Protection Agency (2024). Targets include reducing soil N_2O emissions from fertilizer application by 30% below 2020 levels by 2030, as outlined in the 2030 Emissions Reduction Plan: Clean Air, Strong Economy (2023). The Canadian government has set a second target of achieving net-zero greenhouse gas emissions (GHG) by 2050, as outlined in the Net-Zero Emissions by 2050 (2023). Optimizing fertilization practices is part of the solution to achieve these targets. By reducing urea application rates and minimizing N losses, substantial progress can be made towards the reduction of soil N_2O emissions. Optimizing fertilizer practices aligns with the 4R nutrient stewardship approach, focusing on the right source, rate, timing and placement to mitigate N losses to the environment using the Fertilizer Institute handbook (2024). A Polymer-Coated Urea (PCU) product, such as ESN contains 44% N, and effectively reduces N losses through various mechanisms (Nutrien, 2018). It was demonstrated that N_2O emissions were reduced using ESN ($1.28 \pm 0.22 \text{ kg } N_2O \text{ N ha}^{-1}$) compared to urea ($2.48 \pm 0.34 \text{ kg } N_2O \text{ N ha}^{-1}$) and SuperU ($2.58 \pm 0.30 \text{ kg } N_2O \text{ N ha}^{-1}$) (Asgedom et al., 2014). The polymer coating minimizes leaching, volatilization, and denitrification, and the coating is designed to decompose into the carbon cycle.

Environmental conditions affect PCU efficacy. In the presence of soil water, N release from PCU is positively related to temperature (Cahill et al., 2010). Release of mineral N from coated urea

continued in October and November although the soil was cold (M. Zhang, 1994). However, the release of mineral N was reduced in cold and frozen soil. Enhancing efficacy by using a polymer coating strikes a balance between agronomic efficiency and maximizing crop yield. This allows farmers to apply PCU fertilizer in the fall as N losses are minimized.

Although the formation and coating process of ESN's polymer coating has evolved since its inception in 1998, notable refinements occurred since 2005. The product originated under Agrium which contained both acute and chronic oral toxicity in addition to acute toxicity to fish, invertebrates, birds and algae (Agrium, 2005). ESN releases ammonia (NH_3) which is a toxic hazard to fish, and urea will promote algae growth which may degrade water quality (Agrium, 2005). However, it is important to note the absence of this toxicological information in subsequent Safety Data Sheets (SDS) (Nutrien, 2012, 2018). However, the composition on ingredients changed for the 2018 SDS but did not for the 2012 SDS compared to the 2005 SDS. All three versions of the SDS state that the recipient assumes all risk in connection with the use of the material. Therefore, the removal of toxicological information could affect how the product is perceived.

There is a lack of publicly available information for the potential redistribution and degradation of ESN's polymer coatings. To inform producers of all potential risks in connection with using the product, data is needed on the redistribution and rate of degradation of ESN's polymer coatings. This data can be used to monitor movement of the polymer coating across the soil surface, and to determine whether sufficient concentration to harm aquatic animals leaves the agroecosystem. Therefore, producers can be informed surrounding environmental sustainability and stewardship while using PCU products.

The lack of information surrounding ESN's rate of degradation generates questions about the degradability of PCU products. A wide range for the rate of degradation occurs for polymer using the PoLyInfo database, ranging from 0.0003 – 100% weight loss day⁻¹ (Yuan et al., 2023). Certain polymer structures have low rates of degradation, raising concerns about their environmental impact. Biodegradable plastics undergo physical and biological decomposition which ultimately transforms the polymer into CO₂, biomass, and water as defined by the European Parliament (2019). ESN's polymer coating, primarily composed of castor oil and polymethylene polyphenylene isocyanate (PPI), is reported to degrade over approximately 18-24 months in soil, yielding CO₂, NH₃, and water (Nutrien, 2018; ESN, 2023). However, the degradation process is contingent upon environmental conditions (e.g., soil water content, temperature, microbial activity, and ultraviolet radiation). Soil temperature was more of a limiting factor compared to soil moisture for N release (Ransom et al., 2020). A humid continental climate with mild summers and no distinct dry season (Köppen climate classification Dfb) is recorded across southern Manitoba (Beck et al., 2023). The subhumid climate of southern Manitoba had an average temperature of 2°C and 489.4-mm of precipitation annually between 1991-2020 (Environment Canada, 2024). Microbial activity (measured as CO₂ production) was significantly increased in soil incubation at 20°C compared to 10°C (Delanau et al., 2024). The rate of water and urea diffusion depends on temperature, with the rate doubling with every 10°C change (Adams et al., 2013). Therefore, it is suspected that reduced microbial activity due to environmental conditions throughout much of the year in Manitoba is likely to slow the polymer coating's degradation rate. Slower degradation rates of polymer coating within the environment could alter their biodegradability status. Research documents on PCU products focus on N efficiency but often makes no mention of their degradability. Therefore, conducting publicly

accessible research for polymer coating degradation rates within Manitoba could assist in providing clear understanding of polymer coating degradation to both producers and scientists across the Canadian prairies.

1.1 Degradation of Plastics and Polymers

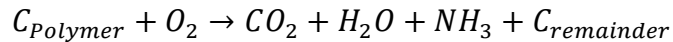
Biodegradable polymers (BPs) offer a distinct advantage over traditional plastic materials due to their faster decomposition rates. Traditional oil-based plastics are characterized by long carbon molecule chains which pose challenges in agriculture as they decompose slowly and may produce undesirable byproducts. The shorter polymer chains of BPs lead to faster fragmentation and degradation, with more complex chemical structures of polymers requiring additional enzymes or coenzymes to fragment (Narancic & O'Connor, 2019). BPs can be made using microbial synthesis fermentation. Microbial synthesis plastics contain an aliphatic structure and ester groups along the main chemical chain (Belal & Farid, 2016). BPs are held together by singular bonds which are more readily broken down.

Polymer coating degradation progresses through several phases, each breaking down the carbon chain. The biodegradation phases occur in order of bio-deterioration, bio-fragmentation, and bio-assimilation (Emadian et al., 2017). Initially, bio-deterioration occurs as microorganisms aggregate on the polymer coating surface, forming a biofilm that can alter its chemical properties. Subsequently, bio-fragmentation occurs when the chemical properties of the biodegradable polymers reach the threshold energy required to break the polymer into monomers and oligomers in the presence of depolymerase produced by the microorganisms (Emadian et al., 2017). Changes in surface features and mass loss occur together during the bio-fragmentation and microbial assimilation phases (Folino et al., 2020). Microorganisms may break the molecular bonds of polymers into monomers, dimers or oligomers using extracellular enzymes. Monomers,

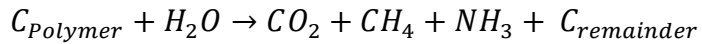
dimers, and oligomers can pass through the cell membrane and be used as an energy source for the bacteria (Gu & Gu, 2005). During the bio-assimilation phase, BPs are mineralized into water, biomass, and CO₂ in aerobic soil conditions (Briassoulis & Mistriotis, 2018; Tokiwa et al., 2009a). The relative molecular weights of polymers decrease during the bio-assimilation phase (Oberbeckmann & Labrenz, 2019). Therefore, mass loss can be measured as CO₂ evolution during the bio-assimilation phase.

Soil moisture play a critical role in the degradation process of BPs. Reduced oxygen availability and increased water exposure can impact the decomposition process of the polymer coating. These anaerobic conditions occur in depressional areas in agricultural soils, non-arable soils (wetlands), or following snowmelt or large precipitation events. Under anaerobic conditions, the energy stored in organic matter is mainly released as methane, and due to the lack of oxygen in the process, less heat and less microbial biomass are produced (Bátori et al., 2018). The bio-assimilation process releases methane (CH₄) in addition to CO₂ for faster polymer decomposition (Briassoulis & Mistriotis, 2018). Although a faster degradation occurs under anaerobic conditions, the release of CH₄ in addition to CO₂ is a net increase in GHG emissions. CH₄ has a 27-30 times increased global warming potential than CO₂ as outlined by the United States Environmental Protection Agency (2024).

The typical aerobic biodegradation of the polymer coating undergoes the following reaction (ESN, 2023):



The anaerobic biodegradation of the polymer undergoes the following reaction (Bátori et al., 2018):



The physical integrity of the polymer coating is contingent upon its formulation, physical properties, and manufacturing process. PCU fertilizer must strike a balance between releasing urea gradually while maintaining structural integrity. Besides the covalent forces of polymer molecules, various kinds of weak forces among macromolecular chains affect not only the formation of polymer aggregates, but also the structure and physical properties and function of the polymer aggregate (Tokiwa et al., 2009a). In addition to the functioning of the PCU, both the chemical and physical properties also play a role in the degradation process of the polymer coating in the soil.

The chemical structure of polymers determines the structure's characteristics and byproducts. Chemical structures of polymers and their associated physical properties for assessing biodegradability include average molecular weight, mean instance mass, molecular weight distribution, monomer composition and relative abundance, degree of crystallinity, degree of substitution, configuration, conformation, ionic charge and charge density, reactive functional groups, crosslinking, nature and length of sidechains, and surface properties (Folino et al., 2023; Massardier-Nageotte et al., 2006; Mukherjee et al., 2023). The physio-chemical properties of the biodegradable plastic are a stronger indication on the ability of degradation rather than the type of material that were used to synthesize it (Folino et al., 2023). In this case, ESN's polymer coating is influenced by its castor oil and polymer with PPI structure. The stability of the polymer matrix can affect its degradation rate and overall biodegradability. However, the difference in polymer coating formulation required to extend the release of urea compared to additives could potentially impede their degradation.

ESN, N stabilizers, and urease inhibitors target the protection of urea from the environment by reducing N loss. The use of these nitrification inhibitors is to control the leaching and denitrification losses from the soil. However, ESN protects against volatilization more effectively than urease inhibitors and for longer (ESN, 2023). For example, nitrification inhibitors delay the bacterial oxidation of the ammonium ion (NH_4^+) by depressing over a certain period of time the activity of *Nitrosomonas* bacteria in the soil (Trenkel, 2010). Additional analysis of microbial community, abundance, and activity may provide supplementary information for factors that influence degradation rates of ESN. Overall, the scope of PCU polymer coating formulations tries to balance stability and biodegradability.

Additives incorporated into the polymer coating matrix plays a crucial role in reducing the rate of degradation needed to achieve a controlled, slow-release mechanism. Additives alter the complexity and crystallization of the polymer structure, thereby enhancing its strength. The strength of the polymer coating is proportional to the energy and time required for microbial depolymerases to break down the polymer into monomers and oligomers. The amorphous domains of biodegradable plastics are more susceptible to decomposition (Tokiwa et al., 2009b). Increased crystallization of the polymer structure can influence the behavior of the amorphous domain, impacting the overall decomposition process. Bonds within the amorphous domain are typically easier to break than those in the crystalline domain, leading to faster decomposition. The formulation of the polymer coating structural characteristics can influence its degradation rate which affects overall environmental impact.

The morphology of the BP structures is important when modelling their properties, behavior, and performance. Morphology of the BP structure refers to the alignment of polymer chains with the polymer coating, which is influenced by composition, creation process and additives. The PCU

polymer coating may exhibit a microphase-separated morphology. Microphase separation occurs as a result of stronger intermolecular attractions, lengths of hard and rigid segments cluster together that push out soft segments that would affect those intermolecular attractions. As a result of mixed soft and harder segments, the softer segments of the polymer chain can be compressed while the harder segments maintain the structure of the material. Microphase-separated morphologies are characterized by improved rigidity, barrier properties, and controlled release behaviors. Lower rigidity may cause compressions of the polymer coating within the soil, leading to observations of collapsed bowl-like structures. Block copolymer membranes can be designed for separation processes by controlling penetrant solubility through appropriate chemical modification and penetrant diffusion through manipulation of nano-structural characteristics (Zielinski, 2001). The chemical additives of most PCU polymer coatings were most likely introduced to control the release of N from the coatings.

The physical characteristics of a polymer coating within the soil may affect their decomposition and degradation rate. Microbial activity leads to the formation of biofilms on the surface of the polymer coating. Biofilm formation primarily occurs on the capsules surface where microbial activity is concentrated. The decomposition of the polymer coating is closely tied to the surface area of the polymer coating and microbial activity breaking down the polymer structure (Chamas et al., 2020). Decomposition is dependent on the surface area of the polymer coating as a result of microbial activity. (Folino et al., 2023; Massardier-Nageotte et al., 2006)

The biodegradation of plastic materials exhibits variable decomposition rates over time. Most serious abrasion of PCU, specifically ESN, occurred when transferring the product in equipment containing scaly deposits (Beres et al., 2012). Abrasion during product transfer can lead to altered surface areas or cracking of polymer coating capsules and increases the exposed surface

areas. The biodegradation rate plateaus when microbial activity occurs across the maximum surface area of a BP (Harrison et al., 2018; Lucas et al., 2008). Additionally, accelerated degradation may occur during the early phases as the biofilm expands, with microbial activity being a key driver of degradation rates during this period affecting the rate of degradation. In a lab-based study, prokaryotic and eukaryotic microorganisms were found to contribute to the biodegradation process of biodegradable plastics (Li et al., 2015). Stimulation of these microorganism groups could potentially increase polymer coating degradation rates.

PCU polymer coating degradation may be affected by abiotic factors. BPs can be abiotically biodegraded by ultraviolet radiation, high temperatures, air, water, and applied forces (Pan et al., 2023). Higher levels of solar radiation and water stimulate microbial activity which can enhance the polymer coating degradation rate. BPs were observed to be biodegradable but the degradation process under natural conditions may not be consistent (Nazareth et al., 2019). For example, Manitoba's environment includes significant periods of sub-zero weather which could result in inconsistent polymer coating degradation over time. As observed by Nazareth et al. (2019), BP biodegradation will be reduced in natural settings under non-optimal conditions. Nonoptimal conditions may result in decreased degradation rates. The decreased degradation rates impact their environmental legacy, which include accumulation, redistribution of BP within the soil, and potential transport between ecosystems. A controlled environment provides an opportunity to analyze optimal polymer coating degradation rates. Although information can be acquired with controlled environments, such as in a greenhouse, it cannot describe the degradation rate pattern under natural climatic conditions. Comparing the polymer coating degradation rates between the controlled and uncontrolled environments can be used to demonstrate the importance of abiotic factors and microbial activity on degradation.

The American Society for Testing and Materials (ASTM), and the International Organization for Standardization (ISO) are classified as the gold standards for biodegradability testing. These two standardized testing formats are essentially synonymous with the Americas and the rest of the world. Regulations from the European parliament were updated as of June 5th, 2019, for the biodegradability requirements. The European Commission proposed that the polymer coating of controlled release fertilizers shall comply with specific biodegradability requirements of 90% biodegradation in natural soil conditions and aquatic environments across the EU within 48 months after the end of the claimed longevity period (Šerá et al., 2020).

BPs degradation can be observed by the release of CO₂ and mass loss during the chemical reaction to byproducts. Biodegradation in soils can be assessed using the ASTM D5988 or EN 17033 (Folino et al., 2020). Measurements of CO₂ evolution are monitored under laboratory conditions to measure the aerobic biodegradability of the plastic material within the ASTM D5988 (ASTM, 2023). Requirements of the ASTM D5988 include topsoil with particles smaller than 2-mm for proper aeration, a test dosage of 200-1000 mg of BP carbon for 500 g soil, and 25 °C temperature. The ASTM D5988 requirements are necessary to achieve optimal CO₂ evolution and mass reduction of polymers. Biodegradation under aerobic conditions can be expressed by mass loss, surface erosion, reduction of molecular weight, evolution of CO₂, and the loss of mechanical properties (Folino et al., 2020; Ruggero et al., 2019).

The degradation rate and full degradation of BP materials can vary across different ecosystems, reflecting the unique environmental conditions present within each ecosystem. Inland water systems, which may receive polymer coatings transported by surface runoff from adjacent agricultural soils and urban areas, represents entirely distinct conditions for polymer degradation. ASTM D7473 is the standard used for assessing biodegradation in marine environments,

specifically for non-floating plastic materials. However, applying this standard to evaluate the degradation of polymer coatings in inland water systems may not be straightforward. The rate of biodegradation by microbial degradation in an inland water system may be further slowed based on its polymer structure (Sashiwa et al., 2018). The standard of addressing mass loss as a function of time of the BP material in an inland water system cannot be used to demonstrate biodegradation (Sashiwa et al., 2018). Comparing the mass loss of BPs between agricultural soils and inland water systems are challenging due to differing environmental conditions and degradation processes involved. There are currently no publicly available documentation specifically addressing the degradation of PCU in inland water systems. However, sources of literature in Manitoba demonstrate that particulate N can enter water bodies via surface runoff (Tiessen et al., 2010; Li et al., 2011; Liu et al., 2014). Therefore, it could be possible that PCU are additionally entering water bodies via surface runoff.

Additional ASTM standard tests, such as ASTM D6868 could offer valuable insight into the degradation of polymer coatings and their impact on soil and crops. ASTM D6868 assesses the material's ability to compost, ensuring that they do not adversely affect plant growth. The ASTM D6868 includes that germination and plant biomass should not be reduced below 90 % of a blank compost (Folino et al., 2023). The remaining residue of starch-based biodegradable plastics should not be toxic for living organisms (Gómez & Michel, 2013).

1.2 Mobility of Plastics and Polymers in Agroecosystems

Substantial pathways of soil erosion include tillage, water, and wind events, which can affect polymer coating redistribution in an agroecosystem. These pathways of soil erosion factor into the redistribution of polymer coatings across the landscape. For example, the loss of soil aggregates due to wind erosion can lead to topsoil particle loss. Reducing the topsoil layer may

expose polymer coatings to the surface. Soil texture, wind duration and shear velocity affect the severity of wind erosion and dust emission (Zuo et al., 2023). A sufficient wind force can transport both soil and plastic from the soil surface, particularly affecting upland areas within agroecosystems. The threshold wind velocity which caused MP 100-1000 μm in longest axis to be transported occurs between 25-43 km h^{-1} (Rezaei et al., 2022). Equivalently, MPs with sizes larger than 1-mm were displaced by wind speeds above this threshold. Heavier MPs required higher wind velocities for transportation. Given that PCU fertilizer applications are targeted within the topsoil layer, any reduction in topsoil caused by soil erosion or vertical displacement by tillage erosion increases the likelihood of wind transport. In a field study by Rezaei et al., (2022), between 0.04-78.08 MP g^{-1} was eroded by the wind in Iran. Therefore, the mobility of MPs observed within this study suggests that agricultural soils act as a temporary sink and dynamic secondary source. The importance of wind erosion highlights how a force of wind acting on exposed polymer coatings on the soil surface can transport them from the agricultural ecosystem to an adjacent ecosystem.

Redistribution of polymer coating capsules within the topsoil may be inevitable due to mechanical activities such as tillage, seeding and fertilizer applications. MP abundance, size, shape, and concentration was uniform across soil depths between 0-30 cm of greenhouses, crop fields, and vegetable fields around Urumqi, China (Li et al., 2023). This can result from MPs within the soil being vertically displaced when topsoil is agitated by tillage. The vertical displacement of polymer coatings, being another form of MP, may additionally undergo vertical displacement by tillage. For example, the mixing of soil particles, soil aggregates, and polymer coatings within the topsoil can lead to their vertical redistribution. MPs can be commonly observed attached to soil aggregates and soil particles. However, if the soil aggregates are

separated into smaller particles, then the attached MPs should become free and more readily able to move. Disaggregation of soil can occur during tillage events. An increased soil detachment rate occurred under increased tillage intensity (Wang et al., 2016). Separation of soil aggregates during a higher tillage intensity could separate the polymer coating from soil aggregates. Unbound polymer coatings that are exposed to the soil surface have a higher probability of movement. Landscapes with large slope gradients may be more susceptible to tillage erosion, which in turn could affect the lateral mobility of polymer coatings. Tillage erosion rates increased as a power function with increasing inflow rate and slope gradient and decreased as a power function with increased tillage depth, demonstrating that slope gradient had the greatest impact on soil erosion rate (Zhao et al., 2023). As soil is eroded from the surface, previously buried polymer coatings could become exposed to the soil surface. Exposed polymer coatings could then be mobilized by wind or water across the landscape and removed from the agroecosystem. Therefore, the redistribution of exposed polymer coatings could be further increased with larger slope gradient. Adoption of no-tillage and reduced-tillage practices minimizes soil disturbance, soil erosion, and nutrient losses from agricultural soils (AAFC, 2008; Li et al., 2011). No tillage and reduced tillage practices may minimize the redistribution of polymer coatings associated with tillage events by reducing the quantity that are detached from soil aggregates assuming banded application.

The impact of water erosion is affected by soil characteristics and landscape properties. For example, soil characteristics such as antecedent soil water, water-holding capacity, and porosity influences the amount of surface runoff during a rainfall event. These factors determine how much water the soil can hold and how easily the water can move through it. The antecedent soil water determines how much water is within the soil before the precipitation event. When the soil

pores become saturated during the precipitation event, water infiltration is reduced. When excess water is supplied during rainfall or snowmelt, the water that is not infiltrated moves laterally across the soil's surface as surface runoff. For example, between 15-20% of precipitation volume leaves the field via surface runoff in the South Tobacco Creek watershed near Miami, MB and primarily occurred during snowmelt events (Li et al., 2011). Therefore, only a small portion of the precipitation volume occurs as surface runoff. No-till and conservation tillage practices have been shown to reduce water erosion compared to conventional tillage practices (e.g., Li et al., 2012; Peng et al., 2023). However, intense rainfall activity weakens the ability of tillage practices to control water erosion (Zhao et al., 2023). Adoption of no- reduced- tillage practices may reduce water erosion, which could reduce the redistribution of polymer coatings.

Water erosion induced by precipitation and snowmelt events are influenced by various factors including soil/farm management practices, soil and slope characteristics and event intensity. Tillage can alter rainwater distribution by increasing depressional storage and runoff while reducing water infiltration (Zhao et al., 2023). For example, tillage breaks apart soil aggregates, affecting the soil structure and water infiltration, and potentially exposing polymer coatings to the soil surface. As separation of soil aggregates occur, porous space within the soil can be disrupted leading to increased runoff and reduced infiltration. Field characteristics such as slope gradient add complexity and may alter the flow patterns within an agroecosystem. A significant difference in mean water flow velocity occurred for a slope of 15° and effective sheer stress were observed across slope positions (Wang et al., 2016). The increased water flow velocity can result in higher water erosion. Additionally, the effective sheer stress could affect soil aggregates stability on the soil surface resulting in exposed polymer coatings. Therefore, an elevated water flow velocity could expose previously buried polymer coatings close to the soil surface. This

would include a net redistribution of polymer coatings downslope resulting in higher concentration in lower-elevation areas. Low-elevation areas contained higher MP pollution than high-elevation areas caused by surface water runoff (Zhou et al., 2023). Therefore, polymer coatings could be susceptible to lateral redistribution by surface runoff and further affected by water erosion.

The loss of top-soil aggregates may severely affect the lateral movement of polymer coatings due to their exposure to the soil surface. The impact of exposure to the soil surface is apparent due to the buoyancy of the polymer coating and the effective sheer stress caused by the flow of water across the soil surface. An applied force along the surface of the polymer coating may remove soil, cleaning the surface, which may result in a floating polymer coating. This applied force is dependent on the surface runoff volume. However, the movement of polymer coatings beneath the soil surface could affect their probability of becoming exposed. Movement of microplastics within soil are influenced by soil macropores, organic matter and soil biota (Rillig et al., 2017). For example, the soil macropore space between soil aggregates contains preferential movement of water, air, and soil biota. In the case that polymer coatings within the soil matrix is absent from soil on its surface it is possible that additional polymer coatings could be carried up the soil profile given a preferential pathway to the surface by infiltrating water through the soil microporous space. This could occur under stagnant and laminar flow due to overall precipitation volume and maximized infiltration capacity. The number and volume of rills alter the flow path and affect the amount of soil translocated on steep slopes (Wang et al., 2021). For example, precipitation events can increase the redistribution of topsoil from the field to the surrounding environment resulting in exposed polymer coatings. The recovered number of MP has been found to be related to the number and magnitude of surface runoff events (Zemke et al., 2019).

Therefore, it is expected that exposed polymer coatings are likely to be redistributed by surface runoff.

The snowmelt contribution in Manitoba can be affected by ice formation within the field. The downslope flow path can become obstructed by basal ice formation. Soil contributions are eliminated under restricted infiltration because of a basal ice layer forming on the soil surface beneath the snow cover (Roste, 2015). The ice formation may create blockages and form rills on the soil surface. Reduced infiltration and strengthened soil stability caused by ice formation could reduce rates of polymer coating dislodging from soil aggregates. Therefore, reducing the overall impact of polymer coating redistribution from the field to the environment.

1.3 Impacts of Plastics and Polymers on Ecological and Human Health

With PCU fertilizer applied annually, there is a risk of buildup over time if the rate of application is greater than the rate of biodegradation. Additionally, the resistance to biodegradation will have increased (slower degradation) caused by reduced photodegradation (abiotic) (Tian et al., 2022). Photodegradation is caused by the absorption of photon; in order to be effective, the light must be absorbed by the substrate (polymeric system) (Yousif & Haddad, 2013). The absorbed photon becomes potential energy of an electron in the process. The incoming light would remain unchanged; however, the concentration of polymer would be increased with repetitive fertilizer applications. Therefore, a higher concentration of substrate (i.e. polymer coating) per unit area using an equivalent amount of photons would have a lower average absorption rate. Continuous application of PCU fertilizers in cold continental climates could lead to polymer coating accumulation exacerbated by higher concentrations and cold and dry (suboptimal) soil environmental conditions.

The degradation of MP within the agroecosystem can have an impact on both the soil and its ecology. As MPs fragment over time, their potential exposure to soil organisms and their ability to ingest them both increases. The fragmentation of polymer coatings into smaller nanoplastic (NP) fragments could have an increased rate of plastic consumed by soil organisms. The presence of plastic residues and MPs in soil poses a threat to the soil ecosystem by altering the physiochemical properties, hindering the growth and development of vegetation and soil organisms by producing oxidative stress damage (Zhang et al., 2022a). Consequently, the fragmentation of polymer coatings could additionally contribute to changes in soil physiochemical properties affecting crop development. Functional traits of earthworms are affected by ingestion of MP, and the observance of MP particles in chicken feces could eventually affect human health by consumption of chicken (e.g. gizzards) (Huerta Lwanga et al., 2017). The ingestion of polymers through fragmentation over time highlights a potential risk to human health.

Plants may absorb pollutants from plastics throughout their vascular systems. Plants are affected by pollutants on the surface of MPs and may be absorbed through their rhizomes (Avellan et al., 2019; Ge et al., 2021). Additionally, if the plastic particles become small enough, they may be taken up by the root system and into the vegetation. MP and NP can accumulate on the surface of vascular plants. Some portion of NPs even penetrate the plant tissue affecting both aquatic and terrestrial vascular plants (Yin et al., 2021). Through the uptake of MP into the root systems of plants, MPs may travel via the vascular system, which is driven by transpiration (Wang et al., 2022; Fu Yu et al., 2021). Therefore, fragmented polymer coatings may be taken up by the root system. For example, a study by Dong et al., (2021) demonstrated that micron-sized plastics could migrate from hydroponic solution and enter carrot roots in the presence of As (III). Leaf-

to-root translocation of NP in maize plants has also been observed (Sun et al., 2021). The result of plastic uptake into vegetative roots stunts the overall biomass. Plant height, total biomass, shoot biomass, and root biomass were decreased by 12-14% in the presence of plastic residues and MPs (Zhang et al., 2022b). Biodegradable MPs between 1.5-2.5% w/w significantly inhibited root and shoot biomass of *Phaseolus vulgaris L.* (Meng et al., 2021). Additionally, accumulation of plastics caused by slow degradation may inhibit germination. Biodegradable plastic debris significantly inhibited germination viability of soybeans (*Glycine max*) and the inhibitory effect of this plastic increased with concentration (Li et al., 2021). However, the type of plastic material that is used may indicate how much the soil is affected. Biodegradable films showed stronger negative effects on *Triticum aestivum* compared to polyethylene and reduced MP size showed a greater negative effect than macro-plastics (Qi et al., 2018). Polymer coating fragments could potentially affect crop development and yield. The amount of polymer present at BRDC Field 2 (six fertilizer applications) was 0.4% w/w of polymer coating to topsoil based on recovered surface area monolith samples. Therefore, after several fertilizer applications it could become environmentally relevant for areas of reduced degradation. Therefore, more research involving the impact of the degradation of polymer coatings on plant growth is needed.

Plastics adjacent to root systems may introduce pollutants or themselves into the edible portions of crops. In the context of temperate soils where slow degradation may occur, fragmented polymer coating pieces can accumulate which elevates MP concentration near root systems. The uptake of MPs into food crops can have serious health impacts. For example, MPs accumulation in the liver based on 0.1-0.5 mg day⁻¹ has been demonstrated to trigger energy and lipid metabolism disorders, oxidative stress and neurotoxic reaction in mice (Deng et al., 2017). Similarly, systematic consumption of plastic particles can result in bioaccumulation in the livers

and kidneys as well as lymphatic transfer, causing oxidative stress, inflammatory responses and metabolic issues in exposed individuals (Shruti & Kutralam-Muniasamy, 2024). The transfer of plastic or pollutants could be increased under higher concentrations.

Inland water ecosystems encompass lakes, ponds, rivers, streams, and wetlands that biodiversity, regulate water quality and provide habitats for various species (Horton et al., 2017). These interconnected ecosystems are fed by natural drainage systems, groundwater and streams that are influenced by upstream agricultural practices. MPs are frequently present in rivers, lake waters, groundwater, and drinking water (Koelmans et al., 2019). Retention of plastic particles in rivers was lowest for particles of about five μm , and < 1-mm size plastics are preferentially retained (Besseling et al., 2017). Measuring the concentration and mass of polymer coatings in surface runoff over time can confirm whether concentration transported is related to their size. Knowing which sizes and masses of polymer coatings in surface runoff is important for identifying what stages they could be exported. If lower mass polymer coatings were exported in surface runoff, then further degradation measurements using mass as a function of time will use data based on the remaining polymer mass, resulting in measuring a slower degradation.

MPs may additionally affect vegetation surrounding inland water ecosystems. The transport of polymers along water channels is influenced by the flow characteristics of the channel. Plastic material that are less dense than water is buoyant, allowing them to accumulate along the water's surface. Accumulation of MPs along the water's surface occurred for laminar water flow and standing water (Eerkes-Medrano et al., 2015). Therefore, extraction of MPs along the water's surface is possible for laminar water flow and standing water. In laminar water flow, intact polymer coatings can be transported between ecosystems without substantial damage. In contrast, turbulent flow can push polymer coatings below the water's surface or cause them to

become damaged. Under turbulent flow MPs may cycle under the water's surface attaching to submerged plant surfaces (Goss et al., 2018). Vegetation lining the water's edge may trap polymer coatings within its foliage or around their root systems under laminar flow.

Polymer coatings introduced into wetlands may become entrapped in vegetation and subsequently consumed by organisms. As polymer coatings fragment over time, they may further contribute to the transfer of plastic materials through the food chain. Although biodegradable plastics have a shorter life span, they can have adverse effects on soil properties, biology and adsorption role and transport vector for a wide range of chemicals (Campanale et al., 2024).

Therefore, chemicals that are absorbed by the polymers could be transported to wetland environments. Microbial communities in the wetland ecosystem are also vulnerable to the introduction of polymer coatings. MPs change the diversity and metabolic function of the soil microorganisms which significantly altered the soil physio-chemical properties and resulted in limited individual growth and population formation (Yu et al., 2021). Microorganisms may compete for the energy resources provided by the polymer coating, influencing its degradation rate. The colonization process and biofilm formation are often characterized by complex microbial competition and increased species richness (Datta et al., 2016). Therefore, microbial communities on the surface of polymer coatings that carry pollutants may have affected health and functions.

Polymer coatings transported into inland water systems may become entrapped below the water surface, leading to inconsistent degradation rates across water depths and sediment depths. Factors such as water quality, solar radiation, temperature, and nutrient availability influence microbial activity. For example, solar radiation penetrates the water surface and diminishes at lower depths, reducing heat-energy adsorption. A portion of heat-energy is also reflected against

the surface of the water. In addition to lower temperatures, the availability of O₂ and nutrients for microorganisms is reduced at lower depths (Harrison et al., 2018). Limited oxygen and nutrient availability at lower depths further inhibit microbial degradation processes. In benthic environments, the deterioration of plastic materials is reduced and variation in deterioration was measured based on depth (Harrison et al., 2018).

The structure of MP influences their breakdown and persistence in aquatic ecosystems. Different types of plastic have different toxicological qualities, which may harm species differently depending on the duration of exposure, particle concentration, shape, chemical composition, and size (Strungaru et al., 2019). Disturbance to the ecosystem caused by transported polymer coatings containing pollutants could lead to the removal of native species, impaired vegetation growth, or reduce water quality. For example, salinity affected the distribution of the dominant species of planktonic and MPs surface-attached bacteria (Dong et al., 2023). MPs degrade at slower rates in higher concentrations of salinity, and the difference in salinity had no significant effect on ultra high molecular weight polyethylene MPs (Bakir et al., 2014). The crystallization of MP structure and its mass may determine the extent of change in solubility for organic pollutants. Dissolved organic matter contains abundant functional groups, which can interact with natural particles or organic pollutants and affect their fate and transport in the ecosystem (Bakir et al., 2014). A partition equilibrium may be reached from some PCUs NH₃ byproduct and other sources of organic pollutants within the water. Therefore, the degradation of polymer coatings in aquatic ecosystems is dependent on the water chemistry and could affect biota.

Polymer coating fragmentation poses risks to aquatic inhabitants due to the increased likelihood of ingestion and absorption. The average size of plastic particles in the environment was observed to be decreasing, and the global distribution of MP fragments has increased (Barnes et

al., 2009). While fragmentation does not increase the concentration of plastic material in aquatic ecosystems, it does increase the abundance of smaller fragments, which are more likely to be ingested by aquatic organisms. These small plastic fragments may also attach to or be absorbed by vegetation within the ecosystem, further affecting aquatic life. NP caused a statistically significant reduction in cell development and alterations in relevant physiological parameters across multiple aquatic species (Shen et al., 2020). *Daphnia magna* showed increased mortality in a six to seven-day exposure period with $1.11 * 10^{-2}$ mg L⁻¹ of MPs not containing any contaminants (Aljaibachi & Callaghan, 2018; Eltemsah & Bøhn, 2019). Exposure to biodegradable plastics resulted in similar ecotoxicological effects on organisms as conventional MP and NP (Moshhood et al., 2022). MP treatment of increasing particle size significantly affected the assimilation efficiency of amphipod *Gammarus fossarum*, resulting in reduced wet weight (Blarer & Burkhardt-Holm, 2016; Straub et al., 2017). Similarly, polymer coating degradation with variable batch sizes may result in various fragment sizes, which could be hazardous to biotic species and vegetation over time. Biological exposure to biodegradable MP and NP shows a decline in cell growth for aquatic organisms, and the deterioration of MP to NP was detrimental for aquatic organisms (González-Pleiter et al., 2019; Green, 2016; Straub et al., 2017). Polymer coating fragmentation could potentially lead to contamination of inland water systems through groundwater transport. Fragmentation of plastics to nano-plastics or colloids may pass through the macropores of coarse soil and could reach high groundwater tables (Bläsing & Amelung, 2018; Chae & An, 2018). Higher concentrations of transport could occur over time due to further polymer coating fragmentation and substantially affect inland water systems and wetland ecosystems. Negative effects caused by polymer coating fertilizer may proceed to reoccur throughout the soil and inland water system until fully degraded.

1.4 Purpose and Objectives

The primary purpose of this research was to investigate the fate of polymer coatings within Manitoba soils under temperate climate conditions. Both soil characteristics and environmental conditions have been shown to exert strong control on the degradation rates of MP. Therefore, to better understand the role of both of these factors, the primary aim of this project was to assess the degradation rates of polymer coatings in soil under controlled and field conditions. To address the first aim of the project, three objectives were considered.

1. To compare the degradation of polymer coatings between the Stockton/Wheatland and Dezwood soil series under controlled/optimal conditions. The null hypothesis was that the degradation rates of polymer coatings would be the same in both types of soil. The alternative hypothesis was that the degradation rates of polymer coatings would be different in both types of soil.
2. To compare the degradation rates of polymer coatings in the Stockton/Wheatland and Dezwood soils between greenhouse and field settings. The null hypothesis was that the degradation rates of polymer coatings would be the same under natural and controlled environments. The alternative hypothesis was that the degradation rates of polymer coatings would be different under natural and controlled environments.
3. To determine whether the greenhouse or field site polymer coatings fully degrade within the four-year international standard of biodegradability. The null hypothesis was that both the greenhouse and field site's polymer coatings would fully degrade within the international standard. The alternative hypothesis was that either or both the greenhouse or field site's polymer coatings would not fully degrade within the international standard.

The secondary purpose of this research was to determine whether polymer coatings are being transported to other ecosystems. Tracking the mobility of polymer coatings becomes achievable for polymers that do not fully degrade within the international standard of biodegradability. Polymer coatings observed at the BRDC field 2 site, more than four years beyond an international biodegradability standard supports the idea of spatially monitoring polymer coatings across a field site. Therefore, the secondary objectives of this research was to investigate the mobility of polymer coatings across a field site. A field site was selected that had a singular PCU fertilizer application to describe the mobility, redistribution, and loss of polymer coatings over time. To address the secondary purpose of this project, an additional two objectives were considered.

4. To monitor lateral movement of polymer coating within surface runoff across a field site that has historical surface runoff measurements. The null hypothesis was that the polymer coatings would not have any lateral movement across the soils surface post-fertilizer application. The alternative hypothesis was that the polymer coatings undergo lateral movement across the soils surface within surface runoff post-fertilizer application.

5. To monitor if polymer coatings are being exported from cropland in surface runoff. The null hypothesis was that polymer coatings would not be observed in surface runoff. The alternative hypothesis was that polymer coatings would be observed in surface runoff.

2 Methods

2.1 Polymer Persistence in Manitoban Field Sites

Two field sites were selected to assess the degradation of ESN's polymer coating. Both field sites are located within southern Manitoba, Canada and are part of the prairie pothole region (Figure 2-1). Soil samples measured at both field sites were measured surrounding growing seasons. Three sampling periods (the fall of 2022, the spring of 2023, and the fall of 2023) were conducted at both BRDC and STC to determine polymer coating degradation rates.

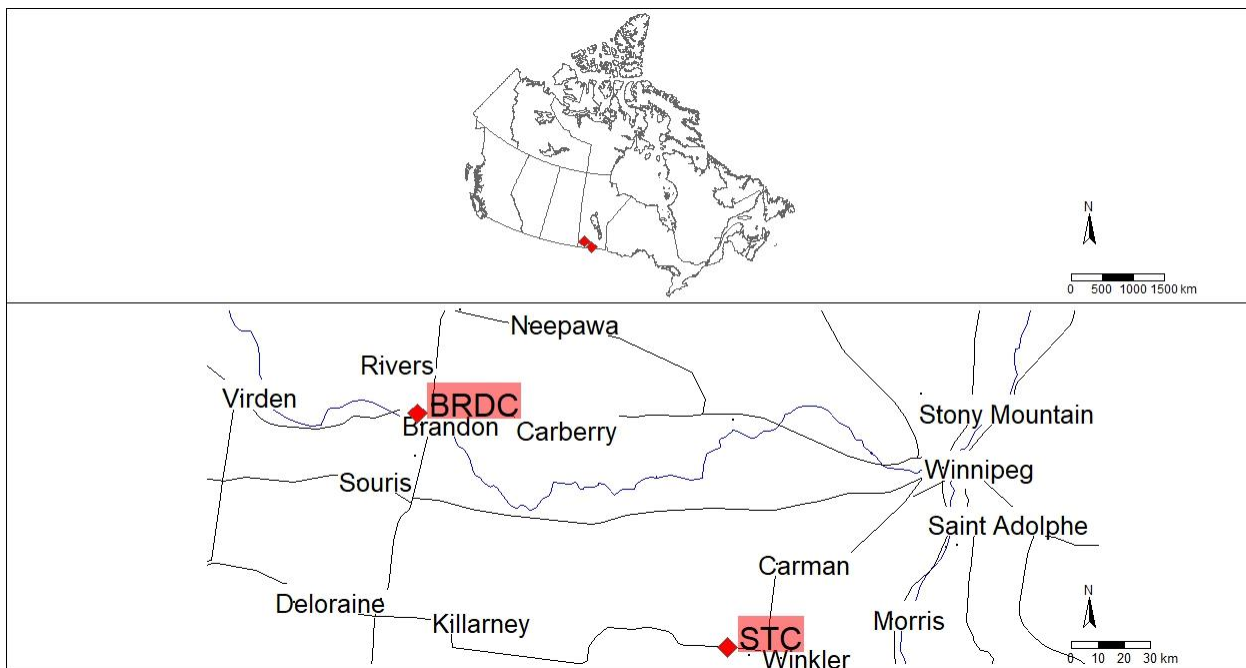


Figure 2-1: Geolocation of the Brandon Research and Development Center (BRDC) and South Tobacco Creek (STC) using rnaturrearth software package in R (Massicotte P, South A (2024) rnaturrearth: World Map Data from Natural Earth, version 1. 0. 1. 9000).

The BRDC is located on the northwest edge of the city of Brandon, at an elevation of 409 m (Figure 2-2). Two fields were selected from BRDC. BRDC Field 1 ($49^{\circ} 53' N$, $100^{\circ} 0' W$) is a part of a national soil erosion study. BRDC Field 2 ($49^{\circ} 52' N$, $99^{\circ} 58' W$) contains various fertilizer treatment studies. Soil characteristics of the two fields include a composition of Orthic

Black Chernozem soils (Stockton and Wheatland Series), slope gradient between 0-5%, imperfect to well drained areas, with negligible to low water erosion (Fitzmaurice et al., 1999). The Stockton Series has weakly to moderately calcareous, sand (FS, LFS, LS) and lacustrine sediments with a coarser texture (Soil Series Descriptions, 2010). The Wheatland Series is developed on a mantle of moderately to strongly calcareous, shallow sandy (FS, LS), with fluvial deposits over moderately to strongly calcareous, sandy-skeletal (CoS, MS) fluvial deposits (Soil Series Descriptions, 2010). Additionally, Wheatland soils can be slightly eroded, non-stony, and non-saline with low available water holding capacity, medium organic matter content, and low natural fertility (Soil Series Descriptions, 2010). BRDC had an annual temperature of 2.2° with an annual precipitation of 473-mm, with 20-25% occurring as snowfall (Fitzmaurice et al., 1999).



Figure 2-2: Brandon Research and Development Center field sites, MB Canada using Google Earth Pro 9.3.6.9796. (January 14, 2024). 49°50'59.06" N, 99°57'53.27" W, eye alt 20.70 km.

BRDC Field 1 received two ESN fertilizer applications at a rate of 220 kg ha⁻¹: the first in 2015 (broadcasted across the soil surface, then worked into the soil), and the second in 2017 banded directly into the soil to a depth between 5-7.5 cm. The first observation of polymer coating persistence occurred at BRDC Field 1. Although polymers were not the main objective of study at BRDC Field 1, polymers were identified, collected, and measured during a soil erosion project. Airborne polymer coatings were collected in the spring of 2022. The hypotheses of degradation and mobility were based surrounding the collection of these polymer coatings. Being the foundation of the hypotheses, BRDC Field 1 was selected as a field site to evaluate the degradation of these polymer coatings. Measurement of polymer coatings at BRDC Field 1 was used to justify whether persistence within the soil was occurring beyond the international standard of biodegradability. Soil sampling within the boundary of the soil erosion project would have affected that study. Hence, four soil sampling points were selected to measure the concentration of polymer coatings within the soil along the corners of the soil erosion plot area.

Extensive fertilizer studies were conducted within BRDC Field 2 (Figure 2-3). Conventional tillage practices occur within BRDC Field 2. BRDC Field 2 received six ESN fertilizer applications at a rate of 220 kg ha⁻¹: the first in 2015 (broadcasted across the soil's surface, then worked into the soil), and in each of 2016, 2017, 2018, 2021, and 2022 banded directly into the soil to a depth of 5-7.5 cm. Extensive fertilizer studies occurred in six plot area segments across the field site. To measure the concentration of polymer coatings without influence from the six plot areas, twelve sampling points were selected equidistantly from the fertilizer trials. BRDC Field 1 and BRDC Field 2 share similar soil characteristics, and collection of polymer coatings could demonstrate the difference between ESN that was just applied to BRDC Field 2 and dated polymer coatings at both field sites. Soil sampling at BRDC Field 2 was used to measure

whether higher amounts of tillage affected mobility of polymer coatings compared to BRDC Field 1. Polymer coating concentration will be measured based on the recovery rate compared to the fertilizer application rates to determine whether a decrease in concentration occurred. A decrease in polymer coating concentration compared to the amount applied would support the mobility of polymer coatings. Preliminary soil sampling was used at BRDC Field 2 to determine the best soil sampling technique to measure polymer coating concentration. Further details of determining the best soil sampling technique can be found in Appendix A: Assessment of soil sampling methods for the quantification of polymer coatings.

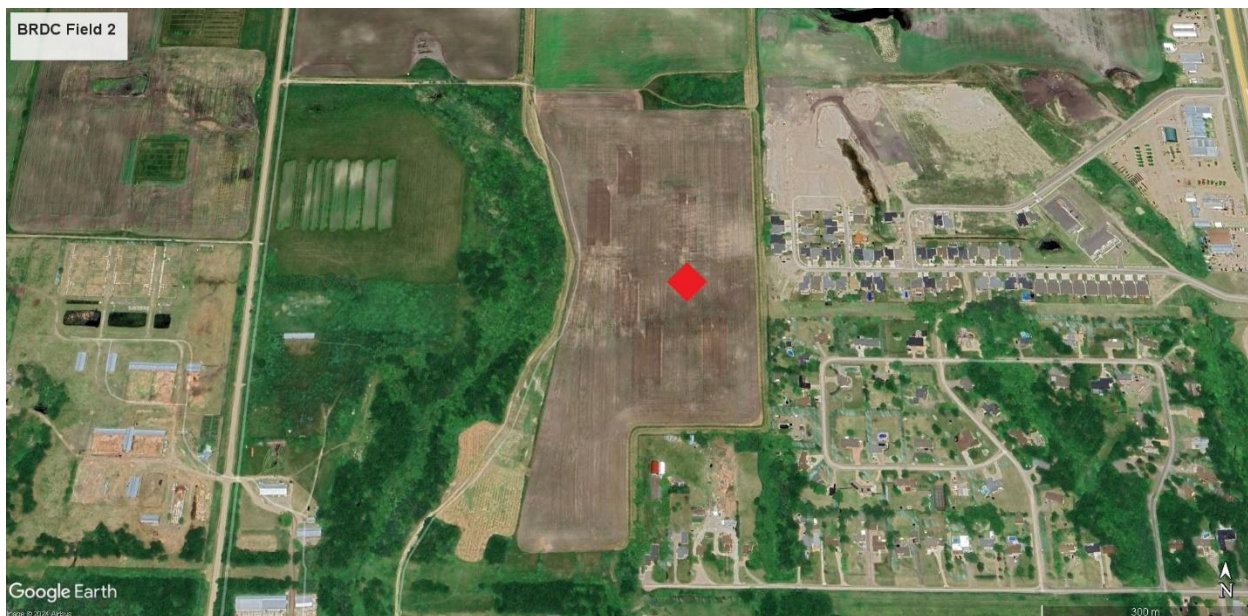


Figure 2-3: Brandon Research and Development Center field two, MB Canada using Google Earth Pro 9.3.6.9796. (January 14, 2024). $49^{\circ}52'33.48''$ N, $99^{\circ}58'31.33''$ W, eye alt 2.34 km.

The STC Watershed is located on the east edge of the Manitoba Escarpment, and within south-central Manitoba. Water quality and the volume of surface runoff have been monitored across 23 locations including the Steppler field sites since the early 1990s (AAFC, 2008). Within the STC Watershed, the Steppler Watershed ($49^{\circ} 20'$ N, $98^{\circ} 22'$ W) contains the twin watersheds field site. The twin watersheds field site has accounted for numerous papers on nutrient losses, tillage

practices, runoff sampling, sediment loss, soil erosion and water quality (e.g., AAFC, 2008; Hope et al., 2002; Li et al., 2011). Soil samples were taken across three landscape elevations in these papers (upper, middle, and lower) to determine the movement of nutrients across the field during surface runoff events. The same soil sampling positions were used as previous AAFC studies to determine the mobility of polymer coatings based on surface runoff. In addition to the soil sampling positions of previous AAFC studies, riparian area soil samples were measured in front of two established edge-of-field weirs to determine the concentration affected by surface runoff. To support the removal of polymer coatings from the field site, the two edge-of-field weirs were used to collect polymer coatings from a snowmelt surface runoff event.

The twin watersheds field site has an elevation of 445 m on the Manitoba Escarpment, containing hummocky to undulating landscape, loamy glacial moraine with Orthic Dark Grey Chernozem soils (predominantly the Dezwood Series) (Li et al., 2012). The Dezwood Series has strongly calcareous, deep, uniform, loamy (L, CL, SiCL) mixed shale, limestone and granite till deposits (Soil Series Descriptions, 2010). Additionally, the Dezwood soil can be slightly eroded and slightly stony with medium available water holding capacity, medium organic matter content and medium to high natural fertility (Soil Series Descriptions, 2010). The soil is moderately to strongly Calcareous, mixes of granitic, limestone and cretaceous shale (Michalyna, 1994). The twin watersheds had crop rotation of cereal/canola dating back to 1991, with the exception of soybean in 2017. ESN fertilizer was broadcast applied at a rate of 110 kg ha⁻¹ on 2022-05-24 using a spin spreader and incorporated into the surface soil with the seeding of canola on 2022-05-25 using an air hoe drill. Following canola harvest, the field was tilled to a depth of 10 to 15 cm using a field cultivator on 2022-10-29. A conventional fertilizer blend was applied in the

spring of 2023 and incorporated into the soil with a single pass of the field cultivator prior to the seeding of spring wheat using the air hoe drill on 2023-05-11.

The landscape at the twin watersheds directs surface runoff towards the two weirs along the northern field edge (Figure 2-4). The slope gradient of the twin watersheds varies from 3-10% and is well drained with moderately rapid runoff (Michalyna, 1994). The Dezwood soil has medium-high available water holding capacity with moderate organic matter content (Lung & Wanhong Y, 2014). The sub humid climate with annual temperature of 3°C receives an annual precipitation of 550-mm with 20-25% occurring as snowfall, and 15-20% of precipitation volume leaves as runoff (AAFC, 2008; Li et al., 2012). Water that flows from the twin watersheds enters the Morris River, which feeds into the Red River, and ultimately into Lake Winnipeg (S. Li et al., 2012).



Figure 2-4: South Tobacco Creek twin watersheds field site, MB Canada using Google Earth Pro 9.3.6.9796. (January 14, 2024). 49°20'16.25" N, 98°21'57.96" W, eye alt 1.93 km. White dots represent soil sampling positions across the field site, and the red diamonds represent the two edge-of-field weirs.

The mobility of nutrients at a specific location can be measured over time based on the reduction of nutrient concentration within soil samples, surface runoff samples, and residue material. The historical soil sampling positions measured the concentration of nutrient levels over time, and were separated into upper, middle, and lower elevations to determine the changes in nutrients content (AAFC, 2008). The concentration of polymer coatings was measured across upper, middle, lower, and riparian elevations to evaluate the redistribution downslope over time. The basis of polymer coatings losses followed the same evaluative methods as the historical data. Firstly, the redistribution of polymer coatings across elevations was evaluated by the reduction of polymer coatings concentration over time. Secondly, the reduction of polymer coatings was measured with runoff measurements to evaluate the net loss from snowmelt. Filtration measurements of polymer coatings were conducted at the two edge-of-field weirs to determine whether polymer coatings were present in surface runoff. The filtration measurement occurred across two days in April of 2023, following the presence of snowmelt water flow through the weir systems.

2.2 Assessment of Polymer Coating Degradation

2.2.1 Field Site Sampling Methodology

A 25 cm x 25 cm square soil sample was excavated with a spade to a depth of 5 cm (volume 3125 cm³). The designated surface area of 625 cm² was vertically indented with the spade and soil was pulled away from the surface monolith to reduce soil compression and maintain stability. The soil monolith was extracted using a spade and placed into containers. The excavated area was filled and leveled post collection. Samples were stored in the fridge at 4 °C. Further discussion of assessing the best soil sampling method may be found within Appendix A: Assessment of soil sampling methods for the quantification of polymer coatings.

The soil samples were disaggregated by hand into smaller soil aggregates to aid finding polymer coatings (Figure 2-5). To dry the soil, it was laid out on racks, then moved into air-drying rooms. The soil remained in the air-drying rooms until sufficiently dried and dried for a minimum of 72 hours. Each sample was further manually disaggregated and sieved through a series of sieves (2-mm followed by 1.18-mm). The stack of sieves were shaken, and polymer coatings were extracted from the sieves using tweezers starting with the 2-mm then followed by the 1.18-mm sieve. The 2-mm sieve filtered out biomass, stone formations, larger aggregates of soil, and soil aggregates containing polymer coatings. Larger aggregates were further broken down, and the polymers were extracted. Polymers coatings extracted from the soil underwent a magnetic stir cleaning process where the polymers were mixed with distilled water for 10 minutes at 500 rpm. The mixture of distilled water and polymer coatings were filtered and dried at 30 °C. The cleaned and dried polymer coatings were counted and then collectively weighed using a Mettler Toledo (ML54 NewClassic MF) balance with 0.1 mg resolution.



Figure 2-5: Embedded polymer capsule in a 5-mm diameter soil aggregate.

2.2.2 Greenhouse Equipment and Setup

The temperature regulated (23-27 °C) greenhouse at Brandon University was used to determine the degradation rate of polymer coatings under optimal conditions. Surface soil samples from BRDC and STC field sites were air-dried and disaggregated by hand to remove pre-existing polymer coatings. The air-dried samples were sieved using a 2-mm and 1.18-mm sieve to acquire coarse soil (> 2-mm), and fine soil (< 2-mm). The ASTM D5988 required the use of < 2-mm soil in the incubation study. Polymer coatings extracted from soil used within the greenhouse incubation were fully intact. Soil aggregates that passed through the 2-mm sieve were composited based on each field site to determine whether polymer coating degradation was different between BRDC Field 1, BRDC Field 2, and STC.

The trial replicates were formed using a plastic tray, 4-inch depth plastic seeding pots, soil, and freshly acquired ESN fertilizer. No presence of preexisting polymer coatings was detected while making the trial replicates. Plastic seeding pots were placed on plastic trays. Soil was added to the plastic seeding pot to form a 2 cm base. ESN fertilizer was applied above the base soil in the plastic seeding pot (Figure 2-6 A) at a target rate of 77 g m⁻² per 800 g soil (i.e. 20 ESN capsules per replicate). Soil was added above the applied fertilizer such that the fertilizer was at a depth of 5 cm (Figure 2-6 B). The number of capsules and total mass of ESN added to each pot were recorded.



Figure 2-6: Fertilizer applied to the soil base (A), and the spatial placement of all replicates within the Brandon University greenhouse (B).

A total of 135 soil replicates created a distribution of replicates for Dezwood (STC field site, n=77), and the Stockton-Wheatland (BRDC field sites, n=58) soils. Soil replicates were used to measure polymer coating degradation over an eight-month period (January to August 2023). Tap water was added uniformly across soil replicates to maintain a consistent soil moisture percentage within the boundaries of aerobic conditions. Additional soil replicates were constructed to measure soil temperature and water content using probes (Model 5TM, Decagon Devices, Inc.) connected to a datalogger (Model ZL6, Meter from January to May 2023; Model EM60G, Decagon Devices, Inc. from May to August 2023).

2.2.3 Sampling Scheme

Two phases existed within the incubation study. The first phase of the incubation contained the presence of urea within the ESN fertilizer. The absence of urea indicated the start of the second

phase. Degradation measurements occurred during the second phase, where measuring the degradation of the polymer coatings was not affected by presence of urea.

The first incubation phase contained a randomized sampling procedure of five replicates using a random generator to determine trial replicate selection (minimum of 2 per location) that were destructively measured every three weeks. The first phase lasted 104 days and assessed the loss of urea from the polymer coatings. Because the urea is 10-20x the mass of the polymer coating, the samples extracted during this phase could not be used to assess the degradation of the polymer coatings. The decrease in mass of the ESN during the first incubation phase was used to assess the release of urea from the polymer coating in the two Manitoba soils studied Appendix D: Release Rate of Urea.

The soil from each sampled replicate was poured into stacking 2-mm and 1.18-mm sieves, shaken, and polymer coatings were extracted using tweezers. Polymers coatings extracted from the replicates were kept separate and underwent a magnetic stir cleaning process to remove soil. The mixture of distilled water and polymer coatings were filtered and dried at a temperature of 30 °C. Each replicate was cleaned and fully dried. All polymer coatings from each respective replicate were weighed collectively and divided by the total coatings recovered to measure the remaining mass of each replicate. Mass percentage was calculated from the difference between initial fertilizer mass and remaining mass.

The second incubation phase contained a randomized selection of 15 replicates that were destructively measured every two weeks during the second phase to construct an analysis of isolated polymer coating degradation. No urea was present within dried polymer coating samples after day 104 based on no crystalline solid material remaining. The second phase lasted 108 days to determine polymer coating degradation. The mass percentage calculation in the absence of

urea using an interval measurement scheme determined the degradation rate of the polymer coating. The mass percentage measurement for the second incubation phase involved the same process of extraction, cleaning, and mass percentage recording of the polymer coatings as described for the first phase.

2.3 Polymer Coating Degradation

The degradation of polymer coatings within the agroecosystem occurs as a result of decomposition. The decomposition process entails polymers breaking down into the byproducts of carbon-based material, CO₂, H₂O, and NH₃. Within the decomposition process, the resulting mass of the remaining product is reduced. The cumulative mass of the polymer coatings within the field study is directly related to the initial polymer product, decomposition process, and products of the decomposition process. A mean capsule mass was derived for each soil sample as the cumulative mass of all capsules divided by the total number of capsules using the following equation:

Equation 2-1: The mean mass of a polymer coating for each elevation defined as the summation of cumulative mass divided by the cumulative count then divided by number of soil samples taken at that elevation.

$$\bar{m} = \frac{1}{n} \sum_{c=1}^n \frac{CM}{CC} \quad (2-1)$$

The decrease in mean polymer mass was assumed to be reflective of the average decomposition rate across each field site since fully intact polymer coatings were recovered.

Three types of models were fitted to the field and greenhouse data to assess the decomposition process of polymer coatings in the agroecosystem. Linear regression, negative exponential and spherical shell models were fitted to the decrease in capsules mass to assess the polymer degradation rates. The extrapolated degradation rates of polymer coatings are projected based on data acquired. The three models will approximate how long the polymer will persist; however,

the results of the three models will vary. For example, the linear model may be indicative of a minimum amount of time required for the polymer coating to deteriorate completely. The polymer degradation rate (r_d) is the differential mass loss per unit time.

Equation 2-2: Polymer degradation rate defined as the differential mass loss per unit time.

$$r_d = -\frac{dm}{dt} \quad (2-2)$$

The general trend of mean capsule polymer mass (m_t) followed a decreasing mass loss ($dm dt^{-1}$) pattern across time (t) based on an initial mean capsule mass (m_0).

Equation 2-3: Linear regression mean polymer coating mass.

$$m_t = \frac{dm}{dt} t + m_0 \quad (2-3)$$

The linear degradation model cannot account for the slowing degradation rate over time. The decomposition follows a negative exponential curve as the polymer coating breaks down. A full decomposition of the polymer coating occurs when the slope of the negative exponential curve is not statistically different from zero.

Equation 2-4: A negative exponential model fit defining the decomposition of the polymer coating.

$$A(t) = A_0 e^{-st} \quad (2-4)$$

The following equations for the degradation rate of plastics are derived from Chamas et al. (2020). Microbial activity occurs on the surface of the polymer coating. Therefore, the degradation by microorganisms on the surface of the polymer coating can be described by the surface degradation rate.

Equation 2-5: Specific surface degradation rate constant defined as the polymer degradation rate divided by the surface characteristics (density and surface area) of the polymer coating.

$$k_d = -\frac{1}{\rho SA} \frac{dm}{dt} \quad (2-5)$$

A vertical shift based on the mean polymer coating capsule mass was implemented to determine the intersection of zero mass at a point in time. Constraints were applied to the negative exponential model. The application of the negative exponential model included constraints involving a positive A_o , positive decay rate, and positive initial mass. The negative exponential fit using the specific surface degradation rate constant can be evaluated as the following:

Equation 2-6: Applied negative exponential fit defined using a spherical shell.

$$m_t = A_o e^{\frac{-4\pi R^2 k_d t}{V_0}} - m_0 \quad (2-6)$$

The polymer coating breaks down over time and becomes smaller during the decomposition process. The degradation of the polymer coating using a spherical shell model describes the degradation of the polymer coating similar to the negative exponential but additionally intersects zero mass. The degradation model assumes that the density of the material is constant across the spherical shell. The mass as a function of time for decreasing radius and surface area is given by the following equation.

Equation 2-7: Mass as a function of time defined by decreasing radius and surface area over time.

$$m_t = \left[(m_o)^{\frac{1}{3}} - \frac{\frac{2}{3}}{3} k_d \left(\frac{\pi * m_o}{V_0 - V_i} \right)^{\frac{1}{3}} t \right]^3 \quad (2-7)$$

A complete degradation time can be described as the following for a decreasing radius and surface area. The spherical shell of the polymer coating is contained within the volume of the outer layer subtracting the inner layer containing urea. The density of the polymer coating was considered constant due to the thin thickness of the polymer coating.

Equation 2-8: Complete degradation time defined by decreasing radius and surface area over time.

$$t_d = \frac{\frac{3}{2}}{6^{\frac{2}{3}} * k_d} \sqrt[3]{\frac{V_0 - V_i}{\pi}} \quad (2-8)$$

The linear regression, spherical shell and negative exponential models were fitted to the data to evaluate the degradation rate of polymer coating and extrapolate a full degradation time. The full degradation time is reached when the fitted model intersects with a zero-polymer mass. The negative exponential regression describes decomposition of the polymer coating but does not intersect zero and cannot evaluate a full degradation time.

BRDC Field 2 was excluded from the field degradation data since the recovered number of polymer coating was much less than the applied amount (Table 5). A reduced number of polymer coatings was observed at BRDC Field 2, and six ESN fertilizer applications were applied between 2015 and 2023. Based on the reduction of recovered polymer coatings at BRDC Field 2, the assessment of polymer coating degradation rates had ambiguity in segregating the degradation based on when it was applied. If mobility of polymer coating occurred at BRDC Field 2, then it would be more likely that polymer in 2015 were removed compared to 2022. This would affect the degradation measurement at BRDC Field 2 and would result in slower degradation compared to BRDC Field 1. Due to these factors, BRDC Field 2 was excluded from the degradation rate analysis and Figure 3-3.

Extrapolating beyond the data was necessary to model the full degradation of polymer coating capsules within the field study. The initial creation of ESN's polymer coating capsules occurred in 1998. The polymer coatings researched within this study were applied in 2015 or later. The linear regression and spherical shell applied models to the field, and incubation data evaluated a full degradation beyond the current year of this research (2024). Extrapolation of polymer coating degradation within this thesis was necessary since fully intact polymer coatings were recovered eight years after fertilizer application with incomplete degradation.

2.4 Tracking Polymer Coatings from Accumulation to Redistribution to Loss

2.4.1 Accumulation of Polymer Coatings

The slow rate of polymer degradation and continuous application of fertilizer with polymer coatings will result in accumulation of polymers within the agroecosystem. The amount of polymer coatings within an agroecosystem was characterized by input and output values. The input of polymer coatings capsules (PCC) was characterized by the amount of applied fertilizer across time, application rate (AR), and the number of applications (n). Polymer coating mass percentage (PCMP) as stated within ESN's SDS is 4% of the total mass (Nutrien, 2018). The mean polymer mass (PM) measured at STC without the presence of urea was $1.226 \text{ mg capsule}^{-1}$ which was used in the calculation of net polymer capsule input. The biofilm formation and expansion on the polymer coating surface was in early development during the growing season. Based on the degradation rate of polymer coatings at the STC field site, the decrease in mass was within two percent over a period of four months period. Based on these factors, it was assumed that limited degradation of the polymer coating occurred before polymer coating samples were extracted from STC four months after fertilizer application. Therefore, the mean polymer coating capsule mass is a close approximation to mean applied capsule mass and was used in the calculation to estimate the number of polymer coatings added during the fertilizer application.

Equation 2-9: Input of polymer coating capsules defined by the application rate, number of applications, and polymer coating mass percentage divided by the mean polymer mass.

$$PCC = \frac{AR * n * PCMP}{PM} \quad (2-9)$$

The field data recovery rate of polymer coatings was compared to the estimated input of polymer coatings to assess whether the concentration of polymer coatings had decreased.

2.4.1.1 Soil Sampling Across Depth

Soil samples were initially sampled within depths of 0-5 cm at BRDC on 2022-10-31 and STC on 2022-10-21 (prior to fall tillage) and 2023-05-11 (prior to spring field management operations). Additional soil measurements followed in the fall of 2023 where samples were taken within depths of 0-5 cm and 5-10 cm at BRDC on 2023-09-27 and STC on 2023-09-19. The 5-10 cm depth soil samples were excavated directly below the 0-5 cm depth soil samples across all sample points to create paired data. The recovered polymer coatings per unit area were the summation of the two sampling depths. The addition of soil excavated at 5-10 cm depths was needed to justify the concentration of polymer coatings redistributed downslope. Soil samples that were collected following the snowmelt surface runoff event were used to determine the net reduction of polymer coatings across different elevations. The amount of polymer coatings that were redistributed could be the difference in polymer coating concentration over time. Soil samples were taken in the 5-10 cm soil layer to assess whether the reduced recovery rate of the polymer coatings in the spring soil samples at STC were associated with vertical movement throughout the soil. The cumulative polymer coatings per unit surface area are required to determine accurately the lateral movement of polymer coatings throughout the landscape, assuming uniform application.

2.4.2 Redistribution of Polymer Coatings

The movement of polymer coatings was measurable at STC due to its single ESN application history and the assumption of a consistent application rate across landscape positions in the field in May 2022. The distribution of polymer coatings was initially measured in the fall of 2022. Further distributions of the polymer coatings across the hillslope were measured by the recovered polymer coatings over time in spring and fall of 2023. The difference in polymer

coatings within the hillslope over time was used to evaluate the redistribution of polymer coatings downslope. Additionally, the mean mass of polymer coatings recovered across the elevation positions were measured. The mean polymer mass in conjunction with elevation position was used to determine whether polymer coatings of lower mass are disproportionately affected by lateral movement.

2.4.3 Loss of Polymer Coatings via Surface Runoff

Polymer coatings at the STC field site weirs were collected using a simple filtration system placed across the upstream side of the v notch (Figure 2-7). A 1-mm screen was applied to the flat surface of a stainless-steel frame. The frame had a flat-rimmed surface which clips were applied to hold the 1-mm screening to collect polymer coatings. Sheets of screens were cut with extra length to wrap around the flat edges of the frame. The 1-mm screening was stretched firmly across the frame's flat surface to filter polymer coatings.



Figure 2-7: Weir filter set against the v-notch of the east weir, with water flow moving downslope (moving towards the top of the image).

2.4.3.1 Surface Runoff Methodology

Measurement of polymer coatings exported by surface runoff occurred on 2023-04-13, and 2023-04-14. Four weir filters were constructed at the start of each day to be applied to the weirs v-notch. The water flow pressure passing through the weir would maintain enough force to keep the weir filter firmly held to the v notch weir. The orientation of the weir filter was set against the wooden walls of the weir to allow the flow pass through. The weir filters were applied to each weir for a maximum duration of two hours each day and switched twice a day. Screening was removed from the frame and replaced to record the polymers coatings that were affected by surface runoff. Polymers were extracted from the screens using tweezers. The samples were dried at 30° C, weighed, and expressed as mean polymer capsule mass as previously described.

The buoyant polymers collected with the surface runoff were used to estimate the amount passing through the weir over time. The accumulation of water volume passing through the weir was calculated based on the flow rate and incremental volume that passed through the surface area of the weir. The calculated flow rate (FR) and volume of water passing through the surface area of the weir were calculated based on depth (D) measurements made with self-logging pressure transducers (Onset HOBO Water Level Data Logger) and staff gauges read manually and from time-lapse photography. The staff gauge with time-lapse photography was used to calibrate the HOBO logger depth used in subsequent calculations.

Equation 2-10: Flow rate calculation defined by water depth through a v-notch weir.

$$FR = 1.37 * D^{2.5} * 1000 \quad (2-10)$$

An incremental volume of water was calculated based on the flow rate over a set interval time of 15 minutes. The accumulated volume of water was the summation of each incremental volume of water passing through the weir. An estimated number of polymer coatings (PC) were

extrapolated based on the sum of polymer coatings (PC_i) passed by an incremented volume of water (V_i) over a time interval multiplied by the total accumulated volume (V):

Equation 2-11: Estimated MPs removed defined by a runoff event ratio multiplied across the cumulative runoff.

$$PC = V \sum_1^n \frac{PC_i}{V_i} \quad (2-11)$$

The estimated net output of polymer coatings via surface runoff was compared with the reduced polymer coating concentration based on polymer per unit area at each sampling position spanning the STC field site. The comparison of polymer coatings within the surface runoff compared to the net reduction across the entire field site was used to determine whether the amount lost in surface runoff accounted for the net reduction across the field site.

2.5 Statistical Analyses

All statistical analyses, summaries, and calculations were undertaken using the R Statistical Software (v4.3.3; R Core Team 2024), through the RStudio Integrated Development Environment v2024.04.1 (RStudio Team 2020). Assessment of BP degradation over time for both incubation and field data were assessed using linear regression with incubation duration, soil type, and their interaction as fixed factors. If the interaction was not significant ($p < 0.05$) the term was removed from the model. Analysis of Variance (ANOVA) was used to determine whether both concentration and mean mass differences were statistically different across field elevation positions. Additionally, ANOVA was used to determine whether the degradation of polymer coatings was statistically different between soil types and between studies. All model assumptions were assessed using DHARMA residual plots (DHARMA v0.4.6; Hartig 2022). Model parameters for the negative exponential and spherical models were fitted using nonlinear least squares. The linear, negative exponential and spherical shell models were compared using

the Akaike information criterion (AIC) to determine the accuracy of the models. All plots were created using the R package ggplot2 (v3.5.1; Wickham 2016).

3 Results

3.1 Polymer Coating Degradation

3.1.1 Comparison of Manitoban Soils Degradation

A comparison between soil types involved the second phase of the incubation study to determine whether the degradation between soil types was different. Polymer coating mass was measured over time within the incubation study (Figure 3-1).

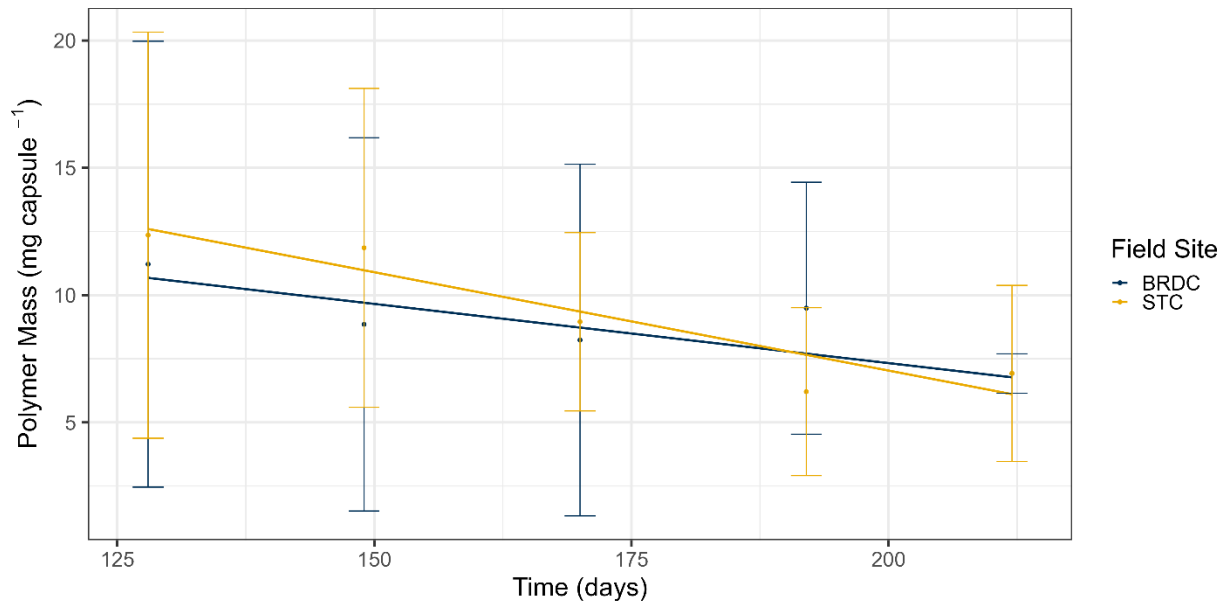


Figure 3-1: No statistical difference between polymer mass and time during the incubation study for two Manitoban soils. Polymer degradation was measured in a controlled greenhouse using 58 Stockton-Wheatland (BRDC) and 77 Dezwood (STC) soils. Statistics performed by ANOVA, comparing the degradation rate between the two soils, error bars indicate standard deviation of polymer coating mass *** p < 0.001.

There was no statistical difference between polymer coating degradation between the Dezwood and Stockton-Wheatland soils. However, polymer degradation for replicates of Dezwood and Stockton-Wheatland soils within the incubation study was statistically different than zero. On average the polymer coating capsules decrease in mass by -0.0007 mg per day (95% CI [-0.000115, -4.88e-05], t-value = -4.948, p-value <0.001). Overall, the amount of variability (i.e.,

standard deviation) in polymer mass decreases over the duration of the incubation study (Figure 3-1).

3.1.2 Extrapolating Polymer Coating Degradation

Three models consisting of linear regression, negative exponential, and spherical shell were applied to the incubation and field studies. The differences in full degradation can be observed between the incubation study and the field study by their extrapolation (Figure 3-2; Figure 3-3). Further discussion of model derivation and applications are found within Appendix C: Model Comparison. All three models reached a full degradation beyond the span of the field and incubation data (Table 1). Within the incubation study, the linear regression projected a full degradation in 312 days, and the spherical shell model projected a full degradation in 588 days, and the negative exponential model projected a full degradation in 831 days.

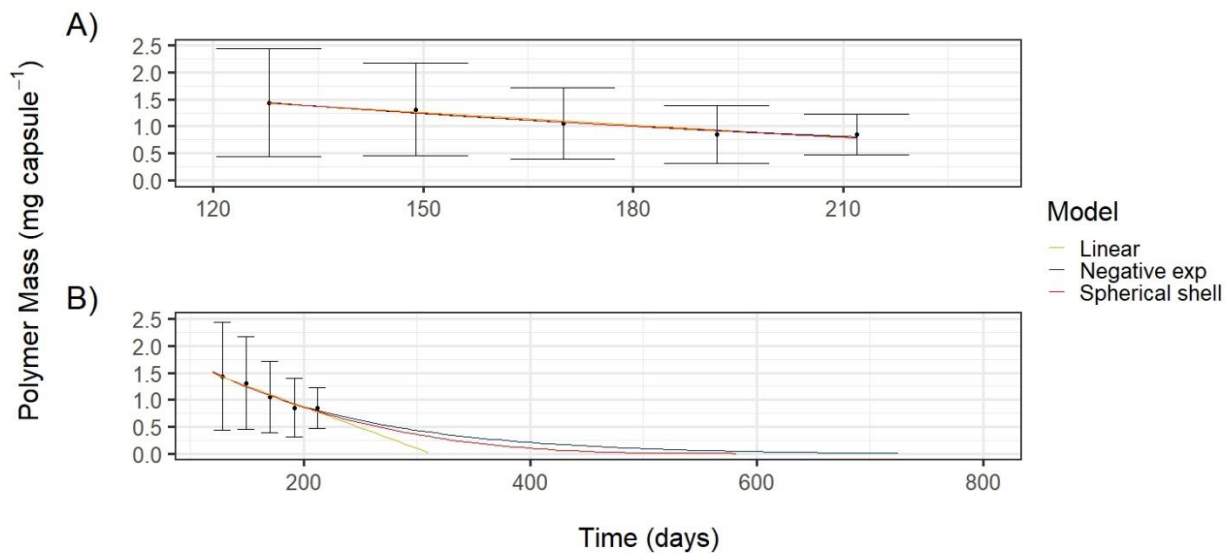


Figure 3-2: Extrapolation of linear regression, negative exponential and spherical shell models measure different full degradation times within the incubation study. (A) The three models were fitted to the incubation data, (B) extrapolated to determine full degradation. All three models projected a full degradation within the four-year biodegradability standard.

Within the field study, the linear regression projected a full degradation in 8986 days, and the spherical shell model projected a full degradation in 24524 days, and the negative exponential

model projected a full degradation in 34232 days. However, the further you extrapolate beyond the data set, the less reliable the models measure degradation.

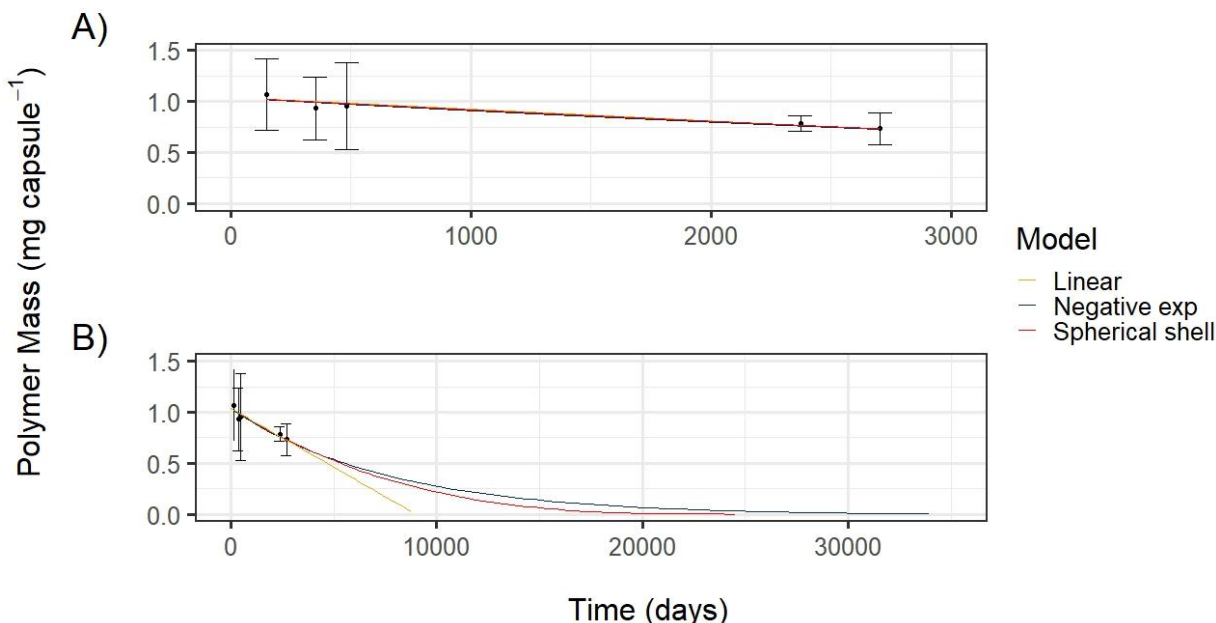


Figure 3-3: Extrapolation of linear regression, negative exponential and spherical shell models measure different full degradation times within the field study. (A) The three models were fitted to the field data, (B) extrapolated to determine full degradation. The three models projected different full degradations with linear regression in 8986 days, spherical shell in 24524 days, and negative exponential in 34232 days.

3.1.3 Field and Greenhouse Degradation Comparison

There was significant difference between the two studies degradation ($F = 62.245$, $p\text{-value} < 0.001$).

The field study degradation rate was 41.7 times slower than the degradation rate of the incubation study using the spherical shell model (Table 1). There was no significant difference in degradation between field sites ($t\text{-value}=0.873$, $p\text{-value} 0.385$), and across time ($t\text{-value} -1.637$, $p\text{-value} 0.105$).

Table 1: Comparison of polymer coating full degradation projections using linear regression, spherical shell, and negative exponential models. The three models were applied to both the incubation and field data to determine the persistence of polymer coatings and compare the difference in degradation between the two studies.

Study	Field Site	Linear Regression Mass Loss ($\mu\text{g day}^{-1}$)	Linear Regression Standard Error ($\mu\text{g day}^{-1}$)	Linear Regression Full Degradation (days)	Specific Surface Degradation Rate (mm day^{-1})	Spherical Shell Full Degradation (days)	Negative Exponential Full Degradation (days)
Incubation	BRDC	57.0	28.5	358	NA	NA	NA
Incubation	STC	94.7	20.4	291	NA	NA	NA
Incubation	Combined	77.4	16.0	312	1.31e-04	588	831
Field	BRDC	0.155	0.42	7446	NA	NA	NA
Field	STC	0.237	0.16	4578	NA	NA	NA
Field	Combined	0.116	0.03	8986	2.20e-06	24524	34232

The degradation of the polymer coating capsules was measured by the negative exponential model as described in section 2.3. The following variables in Table 2 are the fits of the negative exponential to incubation and field data sets. Based on the negative exponential, the variables could explain environmental degradation factors (A), surface degradation of the polymer coating (S), initial mass (K), and time (x).

Table 2: Fitted values for the negative exponential model for the degradation of polymer coating capsules. The initial conditions (A) are based on the starting mass and number of polymers, the decay rate (S) based on the polymer type/composition/molecular weight, temperature, moisture, size, shape, and mean capsule mass (K).

Study	Variable	Mass Equivalent	Estimate
Incubation	A	Polymer Mass	3.5
Incubation	S	Polymer Mass	0.0069
Incubation	K	Polymer Mass	0.0123
Field	A	Polymer Mass	1.05
Field	S	Polymer Mass	0.00013
Field	K	Polymer Mass	0.0123

The confidence limits in Table 3 were measured using a 0.95 confidence level. The field data degradation confidence limits of linear regressions were not statistically different from zero (i.e. contain zero) (Table 3). When combining BRDC and STC, polymer degradation is statistically different than zero (Table 3). Based on the difference in mean polymer coating mass observed at BRDC Field 1 and STC, degradation is occurring, however, at a very slow rate at field sites.

Table 3: Field data comparison of linear regression analysis applied to Wheatland/Stockton (BRDC) and Dezwood (STC) soils. The estimated marginal means of linear trends upper limit for both soils contained zero.

Field Site	Mass Loss ($\mu\text{g day}^{-1}$)	Standard Error ($\mu\text{g day}^{-1}$)	Degrees of Freedom	Lower Confidence limit ($\mu\text{g day}^{-1}$)	Upper Confidence Limit ($\mu\text{g day}^{-1}$)
BRDC	0.155	0.42	206	0.977	-0.668
STC	0.237	0.16	206	0.553	-0.079
Combined	0.116	0.03	206	0.178	0.054

There was no difference between AIC values between the three models (Table 4). Therefore, the three models could be interchangeable for interpreting polymer coating degradation. While the three models are not statistically different, the selection of the best applicable model is important to describe the persistence of polymer coatings within the soil. The selection of the model in the field study can vary between 24 and 94 years for full degradation based on model selection.

Table 4: The Akaike Information Criterion (AIC) values using linear regression, spherical shell, and negative exponential models. No statistical difference measured between the linear regression, spherical shell, and negative exponential models.

Study	Model	AIC
Incubation	Linear Regression	317.04
Incubation	Negative Exponential	316.67
Incubation	Spherical Shell	317.04
Field	Linear Regression	-24.32
Field	Negative Exponential	-24.52
Field	Spherical Shell	-24.45

The two studies can be qualitatively compared using data from STC since the incubation and field studies were measured on a similar time scale. The comparison of the polymer coating degradation between studies was conducted qualitatively to visualize the difference in degradation between the incubation and field study. Figure 3-4 visualizes the difference in degradation between the two data sets using both a linear regression model (A), and spherical shell model (B).

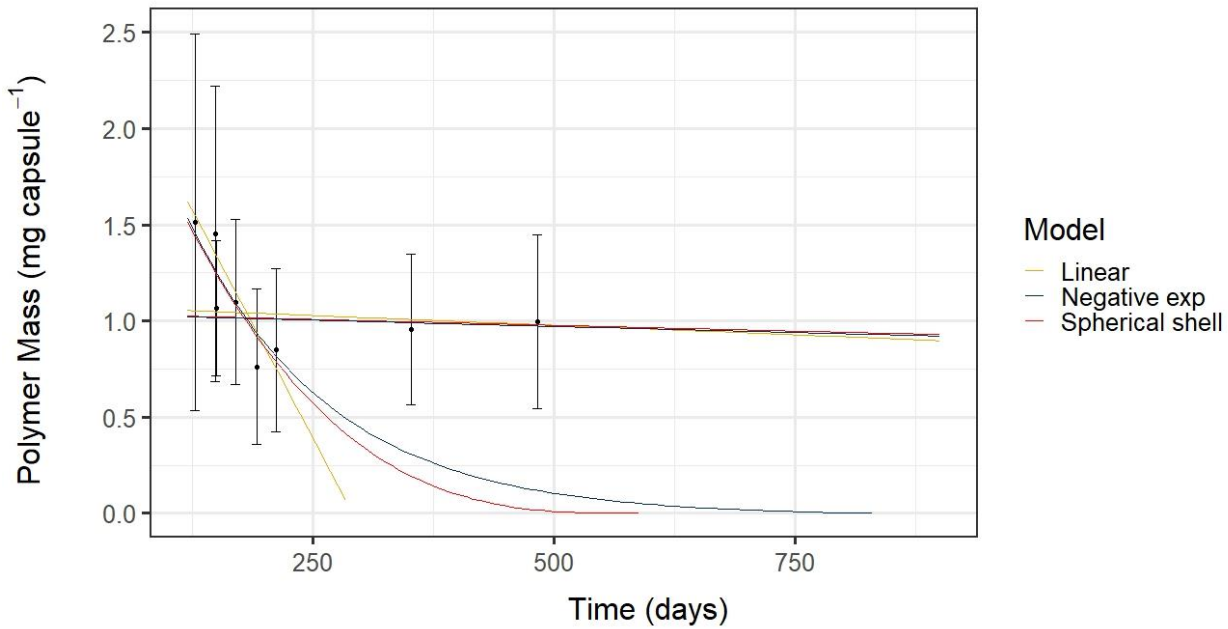


*Figure 3-4: Visualization of the statistical difference between incubation and field studies using the linear, negative exponential and spherical shell models. Statistics performed by ANOVA, comparing the degradation rate between the two studies, error bars indicate standard deviation of polymer coating mass **** $p < 0.001$.*

3.2 Tracking Polymer Coatings from Accumulation to Redistribution to Loss

3.2.1 Accumulation and Redistribution of Polymer Coatings

The estimated amount of polymer coating capsules applied per unit area was calculated and compared with recovery rates at the two field sites (Table 5). The concentration of polymer coatings was measured over time at BRDC and STC. Concentration measurements before the fall of 2023 were collected within the 0-5 cm soil layer. Additional measurements in the vertical direction were needed to verify lateral mobility of polymer coatings. Concentration measurements in the fall of 2023 were collected from the 0-10 cm soil layer to reconcile the difference between recovered and applied polymer coatings.

Table 5: Estimated and recovered number ± standard error of polymer coating capsules at the field sites over time. Fall 2022 and Spring 2023 were sampled to a depth of 5cm and Fall 2023 to a depth of 10cm. ND = no data.

Field Site	Application Rate (g m⁻²)	Number of Fertilizer Applications	Estimated Polymer Coating (capsules m⁻²)	Fall 2022 (capsules m⁻²)	Spring 2023 (capsules m⁻²)	Fall 2023 (capsules m⁻²)
BRDC Field 1	22	2	1435	944 ± 213	ND	1468 ± 341
BRDC Field 2	22	6	4306	1895 ± 277	ND	3175 ± 320
STC	11	1	359	403 ± 40	348 ± 34	305 ± 25

A net decrease in polymer coating concentration occurred over a period of a year at STC regardless of additional soil per unit area in the fall of 2023. However, the distribution of polymer coatings concentration compared with Table 5 demonstrates that the upper landscape elevation was not significantly lower using an ANOVA (p value of 0.237) than the concentration across the field site elevations. This could suggest that redistribution of polymer coatings could be affected by larger slope gradients. The recovered amount of polymer at BRDC Field 1 compared to the estimated amount of polymer coatings over a period of seven years. This could suggest that polymer coatings are not significantly redistributed across field sites with low slope gradients.

Polymer coatings were observed to vertically shift within the soil across all field sites (Figure 3-5). The recovered polymer coatings within the 5-10 cm layer were greater than the 0-5 cm layer at BRDC Field 2 where banded (subsurface) fertilizer application and deeper tillage practices occurred (Figure 3-5).

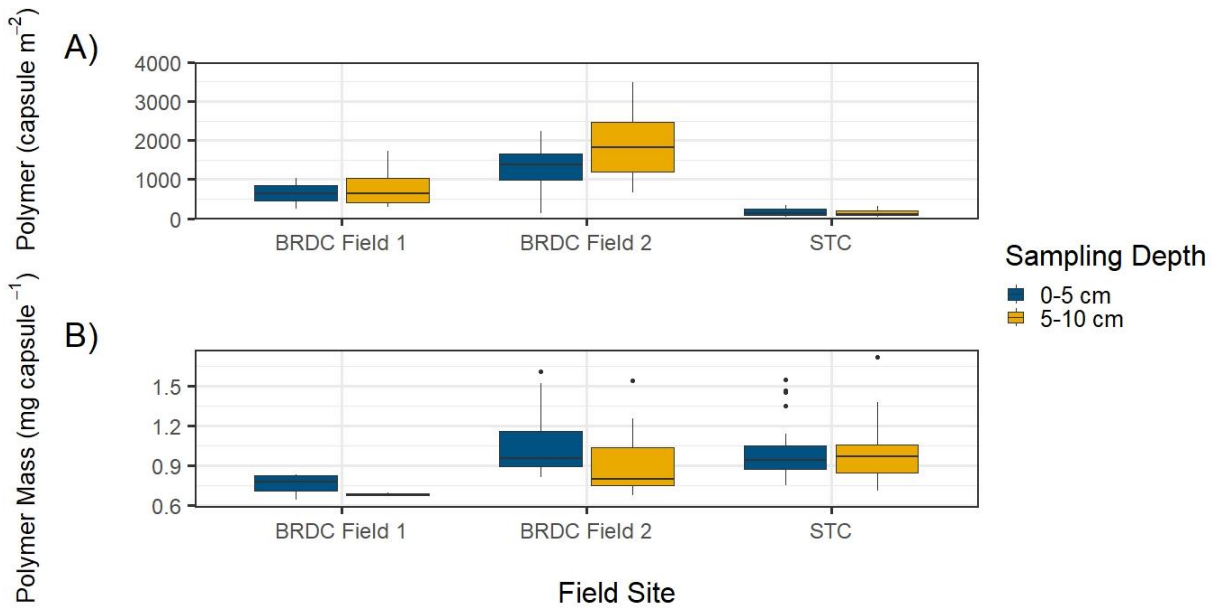


Figure 3-5: Statistical difference in polymer coating concentration at STC and polymer coating mass at BRDC Field 2 when comparing sampling depth of 0-5 cm and 5-10 cm over time, error bars indicate standard deviation. (A) Polymer coating concentration measured across BRDC Field 1, BRDC Field 2, and STC field sites, (B) polymer coating mass measured across BRDC Field 1, BRDC Field 2, and STC field sites. Statistics are performed by a one-way ANOVA, comparing the polymer coating concentration at BRDC Field 1, BRDC Field 2, and STC **** p = 0.921, p = 0.376, p = 0.0008, and comparing polymer mass across sampling depths at BRDC Field 1, BRDC Field 2, and STC **** p = 0.257, p = 0.008, p = 0.918.

There was a statistical difference in polymer coating concentration at STC for sampling depths of 0-5 cm and 5-10 cm using a one-way ANOVA ($F = 12.044$, $p = 0.0008$). The concentration of polymer coatings in 0-5 cm was higher than the concentration measured in 5-10 cm. This would suggest that polymer coatings have not moved vertically downward through the soil after a year.

At BRDC Field 2, the mean mass of polymer coating capsules was statistically different for sampling depths of 0-5 cm and 5-10 cm using a one-way ANOVA ($F = 7.8875$, $p = 0.008$).

Fertilizer was banded yearly at BRDC since the first ESN application seven years prior, which could suggest that smaller polymer coating capsules are more likely to move vertically downward through the soil during tillage and seeding events.

Table 6: The mean polymer coating capsule mass and standard error across 0-5 cm, 5-10 cm, and 0-10 cm soil depths spanning BRDC Field 1, BRDC Field 2, and STC. A statistical differences between mean polymer coating capsules across 0-5 cm, 5-10 cm soil depths occurred at BRDC Field 2.

Field Site	Polymer Coating	Polymer Coating	Polymer Coating
	0-5 cm (mg capsule⁻¹)	5-10 cm (mg capsule⁻¹)	0-10 cm (mg capsule⁻¹)
BRDC Field 1	0.758 ± 0.04	0.684 ± 0.02	0.733 ± 0.03
BRDC Field 2	1.028 ± 0.08	0.922 ± 0.07	0.975 ± 0.05
STC	0.992 ± 0.05	0.978 ± 0.06	0.985 ± 0.04

The mean mass of polymer coating capsules within the 5-10 cm layer at STC lower and middle elevations were observed to be higher than the 0-5 cm layer (Table 7). The mean mass of polymer coating capsules at STC were observed to decrease with descending elevation in the 0-5 cm soil layer (Table 7). However, there was no statistical difference between polymer coatings mass in the 0-5 cm and 5-10 cm soil layer across elevations at STC (Table 7). Additionally, there was no statistical difference in the mean mass of polymer coating capsules between elevations within the field in the 0-5 cm soil layer at STC (Table 7).

Table 7: The mean polymer coating capsule mass and standard error across 0-5 cm, 5-10 cm, and 0-10 cm soil depths spanning upper, middle, lower, and riparian elevations at South Tobacco Creek. No statistical differences between polymer coating capsule mass between 0-5 cm and 5-10 cm soil depths. No polymer coating capsules were observed within the riparian 5-10 cm soil depth.

STC	Polymer Coating	Polymer Coating	Polymer Coating
	0-5 cm (mg capsule⁻¹)	5-10 cm (mg capsule⁻¹)	0-10 cm (mg capsule⁻¹)
All Field Elevations	0.992 ± 0.05	0.978 ± 0.06	0.985 ± 0.04
Upper	1.027 ± 0.10	0.943 ± 0.07	0.985 ± 0.06
Middle	0.984 ± 0.08	1.033 ± 0.11	1.009 ± 0.07
Lower	0.924 ± 0.12	0.991 ± 0.05	0.961 ± 0.07
Riparian	0.835 ± 0.05	0 ± 0	0.835 ± 0.05

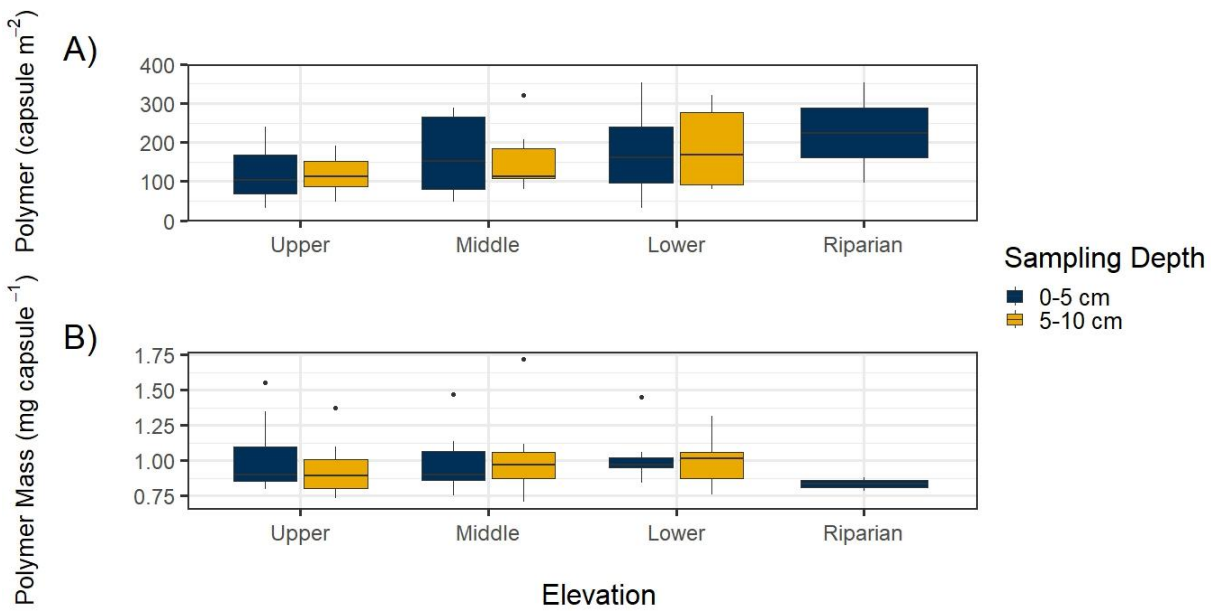


Figure 3-6: Polymer coating concentration increased with descending elevations, and polymer mass was lower in the riparian compared to field elevations at STC, error bars indicate standard deviation. (A) Polymer coating concentration measured across STC elevations, (B) polymer coating mass measured across STC elevations. Statistics are performed by a one-way ANOVA, comparing the polymer coating concentration across upper; middle; lower; and riparian elevations at STC *** $p = 0.0341$, and comparing polymer mass across upper; middle; lower; and riparian elevations at STC *** $p = 0.02292$.

The concentration of polymer coatings should be equivalent across the landscape, assuming an even application of PCU fertilizer at STC. However, the recovered number of polymer coating capsules increased with descending elevation. There was a statistical difference in polymer coating concentration across hillslope elevations using a one-way ANOVA ($F = 3.0062$, $p = 0.0341$). The mid and lower slope positions had 33 and 43 % more capsules as compared to the upper position, respectively. The recovered polymer coatings in Table 8 provides evidence that polymer coatings can shift both laterally and vertically within the soil compared to the even application (359 polymer coatings m^{-2}). This provides further evidence for mobility since polymer coating degradation in 3.1.2 was measured to take more than 67 years. Additionally, there was a statistically difference in mean polymer coating mass between the riparian and field elevations using a one-way ANOVA ($F = 4.4352$, $p = 0.02292$). This could suggest that polymer coatings with less mass are more likely to be redistributed downslope.

Table 8: The recovered number of polymer coating capsules ± standard error across 0-5 cm, 5-10 cm, and 0-10 cm soil depths spanning upper, middle, lower, and riparian elevations at South Tobacco Creek 16- months after ESN application. A statistical difference in polymer coating concentration occurred across hillslope elevations. ND = not detected.

Slope Position	Polymer Coatings	Polymer Coatings	Polymer Coatings
	0-5 cm (capsules m⁻²)	5-10 cm (capsules m⁻²)	0-10 cm (capsules m⁻²)
Upper	122 ± 29	118 ± 18	240 ± 33
Middle	168 ± 36	152 ± 28	320 ± 45
Lower	170 ± 37	184 ± 35	344 ± 49
Riparian	224 ± 128	ND	224 ± 128

There was a statistical difference in polymer coating concentration over time at STC using a one-way ANOVA ($F = 32.553$, $p < 0.0001$). Approximately half of the polymer coatings capsules were observed to be below the depth of initial application (0-5 cm) (Table 8). No subsequent ESN fertilizer was applied to the field during the study. The concentration of PCU fertilizer should remain constant across landscape elevations assuming no lateral movement. If redistribution of polymer coatings were occurring at STC, then they should move downslope. A decrease in polymer coatings can be observed in the upper landscape elevation suggesting lateral movement downslope. Additionally, an increase in polymer coating concentration occurred in the middle elevation and a decrease in concentration in the upper elevation occurred between the spring and fall of 2023 (Figure 3-7). This supports polymer coatings moving laterally downslope by field equipment.

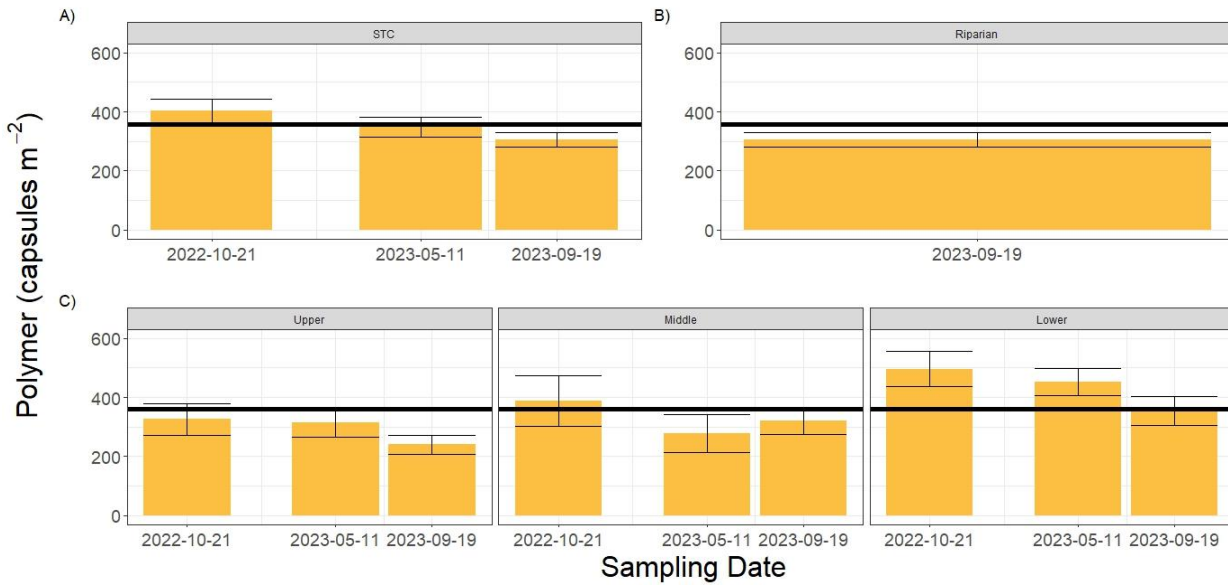


*Figure 3-7: Polymer coating concentration decreased over time, and polymer coatings were observed within the riparian at STC, error bars indicate standard deviation. (A) Overall decline of polymer coating concentration at STC, (B) observance of polymer coating mass within the riparian area, and (C) polymer coating concentration across field elevations over time. Statistics are performed by a one-way ANOVA, comparing the polymer coating concentration over time across upper, middle, lower, and riparian elevations at STC **** p < 0.0001.*

3.2.2 Loss of Polymer Coatings via Surface Runoff

Two main surface runoff events occurred during the 2023 snowmelt period, the first main snowmelt event occurred between 2023-04-12 and 2023-04-14. The Polymer coatings transported in Table 9 was extrapolated from the polymer coatings collected during each weir filter interval measured on 2023-04-13 and 2023-04-14. The Concentration of polymer coatings removed from the agroecosystem was approximately equivalent across the west and east weir (Table 9). Polymer coating capsules that were observed to redistribute in surface runoff most likely originated from the soil surface at the lower elevation (Figure 3-7). Polymer coatings collected from the surface runoff samples had a mean polymer capsule mass of 1.124 ± 0.3 mg. The recovered ratio of polymer coatings between the second and third day of 11:4 was a result of decreased water volume through the weir on the third day.

Table 9: Comparison of the amount of polymer coating capsules transported during the surface runoff event at STC during the spring of 2023 between the west and east weir. The amount of polymer coating capsules recovered was dependent on the accumulated volume through the weir.

Weir	Accumulated Volume (L)	Transport Rate (capsules L ⁻¹)	Field Area (m ²)	Polymer Coating Transported (capsules)	Polymer Coating Lost (capsules m ⁻²)
West	4.25e+06	4.65e-05	4.00e+04	198	4.95e-03
East	3.94e+06	4.69e-05	5.15e+04	185	3.59e-03

A net output of polymer coatings was observed in surface runoff but statistically insignificant compared with the amount applied to the twin watershed field site (Table 5). Therefore, the net reduction in polymer coatings from surface runoff cannot solely describe the reduction in polymer coatings throughout the year but may contribute to the reduction observed over time.

4 Discussion

4.1 Polymer Coating Degradation

The polymer coating degradation rates of the two soil types within the greenhouse incubation study were compared and found to be the same over the observation period (Figure 3-1). The greenhouse incubation study was based on the specification within the ASTM D5988 to evaluate the mass loss of polymer coatings over time. Although the ASTM D5988 was designed to measure CO₂ evolution, a simpler approach where the mass loss of polymer coatings was measured directly over time was taken since the degradation results in both CO₂ evolution and a net mass loss. Uniform replicates within the incubation study were used to measure the degradation of the polymer coating. Uniform replications were needed since microbial decomposition and CO₂ evolution can be dependent on the soil pore structure. Previous research has shown that the soil pore structure affected the soil CO₂ concentration and that greenhouse gas fluxes increased from fine to medium to coarse texture soil (Du et al., 2023). While chemical and physical factors play a prominent role in small aggregate formation in clay soils, biological processes are important for development of large aggregates and macropores, and they are the primary factor for aggregation of sandy soils (USDA, 2022). Sand particles are rougher in texture than clay particles. The sand particles are less likely to form a tight soil matrix resulting in larger macropore space and allowing water to drain faster. Therefore, larger macropores found within sandier soil are less likely to retain water. However, the macropore space is built from the culmination of soil mineral particles over time. A higher clay content within soil can reduce the macropore space within the soil matrix. For example, clay soil can expand when wet, reducing the macropore space within the soil matrix. This would result in soil being drained slower and increased water retention. Therefore, a higher clay content could increase the retention of water

that could affect polymer coating degradation rates. Additionally, clay particles have a net negative charge which may attract the dipole of the water molecule. This attraction could retain water in proximity to the polymer coating. Within the incubation study, a faster rate of urea release was observed from the soil composition with higher clay content (STC) as expected (Appendix D: Release Rate of Urea). This occurred since the release of urea from the polymer coating occurs in response to soil temperature and moisture. However, the two soil types did not have statistically different degradation rates.

The polymer coating degradation rates of the two soil types in a greenhouse incubation and field study were statistically different. The slower degradation observed within the field study compared to the incubation study underscores the importance of environmental conditions on polymer coating degradation rates. Site-specific factors including soil temperature and moisture dynamics, inherent soil biotic communities and plastic film characteristics (mulch fragment size) will control biodegradation rates, and in-field conditions are often less ideal for degradation (Griffin-LaHue et al., 2022). Therefore, a reduction in MP degradation under cooler temperatures in a continental climate could explain the increased persistence of the polymer coating.

Additionally, it was demonstrated that slower degradation occurred in cooler than in warmer climates and that degradation is reduced in extremes of dry or wet soils (Costa et al., 2014; Sintim et al., 2020). Polymer coating degradation within the environment can vary due to fluctuations in soil moisture levels from dry or wet seasonal variance. The rate of plasticizers release from PVC and its degradation were influenced by the initial plasticizer content, environmental conditions (abiotic/biotic), and other physiochemical properties (Panahi et al., 2024). Therefore, suboptimal conditions for microbial activity such as low soil temperatures and moisture can contribute to slower degradation rates. Two factors for microorganisms' ability to

degrade MPs stem from soil temperature and soil moisture. For example, soil temperature affects the metabolic rate of microorganisms and soil moisture content dictates water availability essential for cellular structure and function. Overall, the greenhouse incubation study had approximately five times the accumulated heat units compared to the field study (Appendix B: Soil Temperature and Water Content in the Field and Greenhouse Studies). Therefore, the consistent temperature and moisture supplied during the greenhouse incubation study resulted in faster polymer coating degradation. Further details of the difference between the soil temperature and moisture content between field and greenhouse incubation study is discussed in Appendix B: Soil Temperature and Water Content in the Field and Greenhouse Studies.

Water retention is affected by the soil pore structure and soil composition, which can increase the degradation rate of polymer coatings. Soil at BRDC (loamy-sand) contains higher sand content than STC (loam), and STC contains higher clay content than BRDC. Since BRDC has a higher sand content than STC it will typically retain less water. Therefore, it was expected that the degradation rate of STC would be greater than the BRDC soil. There was no statistical difference in total N concentration between BRDC ($0.303 \pm 0.018\%$) and STC ($0.284 \pm 0.007\%$). However, there was a statistical difference in organic C content between BRDC ($3.211 \pm 0.202\%$) and STC ($3.566 \pm 0.097\%$). Further soil organic carbon and nitrogen details can be found in Appendix E: Soil Organic Carbon and Nitrogen. It is possible that higher soil organic carbon could increase polymer degradation rate due to higher water retention. Soil organic matter increases soil porosity, which improves water retention capacity (De Jonge, 1996; Kučerík et al., 2018. Increased water retention results in more water in proximity to the polymer coating. Polymers can be abiotically biodegraded by ultraviolet radiation, high temperatures, air, water, and applied forces (Pan et al., 2023). Therefore, higher organic C content could increase polymer

degradation rates. However, organic matter content could affect polymer degradation due to pollutant sorption caused by the movement of the water within the soil. Movement of water within the soil is influenced by the soil macropores space, and organic matter content (Rillig et al., 2017). The movement of water within the soil could direct water away from the polymer resulting in insufficient water for microbial activity. Polymer degraded by microbial activity can be constrained by insufficient water (Y. Cui et al., 2020). Alternatively, the movement of water could contain organic micropollutants. MP sorption is significantly influenced by the physiochemical characteristics of the soil, particularly by the amount of organic carbon present (Hüffer et al., 2018). The interaction between MPs and organic micropollutants may modify biodegradation (Poursat et al., 2024). Therefore, further research of the effect of organic matter content on MP degradation is needed.

Seasonal variation in temperature within the agricultural region of Manitoba may influence the degradation of the polymer coating. Brandon Manitoba has a mean temperature of approximately 2°C and winter temperatures normally below zero (Environment Canada, 2024). Microbial activity is affected by temperature and thermal fluctuations. A significant increase was observed in Delanau et al., (2024) where microbial activity (measured as CO₂ production) for soil incubated at 20°C compared to 10°C, and microbial activity increased with incubation temperature. Additionally, the productivity of microbial populations is dependent on ranges of temperatures and nutrient quantities within inland waters ecosystems (Cramer, 2008). Therefore, polymer coatings may take longer to degrade due to the fluctuating and reduced temperatures in both soil and inland water ecosystems. This can explain why an observed slower degradation in the field study was observed compared to the greenhouse incubation study. Finally, the rate of degradation observed within the greenhouse incubation and field study was compared to the

four-year international standard of biodegradability. In this thesis, the linear regression full degradation was extrapolated to 312 days, the spherical shell full degradation to 588 days, and the negative exponential full degradation was extrapolated to 831 days for the greenhouse study. The extrapolated degradation of polymer coatings in the incubation study met the international biodegradability standard. However, for the field study, the linear regression full degradation was extrapolated to 8986 days, the spherical shell full degradation to 24524 days, and the negative exponential full degradation to 34232 days. Therefore, the extrapolated degradation of polymer coatings in the field study did not meet the international biodegradability standard.

The AIC values indicated that the three degradation models were equivalent (Table 4). However, the full degradation of the polymer coatings based on the three models are quite different. The negative exponential would reach a horizontal asymptote rather than intersect zero mass. Therefore, calculating whether the slope of the negative exponential is statistically different than zero can be used to determine whether the number of aerobic biodegradation reactions occurring is significant. This would indicate that the degradation of the polymer coating has slowed resulting in a longer degradation process beyond what was observable in both the greenhouse and field studies. The linear regression degradation model has limitations in assessing the full degradation of the polymer coatings. The linear regression models the degradation rate with a constant exposed surface area (Chamas et al., 2020). The linear regression model would describe the faster possible degradation rate based on maximum surface area. However, the linear regression model assumes that the degradation rate is constant over time. Therefore, the linear regression model would not be able to account for the spherical shell decrease in radii and decrease in degradation rate of the polymer coating. Although knowing the fastest possible degradation rate can be useful, choosing the correct model can substantially affect the assessment

of biodegradability and time until full degradation of the polymer coatings. Therefore, creating a spherical shell model was the most appropriate model for demonstrating polymer coating capsules degradation.

4.1.1 Slow Degradation Rate Implications

The slower degradation observed within the field study may result in the accumulation of polymer coatings within the agroecosystem. The time required for polymer coatings to degrade fully using the models projected exceeds the history of polymer coating development (1998-2005 and 2005-2024). The buildup of plastics in the soil has the potential to impede their degradation rates (Tian et al., 2022). Additionally, increasing concentration of plastics negatively affects nutrient cycling (Graf et al., 2023). It was demonstrated by Graf et al., (2023) that effects of microplastics on soil and plant health is negligible in the short-term (<10 years of plastic application), however, beyond this has a clear negative effect on plant growth and microbial biomass. Therefore, the degradation of the polymer coatings within this thesis may not fully realize negative effects on plant growth and microbial biomass. However, slow degradation not only affects growth. Plastics are capable of adsorbing other merging contaminants leading to the removal of contaminants adsorbed on their surface (Di Natale et al., 2022). Secondly, plastics of various sizes can absorb organic and inorganic contaminants and their ability to transfer upon ingestion, which may affect the long-term health of humans (Fred-Ahmadu et al., 2020). Therefore, further research is needed to look at how polymer coating degradation affects biomass and long-term human health.

To assess how polymer coating degradation may affect biomass and human health, using a degradation model that utilizes the physical characteristics of the spherical shell was necessary. When degradation occurs principally at exposed surfaces, the degradation rate is proportional to

the exposed surface area (Chamas et al., 2020). Therefore, polymer coating degradation is a factor of the spherical shell outer surface area. Larger spherical shells (larger radius) will degrade faster than smaller spherical shells (smaller radius) because of surface area exposure decreasing with radii. This would describe the compression of higher mean polymer coating mass over time. Additionally, the specific surface degradation rate in Table 1 represents the mean value observed throughout the duration of polymer coating degradation. The specific surface degradation rate describes the loss of polymer as a function of the polymer coating exposed surface area. However, if a polymer coating has been cleaved or fragmented, it would undergo faster degradation. Damage to the polymer coating of ESN occurred during fertilizer mixing and loading, and greater capsule damage was observed at higher airflow speeds (Heard et al., 2010). Faster degradation would occur as more surface area is exposed, being the sum of the outer and inner surface areas. Spontaneous fragmentation resulted in a discontinuity where the surface area and degradation rate abruptly increased (Chamas et al., 2020). Therefore, degradation would occur on both the inner and outer surfaces of the fragment. Alternatively, the initial degradation rate observed in both studies may be higher due to the exposed surface area available. The degradation of polymer is dependent on its surface area. A spherical shell with surface area ($4\pi r^2$), would have a degradation curve related to its radius. Since a reduction in surface area occurs as the spherical shell becomes smaller, the rate of degradation is reduced. Therefore, as the spherical shell exposed surface area is reduced, the larger spherical shells will ‘catch up’ in degradation to smaller polymer coatings. This could be observed as the reduction of standard deviations over time observed within Figure 3-2.

Utilizing mass percentage has been widely accepted for decomposition of plant litter. However, using mass percentage as a metric for characterizing polymer degradation could offer versatility

and robustness across various types of polymer research. A summary of degradation efficiency was created by Lin et al. (2022) that describes a wide range of degradation across plastics and microorganisms in soil. This demonstrates that polymers could exhibit varying degradation rates and behaviors, necessitating a uniform method to characterize degradation across different forms and structures of polymers. Therefore, mass percentage could provide a standardized approach to describe effectively the degradation relationship between polymer blends and batches. Mass percentage could account for differences in polymer coating batches, which includes variations in thickness and size. Hence, mass percentage could enable accurate degradation rate comparisons across different batches for future studies.

The implication of slower degradation extends beyond local environmental impacts to potentially impact downstream. Regardless of polymer coating concentration, the persistence of polymer coatings in the environment could result in transport from agroecosystems via surface runoff over time. The volume of surface runoff in the spring of 2024 was normal and within the expected yearly range. Therefore, it would be likely that polymer coatings in future years may also be exported in surface runoff. However, surface runoff is not the only potential export of polymer coatings once they fragment. The downward movement of MPs and NPs through soil may reach groundwater for transport (Xu et al., 2023). Therefore, further research of polymer coatings at lower depths is needed to both confirm the presence of polymer coatings below 10 cm and to observe if fragmented capsules are moving towards groundwater. Additional research is required to address polymer coating mobility in extreme cases of surface runoff.

4.1.2 Limitations of Polymer Coating Degradation

The significance of these findings are not without limitations due to data compactness without full degradation. BRDC Field 2 was excluded from the data set due to repetitive fertilizer

application and reduced recovery rate. If polymer coatings were removed with mass disparities, then the degradation rate analysis would be affected. Therefore, soil samples at depths greater than 10 cm at BRDC and STC are needed to confirm whether a shift in polymer coating concentration occurred. Removal of one field site grouped data points surrounding two points in time. The limitation of grouped data was a result of limited access to field sites with specific PCU application history. Additionally, field data was collected before seeding in the spring and after harvest in the fall to minimize crop disturbance. Therefore, limiting the availability of data points and highlighting that polymer degradation needs to be monitored longitudinally over time.

The largest limiting factor for determining the full degradation of polymer coatings was the duration of the studies. Time was the largest source of error since the later stages of polymer coating degradation are not measured. Polymer coating degradation was extrapolated beyond the data, which creates uncertainty in the time that the polymer coatings need to fully degrade. The degradation of the polymer coatings observed meets the four-year international biodegradability standard within the greenhouse incubation study. However, the full degradation of polymer coatings were not observed, and the incubation study should be evaluated to full degradation.

The field study demonstrated that long-term studies are needed to evaluate their full degradation and degradation rates over time in the natural environment. Another limiting factor was due to the constraints surrounding measurements. A minimum amount of polymer mass was needed to measure the subtle differences in mass over time. The level of noise was influenced by the physical properties of the polymer coatings such as thickness and size. This was addressed by using a standardized mass requirement range across 20 ESN capsules from a single batch.

PCU fertilizer applications are used across North America yet there is limited information for the degradation of polymer coatings. Identification of the main soil and climate drivers are needed to

create an interaction relationship for complex polymer degradation. For example, determining the degradation across different climate conditions are needed to identify whether the degradation of polymer coatings is consistent between climates. Expanding to different soil types is needed to determine whether there is a significant difference due to water content within the soil. Using extremes on the soil textural triangle would determine whether a significant difference in degradation occurs between the soil types due to different water contents. This could be done within an incubation study or field study to confirm whether this occurs. Information presented by Nutrien suggests that the polymer coating fully degrades within soil within two years. This information suggests that the soil temperature is a driving factor for degradation rates. However, further studies are required to verify the significance of each parameter to polymer degradation.

4.2 Tracking Polymer Coatings Redistribution and Loss

The distribution of polymer coatings was compared over time to assess whether redistribution occurred. It was observed that the polymer coatings underwent some lateral movement. Within the lateral and vertical redistribution of polymer coatings, various methods for redistribution were observed and noted such as wind, tillage, and water erosion events. For example, the redistribution of polymer coatings was supported by observed airborne polymer coatings.

Airborne polymer coatings collected in Modified Wilson and Cooke samplers were recorded at BRDC Field 1. Observance of polymer coatings in elevated canisters confirms that wind erosion is a factor for polymer coating redistribution. The observance of MPs (< 5-mm) to become airborne occurred between wind speeds of $7\text{--}12 \text{ m s}^{-1}$ (Rezaei et al., 2022). Similarly, wind speeds above 43 km h^{-1} are able to move MPs with sizes larger than 1-mm. Therefore, polymer coatings with 2-mm diameter could be expected to become airborne given wind speeds

surpassing 43 km h⁻¹. Additionally, MPs can be similar to physical tracers that move throughout the landscape. Dyed limestone chips (tracers) were implemented to measure the relationship between tillage translocation and slope gradient which confirmed that slope gradient was the predominant factor driving tillage translocation (Li et al., 2007). Additionally, heavier 11-mm steel hexagonal nuts had been observed to move towards downslope positions (Lindstrom et al., 1990). Redistribution of polymer coatings were measured based on concentration and their mean mass to conclude whether lateral movement occurred. Polymer coating concentration increased with descending elevation (Table 8, Figure 3-6). The mean mass was not statistically significant between field slope positions. Therefore, the observed redistribution of polymer coatings towards downslope positions was expected.

The loss of polymer coatings was monitored by surface runoff to determine whether polymer coatings were exported from the field. Between 0.2-0.4% of MPs were mobilized by water runoff in a singular year from agricultural plots within central Spain with a semi-arid climate, 430-mm of yearly rainfall, and a slope gradient of 5% (Schell et al., 2022). At STC with a slope gradient between 3-10%, 550-mm of annual precipitation of which 20-25% being snowfall, between 15-20% of precipitation volume leaves the field as surface runoff. It could be expected that a percentage of microplastics could be mobilized by snowmelt surface runoff. This is supported by evidence of exposed polymer coatings on the soil surface by measurement of airborne samples. Low-density polymer coatings can be susceptible to redistribution and export across the soil surface. Therefore, polymer coatings on the soil surface could be affected by surface runoff events. This was confirmed by measurement of polymer coatings exported in surface runoff (Table 9) and observed within the riparian buffer zone (Table 8).

4.2.1 Redistribution and Loss Implications

Wetlands often serve as transitional zones between the terrestrial and aquatic ecosystems.

Wetlands are characterized by saturated soils, occurring in geomorphologically mature terrains of gentle slopes and shallow depressional areas. The prairie pothole region within Manitoba contains thousands of shallow wetlands classified as potholes created by glacial activity. The proximity of agricultural fields to wetland areas in Manitoba's prairie pothole region highlights the potential risk of polymer coating transport to these habitats. Therefore, the biota within these habitats may be affected over time. Within 3.2.2, polymer coatings were measured in surface runoff, which could affect neighboring ecosystems. For example, woodland soil and freshwater sediments were potential destinations of MP migration across an MP abundant watershed (Qiu et al., 2023). Therefore, polymer coatings within surface runoff could be transported to pothole wetland areas or down the water channel.

One effective measure for mitigating the transport of nutrients, particles, and potentially polymer coatings are riparian buffer zones. Riparian vegetation acts as a trap for plastics, and plastics that had floating properties were entrapped after flood events (Cesarini & Scalici, 2022). Therefore, the riparian buffer zone located along the edge of the field may act as a filter for polymer coatings under a low steady flow. However, for buoyant polymer coatings the effectiveness of the riparian buffer is reduced for water levels surpassing the riparian buffer. Up to 70% of the annual runoff at the STC watershed occurs during the snowmelt period in Manitoba (Liu et al., 2014). Since a large percentage of water volume leaves during snowmelt surface runoff events it can be expected that the riparian buffer could be less effective. Additionally, buoyant polymer coatings collected from the runoff weirs were absent from attached soil. Polymer coatings collected from the runoff weirs had a mean polymer capsule mass of 1.124 ± 0.3 mg that are

equivalent to the mean mass within the field soil samples (Table 7). Therefore, if any polymer coatings become exposed to the soil surface, then they could be redistributed by surface runoff. Polymer coatings observed in the riparian buffer zone could be transported in subsequent surface runoff events. The effectiveness of the riparian buffer for capturing polymer coatings is supported by the absence of polymer coatings in the 5-10 cm layer (Table 8). Therefore, vertical movement in this range was negligible where thick vegetative roots impeded vertical movement of polymer coatings.

4.2.2 Limitations of Redistribution and Loss

The riparian buffer zone that collected polymer coatings was much smaller than the area that could be sampled in the cropland field at STC. A two-point transect was conducted at each weir to measure concentration and mean mass. The ANOVA resulted in no statistical difference of a polymers mean mass between the riparian and field slope positions. Additional data points were needed to conclude that the mean mass of the polymer coatings removed were significantly lower than those in the field. However, there are consequences with the removal of soil from the riparian buffer zone during sampling campaigns. The regrowth of excavated sections of the riparian buffer zone would be hindered by the removal of soil. The dampened regrowth could affect the ability to capture polymer coatings in surface runoff in subsequent precipitation events. Cesarini & Scalici (2022) found that the type of vegetation affected the retention of plastics. Therefore, the effectiveness of the riparian buffer is dependent on the density, quality, and surface area of the vegetation. The number of polymer coatings captured within four riparian buffer zone measurements was equivalent to the extrapolated number of polymer coatings exported by surface runoff (Table 8; Table 9). Therefore, the number of destructive riparian buffer zone excavations must be considered and minimized if possible.

The quantity of polymer coating exported during surface runoff was affected by blockage events. The main blockage event elevated the water level at the weir (Equation 2-10). The extrapolation of polymer coatings through the weir systems was calculated based on the depth of the transducer. A correction was applied to the depth of the transducer during this period. However, the backup of water caused by blockage allowed for elevated water levels surpassing the riparian buffer. Buoyant polymer coatings under stagnant or laminar water conditions were expected to accumulate on the water's surface. This is supported by the observance of MPs accumulation along the water's surface during laminar water flow and standing water (Eerkes-Medrano et al., 2015). Therefore, the riparian buffer was less effective at capturing polymer coatings during this surface runoff event. The reduced effectiveness of the riparian buffer is apparent as the buoyant polymer coatings are suspended above the vegetation. Secondly, the 1-mm screening needed to capture polymer coating collected crop residue, ice and clumps of snow over time (Figure 4-1). Polymer coatings may catch and hold onto the snow or ice clumps during these periods and reduce the exported number observed. Therefore, the amount of polymer coating exported could be higher than what was observed.



Figure 4-1: Backup of ice on the weir filter.

The redistribution and export of polymer coatings could affect degradation measurements. Degradation as a function of elevation position was conducted at STC due to the singular fertilizer application. Polymer coating concentration increased with descending elevation (Table 8). However, measuring depths beyond 10 cm is needed to confirm that quantification in 0-10 cm was sufficient to determine redistribution quantities. The mean mass of riparian position polymer coatings within Table 8 were less than that of field positions. This could be described by an increased degradation of polymer coatings affected by higher moisture content. A moisture content gradient may be observed across the landscape as rainwater or snowmelt moves downslope (Wang et al., 2021). Therefore, an increased moisture content within the lower elevation positions may have faster polymer coating degradation as a result. This could affect evaluating the mean mass of polymer coatings over time.

4.3 Future Steps

There are several questions that are left to be further analyzed following the results presented within this thesis. There is a need to better understand the impacts of soil characteristics on polymer coating degradation. This would include further quantification of the impact of soil moisture and temperature on polymer coating degradation rates. Additionally, it is required to get data over a long period. Data over a long period could be stitched together with fields containing different application timings pending that their conditions are not statistically significant. However, the field sites would need to be a single PCU fertilizer application. Additional data should include standardization of sampling methodologies to maintain comparability between studies.

Data demonstrating the mobility of polymer coatings via surface runoff indicates that a watershed scale study could be developed. This would include developing a framework to assess

the risk of loss and redistribution from the field. The watershed scale study would include monitoring the movement of polymer coatings in the environment along water channels and determining the distance, identifying the degradation, byproducts, and effects of the polymer coating in different water contents and habitats.

5 Conclusion

5.1 Polymer Coating Degradation

It was found that the two Manitoba soil types had statistically equivalent degradation rates within the field and incubation studies. However, the difference in degradation rates observed between the field and greenhouse studies was statistically significant. Thirdly, the degradation rates within the incubation study suggests that the polymer coating is fully degraded within the international biodegradability standard. However, the degradation rates observed within the field study suggests that the polymer coating does not fully degrade within the international biodegradability standard.

This information is significant since the environmental conditions where the polymer coatings are applied impact the degradation rate of the polymer coating. Effects of ESN's polymer coating could be comparable to other plastic material in Manitoba soils since the full degradation was estimated beyond an international biodegradability standard. Additionally, the degradation of MPs can affect soil pH, P, and K concentrations, hinder growth of vegetation and reduce soil organisms' survival rate and reproduction. Therefore, the degradation products of MPs can have a lasting effect on soil health until full degradation. Furthermore, the spherical shell model estimated the full degradation of the polymer coating in 67 years within the field study. The difference in degradation between the spherical shell model was 42 times slower between the incubation and field studies. Therefore, the difference in degradation rate between the two studies demonstrates how significantly environmental conditions affect the degradation rate of the polymer coatings. Overall, the time required for full degradation of the polymer coatings is multi-generational and only prolonged with further fertilizer applications.

5.2 Tracking Polymer Coatings Mobility

Within monitoring the mobility of polymer coatings, several factors were measured to assess the lateral, vertical redistribution of polymer coatings and loss to the environment. The first source of evidence supporting lateral movement occurred from a reduction of polymer coatings mean mass across descending elevations in the 0-5 cm topsoil layer. The second factor is an increase in polymer coating concentration across descending elevations. Thirdly, a net reduction in polymer coating concentration occurred regardless of taking additional soil in the 5-10 cm topsoil layer in the last sampling period. Vertical movement of polymer coatings was observed surrounding tillage events where polymer was displaced to 5-10 cm at STC. Additionally, a net loss of polymer coatings to the environment was supported by two main factors. Firstly, polymer coatings were observed within the riparian buffer zone. Secondly, exportation of polymer coatings was observed in surface runoff at both weirs. Therefore, both the lateral movement and observance in surface runoff provide sufficient evidence that polymer coatings are being redistributed within and from the agroecosystem.

The significance of observing polymer coatings redistribution is increasingly more important because of the slow degradation of the polymer coatings. Documentation within the introduction section on movement of plastics may also apply to polymer coatings. Therefore, redistribution of polymer coatings may occur from wind, tillage, and water erosion. Polymer coatings with lower mass were observed within the 0-5 cm layer in the lower sections suggesting that polymers with lower mean mass may be more likely affected by redistribution. Furthermore, polymer coatings mean mass decreases over time but may last between 24 to 94 years within the agroecosystem. Polymer coatings may be more likely to be redistributed over time as further reduction in polymer mass occurs. Polymer coating within the STC field site may redistribute over the

entirety of the 67-year degradation suggesting that the agroecosystem may act as a temporary sink for polymer coatings. The recovered polymer coatings mean mass from the surface runoff data supports that any exposed polymer may be transported since polymer coatings in the surface runoff were equivalent to the mean mass across the entire field. All of the polymer coatings lost to the environment entails accumulation within inland water systems and other ecosystems.

Therefore, the effects of MPs and NPs affecting cellular development and their ability to act as a vector of pollutants may influence aquatic inhabitants. Additionally, the polymer coatings within the soil may fragment and reach the groundwater table. Therefore, mobility of polymer-coated fertilizers may occur throughout their entire degradation.

Overall, our understanding of polymer-coated degradation is limited. Therefore, my research should serve as a launching point for further research. Further research surrounding polymer coatings cannot be simply overlooked or neglected until consequences are evident. Negative effects of polymer coating may persist for up to 67 years using the spherical shell model and effects may be prolonged by subsequent PCU fertilizer applications. Therefore, further research should be conducted to bridge the understanding of the full degradation period, mobility capability of polymer coatings, their effects on water quality, and impacts on human health.

6 References

- AAFC. (2008). *Watershed Evaluation of Beneficial Management Practices (WEBs): South Tobacco Creek/Steppler, Manitoba.*
- Adams, C., Frantz, J., & Bugbee, B. (2013). Macro- and micronutrient-release characteristics of three polymer-coated fertilizers: Theory and measurements. *Journal of Plant Nutrition and Soil Science*, 176(1), 76–88. <https://doi.org/10.1002/jpln.201200156>
- Agrium. (2005). *Material Safety Data Sheet NFPA Classification* PROTECTIVE CLOTHING
PRODUCT NAME/ TRADE NAME SYNONYM CHEMICAL NAME CHEMICAL
FORMULA CHEMICAL FAMILY MATERIAL USES MSDS NUMBER: ESN Polymer
Coated Urea 44-0-0.
- Aljaibachi, R., & Callaghan, A. (2018). Impact of polystyrene microplastics on Daphnia magna mortality and reproduction in relation to food availability. *PeerJ*, 2018(4).
<https://doi.org/10.7717/PEERJ.4601>
- Asgedom, H., Tenuta, M., Flaten, D. N., Gao, X., & Kebreab, E. (2014). Nitrous oxide emissions from a clay soil receiving granular urea formulations and dairy manure. *Agronomy Journal*, 106(2), 732–744. <https://doi.org/10.2134/agronj2013.0096>
- Avellan, A., Yun, J., Zhang, Y., Spielman-Sun, E., Unrine, J. M., Thieme, J., Li, J., Lombi, E., Bland, G., & Lowry, G. V. (2019). Nanoparticle Size and Coating Chemistry Control Foliar Uptake Pathways, Translocation, and Leaf-to-Rhizosphere Transport in Wheat. *ACS Nano*, 13(5), 5291–5305. <https://doi.org/10.1021/ACSNANO.8B09781>

Bakir, A., Rowland, S. J., & Thompson, R. C. (2014). Transport of persistent organic pollutants by microplastics in estuarine conditions. *Estuarine, Coastal and Shelf Science*, 140, 14–21.
<https://doi.org/10.1016/j.ecss.2014.01.004>

Barnes, D. K. A., Galgani, F., Thompson, R. C., & Barlaz, M. (2009). Accumulation and fragmentation of plastic debris in global environments. *Philosophical Transactions of the Royal Society B: Biological Sciences*, 364(1526), 1985–1998.
<https://doi.org/10.1098/RSTB.2008.0205>

Bátori, V., Åkesson, D., Zamani, A., Taherzadeh, M. J., & Sárvári Horváth, I. (2018). Anaerobic degradation of bioplastics: A review. *Waste Management*, 80, 406–413.
<https://doi.org/10.1016/J.WASMAN.2018.09.040>

Belal, E. B., & Farid, M. A. (2016). Production of Poly- β -hydroxybutyric acid (PHB) by *Bacillus cereus*. *International Journal of Current Microbiology and Applied Sciences*, 5(7), 442–460.
<https://doi.org/10.20546/ijcmas.2016.507.048>

Beres, B. L., McKenzie, R. H., Dowbenko, R. E., Badea, C. V., & Spaner, D. M. (2012). Does handling physically alter the coating integrity of ESN urea fertilizer? *Agronomy Journal*, 104(4), 1149–1159. <https://doi.org/10.2134/agronj2012.0044>

Besseling, E., Quik, J. T. K., Sun, M., & Koelmans, A. A. (2017). Fate of nano- and microplastic in freshwater systems: A modeling study. *Environmental Pollution*, 220, 540–548.
<https://doi.org/10.1016/j.envpol.2016.10.001>

Blarer, P., & Burkhardt-Holm, P. (2016). Microplastics affect assimilation efficiency in the freshwater amphipod *Gammarus fossarum*. *Environmental Science and Pollution Research*, 23(23), 23522–23532. <https://doi.org/10.1007/S11356-016-7584-2>

Bläsing, M., & Amelung, W. (2018). Plastics in soil: Analytical methods and possible sources. *Science of The Total Environment*, 612, 422–435.

<https://doi.org/10.1016/J.SCITOTENV.2017.08.086>

Briassoulis, D., & Mistriotis, A. (2018). Key parameters in testing biodegradation of bio-based materials in soil. *Chemosphere*, 207, 18–26.

<https://doi.org/10.1016/j.chemosphere.2018.05.024>

Brodhagen, M., Peyron, M., Miles, C., & Inglis, D. A. (2015). Biodegradable plastic agricultural mulches and key features of microbial degradation. *Applied Microbiology and Biotechnology*, 99(3), 1039–1056. <https://doi.org/10.1007/S00253-014-6267-5>

By, S., & Roste, J. (2005). *Development and Evaluation of a Canadian Prairie Nutrient Transport Model*.

Cahill, S., Osmond, D., & Israel, D. (2010). Nitrogen release from coated urea fertilizers in different soils. *Communications in Soil Science and Plant Analysis*, 41(10), 1245–1256. <https://doi.org/10.1080/00103621003721437>

Campanale, C., Galafassi, S., Di Pippo, F., Pojar, I., Massarelli, C., & Uricchio, V. F. (2024). A critical review of biodegradable plastic mulch films in agriculture: Definitions, scientific background and potential impacts. *TrAC Trends in Analytical Chemistry*, 170, 117391. <https://doi.org/10.1016/J.TRAC.2023.117391>

Cesarini, G., & Scalici, M. (2022). Riparian vegetation as a trap for plastic litter. *Environmental Pollution*, 292, 118410. <https://doi.org/10.1016/J.ENVPOL.2021.118410>

Chae, Y., & An, Y. J. (2018). Current research trends on plastic pollution and ecological impacts on the soil ecosystem: A review. In *Environmental Pollution* (Vol. 240, pp. 387–395). Elsevier Ltd. <https://doi.org/10.1016/j.envpol.2018.05.008>

Chamas, A., Moon, H., Zheng, J., Qiu, Y., Tabassum, T., Jang, J. H., Abu-Omar, M., Scott, S. L., & Suh, S. (2020). Degradation Rates of Plastics in the Environment. *ACS Sustainable Chemistry and Engineering*, 8(9), 3494–3511.
<https://doi.org/10.1021/acssuschemeng.9b06635>

Costa, R., Saraiva, A., Carvalho, L., & Duarte, E. (2014). The use of biodegradable mulch films on strawberry crop in Portugal. *Scientia Horticulturae*, 173, 65–70.
<https://doi.org/10.1016/J.SCIENTA.2014.04.020>

Cramer, W. (2008). Global Change Impacts on the Biosphere. *Encyclopedia of Ecology, Five-Volume Set*, 1736–1741. <https://doi.org/10.1016/B978-008045405-4.00736-9>

Cui, J., Bai, R., Ding, W., Liu, Q., Liu, Q., He, W., Yan, C., & Li, Z. (2024). Potential agricultural contamination and environmental risk of phthalate acid esters arrived from plastic film mulching. *Journal of Environmental Chemical Engineering*, 12(1), 111785.
<https://doi.org/10.1016/J.JECE.2023.111785>

Cui, Y., Wang, X., Zhang, X., Ju, W., Duan, C., Guo, X., Wang, Y., & Fang, L. (2020). Soil moisture mediates microbial carbon and phosphorus metabolism during vegetation succession in a semiarid region. *Soil Biology and Biochemistry*, 147, 107814.
<https://doi.org/10.1016/J.SOILBIO.2020.107814>

Datta, M. S., Sliwerska, E., Gore, J., Polz, M. F., & Cordero, O. X. (2016). Microbial interactions lead to rapid micro-scale successions on model marine particles. *Nature Communications*, 7. <https://doi.org/10.1038/ncomms11965>

De Jonge, M.-H. (1996). *Adsorption of CO₂ and N₂ on Soil Organic Matter: Nature of Porosity, Surface Area, and Diffusion Mechanisms*. <https://pubs.acs.org/sharingguidelines>

Decagon Devices. (2010). *5TM Water Content and Temperature Sensors Operator's Manual*. www.decagon.com

Delanau, C., Aspray, T., Pawlett, M., & Coulon, F. (2024). Investigating the influence of sulphur amendment and temperature on microbial activity in bioremediation of diesel-contaminated soil. *Helijon*, 10(9), e30235. <https://doi.org/10.1016/J.HELJON.2024.E30235>

Deng, Y., Zhang, Y., Lemos, B., & Ren, H. (2017). Tissue accumulation of microplastics in mice and biomarker responses suggest widespread health risks of exposure. *Scientific Reports*, 7. <https://doi.org/10.1038/srep46687>

Di Natale, M. V., Carroccio, S. C., Dattilo, S., Cocca, M., Nicosia, A., Torri, M., Bennici, C. D., Musco, M., Masullo, T., Russo, S., Mazzola, A., & Cuttitta, A. (2022). Polymer aging affects the bioavailability of microplastics-associated contaminants in sea urchin embryos. *Chemosphere*, 309, 136720. <https://doi.org/10.1016/J.CHEMOSPHERE.2022.136720>

Dong, X., Zhu, L., He, Y., Li, C., & Li, D. (2023). Salinity significantly reduces plastic-degrading bacteria from rivers to oceans. *Journal of Hazardous Materials*, 451, 131125. <https://doi.org/10.1016/J.JHAZMAT.2023.131125>

Dong, Y., Gao, M., Qiu, W., & Song, Z. (2021). Uptake of microplastics by carrots in presence of As (III): Combined toxic effects. *Journal of Hazardous Materials*, 411.

<https://doi.org/10.1016/j.jhazmat.2021.125055>

Du, Y., Guo, S., Wang, R., Song, X., & Ju, X. (2023). Soil pore structure mediates the effects of soil oxygen on the dynamics of greenhouse gases during wetting–drying phases. *Science of The Total Environment*, 895, 165192. <https://doi.org/10.1016/J.SCITOTENV.2023.165192>

Eerkes-Medrano, D., Thompson, R. C., & Aldridge, D. C. (2015). Microplastics in freshwater systems: A review of the emerging threats, identification of knowledge gaps and prioritisation of research needs. *Water Research*, 75, 63–82.

<https://doi.org/10.1016/J.WATRES.2015.02.012>

Eltemsah, Y. S., & Bøhn, T. (2019). Acute and chronic effects of polystyrene microplastics on juvenile and adult *Daphnia magna*. *Environmental Pollution*, 254.

<https://doi.org/10.1016/j.envpol.2019.07.087>

Emadian, S. M., Onay, T. T., & Demirel, B. (2017). Biodegradation of bioplastics in natural environments. In *Waste Management* (Vol. 59, pp. 526–536). Elsevier Ltd.

<https://doi.org/10.1016/j.wasman.2016.10.006>

Fairbairn, L., Rezanezhad, F., Gharasoo, M., Parsons, C. T., Macrae, M. L., Slowinski, S., & Van Cappellen, P. (2023). Relationship between soil CO₂ fluxes and soil moisture: Anaerobic sources explain fluxes at high water content. *Geoderma*, 434, 116493.

<https://doi.org/10.1016/J.GEODERMA.2023.116493>

Fitzmaurice, J., E. St. Jacques, A. Waddell, & R.G. Eilers. (1999). *Soils of the Brandon Research Centre*. 1–65.

Folino, A., Karageorgiou, A., Calabrò, P. S., & Komilis, D. (2020). Biodegradation of wasted bioplastics in natural and industrial environments: A review. In *Sustainability (Switzerland)* (Vol. 12, Issue 15). MDPI. <https://doi.org/10.3390/su12156030>

Folino, A., Pangallo, D., & Calabrò, P. S. (2023). Assessing bioplastics biodegradability by standard and research methods: Current trends and open issues. *Journal of Environmental Chemical Engineering*, 11(2), 109424. <https://doi.org/10.1016/J.JECE.2023.109424>

Fred-Ahmadu, O. H., Bhagwat, G., Oluyoye, I., Benson, N. U., Ayejuyo, O. O., & Palanisami, T. (2020). Interaction of chemical contaminants with microplastics: Principles and perspectives. *Science of The Total Environment*, 706, 135978.
<https://doi.org/10.1016/J.SCITOTENV.2019.135978>

Ge, J., Li, H., Liu, P., Zhang, Z., Ouyang, Z., & Guo, X. (2021). Review of the toxic effect of microplastics on terrestrial and aquatic plants. *Science of The Total Environment*, 791, 148333. <https://doi.org/10.1016/J.SCITOTENV.2021.148333>

Gómez, E. F., & Michel, F. C. (2013). Biodegradability of conventional and bio-based plastics and natural fiber composites during composting, anaerobic digestion and long-term soil incubation. *Polymer Degradation and Stability*, 98(12), 2583–2591.
<https://doi.org/10.1016/J.POLYMDEGRADSTAB.2013.09.018>

González-Pleiter, M., Tamayo-Belda, M., Pulido-Reyes, G., Amariei, G., Leganés, F., Rosal, R., & Fernández-Piñas, F. (2019). Secondary nanoplastics released from a biodegradable microplastic severely impact freshwater environments. *Environmental Science: Nano*, 6(5), 1382–1392. <https://doi.org/10.1039/C8EN01427B>

Goss, H., Jaskiel, J., & Rotjan, R. (2018). Thalassia testudinum as a potential vector for incorporating microplastics into benthic marine food webs. *Marine Pollution Bulletin*, 135, 1085–1089. <https://doi.org/10.1016/J.MARPOLBUL.2018.08.024>

Graf, M., Greenfield, L. M., Reay, M. K., Bargiela, R., Williams, G. B., Onyije, C., Lloyd, C. E. M., Bull, I. D., Evershed, R. P., Golyshin, P. N., Chadwick, D. R., & Jones, D. L. (2023). Increasing concentration of pure micro- and macro-LDPE and PP plastic negatively affect crop biomass, nutrient cycling, and microbial biomass. *Journal of Hazardous Materials*, 458, 131932. <https://doi.org/10.1016/J.JHAZMAT.2023.131932>

Green, D. S. (2016). Effects of microplastics on European flat oysters, *Ostrea edulis* and their associated benthic communities. *Environmental Pollution*, 216, 95–103.
<https://doi.org/10.1016/j.envpol.2016.05.043>

Griffin-LaHue, D., Ghimire, S., Yu, Y., Scheenstra, E. J., Miles, C. A., & Flury, M. (2022). In-field degradation of soil-biodegradable plastic mulch films in a Mediterranean climate. *Science of The Total Environment*, 806, 150238.
<https://doi.org/10.1016/J.SCITOTENV.2021.150238>

Gu, J. G., & Gu, J. D. (2005). Methods currently used in testing microbiological degradation and deterioration of a wide range of polymeric materials with various degree of degradability: A review. In *Journal of Polymers and the Environment* (Vol. 13, Issue 1, pp. 65–74). Kluwer Academic/Plenum Publishers. <https://doi.org/10.1007/s10924-004-1230-7>

Harrison, J. P., Boardman, C., O'Callaghan, K., Delort, A. M., & Song, J. (2018). Biodegradability standards for carrier bags and plastic films in aquatic environments: A

critical review. In *Royal Society Open Science* (Vol. 5, Issue 5). Royal Society Publishing.

<https://doi.org/10.1098/rsos.171792>

Heard, J., Ginter, K., & Cropcheck, K. R. (2010). *Field observations of ESN release rates and mechanical damage during application.*

Hope, J., Harker, B., & Townley-Smith, L. (2002). *Long Term Land Use Trends For Water Quality Protection.*

Horton, A. A., Svendsen, C., Williams, R. J., Spurgeon, D. J., & Lahive, E. (2017). Large microplastic particles in sediments of tributaries of the River Thames, UK – Abundance, sources and methods for effective quantification. *Marine Pollution Bulletin*, 114(1), 218–226. <https://doi.org/10.1016/j.marpolbul.2016.09.004>

Huang, T., Wu, Q., Yuan, Y., Zhang, X., Sun, R., Hao, R., Yang, X., Li, C., Qin, X., Song, F., Joseph, C. O., Wang, W., & Siddique, K. H. M. (2024). Effects of plastic film mulching on yield, water use efficiency, and nitrogen use efficiency of different crops in China: A meta-analysis. *Field Crops Research*, 312, 109407. <https://doi.org/10.1016/J.FCR.2024.109407>

Huerta Lwanga, E., Mendoza Vega, J., Ku Quej, V., Chi, J. de los A., Sanchez del Cid, L., Chi, C., Escalona Segura, G., Gertsen, H., Salánki, T., van der Ploeg, M., Koelmans, A. A., & Geissen, V. (2017). Field evidence for transfer of plastic debris along a terrestrial food chain. *Scientific Reports*, 7(1). <https://doi.org/10.1038/s41598-017-14588-2>

Koelmans, A. A., Mohamed Nor, N. H., Hermsen, E., Kooi, M., Mintenig, S. M., & De France, J. (2019). Microplastics in freshwaters and drinking water: Critical review and assessment of data quality. *Water Research*, 155, 410–422. <https://doi.org/10.1016/j.watres.2019.02.054>

Kučerík, J., Ondruch, P., Kunhi Mouvenchery, Y., & Schaumann, G. E. (2018). Formation of Water Molecule Bridges Governs Water Sorption Mechanisms in Soil Organic Matter. *Langmuir*, 34(40), 12174–12182. <https://doi.org/10.1021/acs.langmuir.8b02270>

Laskar, N., & Kumar, U. (2019). Plastics and microplastics: A threat to environment. *Environmental Technology & Innovation*, 14, 100352. <https://doi.org/10.1016/J.ETI.2019.100352>

Li, B., Huang, S., Wang, H., Liu, M., Xue, S., Tang, D., Cheng, W., Fan, T., & Yang, X. (2021). Effects of plastic particles on germination and growth of soybean (*Glycine max*): A pot experiment under field condition. *Environmental Pollution*, 272, 116418. <https://doi.org/10.1016/J.ENVPOL.2020.116418>

Li, M., Witt, T., Xie, F., Warren, F. J., Halley, P. J., & Gilbert, R. G. (2015). Biodegradation of starch films: The roles of molecular and crystalline structure. *Carbohydrate Polymers*, 122, 115–122. <https://doi.org/10.1016/J.CARBPOL.2015.01.011>

Li, S., Elliott, J. A., Tiessen ac, K. H., Yarotski, J., & Lobb, D. A. (2012). *The Effects of Multiple Beneficial Management Practices on Hydrology and Nutrient Losses in a Small Watershed in the*.

Li, S., Elliott, J. A., Tiessen, K. H. D., Yarotski, J., Lobb, D. A., & Flaten, D. N. (2011). The Effects of Multiple Beneficial Management Practices on Hydrology and Nutrient Losses in a Small Watershed in the Canadian Prairies. *Journal of Environmental Quality*, 40(5), 1627–1642. <https://doi.org/10.2134/jeq2011.0054>

Li, S., Lobb, D. A., & Lindstrom, M. J. (2007). Tillage translocation and tillage erosion in cereal-based production in Manitoba, Canada. *Soil and Tillage Research*, 94(1), 164–182.
<https://doi.org/10.1016/J.STILL.2006.07.019>

Li, W., Wang, S., Wufuer, R., Duo, J., & Pan, X. (2023). Distinct soil microplastic distributions under various farmland-use types around Urumqi, China. *Science of the Total Environment*, 857. <https://doi.org/10.1016/j.scitotenv.2022.159573>

Li, Y., Gao, X., Tenuta, M., Gui, D., Li, X., Xue, W., & Zeng, F. (2020). Enhanced efficiency nitrogen fertilizers were not effective in reducing N₂O emissions from a drip-irrigated cotton field in arid region of Northwestern China. *Science of The Total Environment*, 748, 141543. <https://doi.org/10.1016/J.SCITOTENV.2020.141543>

Lin, Z., Jin, T., Zou, T., Xu, L., Xi, B., Xu, D., He, J., Xiong, L., Tang, C., Peng, J., Zhou, Y., & Fei, J. (2022). Current progress on plastic/microplastic degradation: Fact influences and mechanism. *Environmental Pollution*, 304, 119159.
<https://doi.org/10.1016/J.ENVPOL.2022.119159>

Lindstrom, M. J., Nelson, W. W., Schumacher, T. E., & Lemme, G. D. (1990). Soil movement by tillage as affected by slope. *Soil and Tillage Research*, 17(3–4), 255–264.
[https://doi.org/10.1016/0167-1987\(90\)90040-K](https://doi.org/10.1016/0167-1987(90)90040-K)

Liu, K., Elliott, J. A., Lobb, D. A., Flaten, D. N., & Yarotski, J. (2014). Nutrient and Sediment Losses in Snowmelt Runoff from Perennial Forage and Annual Cropland in the Canadian Prairies. *Journal of Environmental Quality*, 43(5), 1644–1655.
<https://doi.org/10.2134/jeq2014.01.0040>

Lucas, N., Bienaime, C., Belloy, C., Queneudec, M., Silvestre, F., & Nava-Saucedo, J. E. (2008). Polymer biodegradation: Mechanisms and estimation techniques – A review. *Chemosphere*, 73(4), 429–442. <https://doi.org/10.1016/J.CHEMOSPHERE.2008.06.064>

Lung, I. K., & WanHong Y. (2014). *Examining the water quantity and quality effects of land management practices in a Canadian Prairie Subwatershed using a GIS-Based distributed model.*

Majaron, V. F., da Silva, M. G., Bortoletto-Santos, R., Klaic, R., Giroto, A., Guimarães, G. G. F., Polito, W. L., Farinas, C. S., & Ribeiro, C. (2020). Synergy between castor oil polyurethane/starch polymer coating and local acidification by *A. niger* for increasing the efficiency of nitrogen fertilization using urea granules. *Industrial Crops and Products*, 154, 112717. <https://doi.org/10.1016/J.INDCROP.2020.112717>

Massardier-Nageotte, V., Pestre, C., Cruard-Pradet, T., & Bayard, R. (2006). Aerobic and anaerobic biodegradability of polymer films and physico-chemical characterization. *Polymer Degradation and Stability*, 91(3), 620–627.

<https://doi.org/10.1016/J.POLYMDEGRADSTAB.2005.02.029>

Meng, F., Yang, X., Riksen, M., Xu, M., & Geissen, V. (2021). Response of common bean (*Phaseolus vulgaris* L.) growth to soil contaminated with microplastics. *Science of The Total Environment*, 755, 142516. <https://doi.org/10.1016/J.SCITOTENV.2020.142516>

Michalyna.W. (1994). *Geomorphology and Soil Quality of the Twin Watershed Area and Project.* Moshhood, T. D., Nawarir, G., Mahmud, F., Mohamad, F., Ahmad, M. H., & AbdulGhani, A. (2022). Biodegradable plastic applications towards sustainability: A recent innovations in

the green product. *Cleaner Engineering and Technology*, 6, 100404.

<https://doi.org/10.1016/J.CLET.2022.100404>

Mukherjee, C., Varghese, D., Krishna, J. S., Boominathan, T., Rakeshkumar, R., Dineshkumar, S., Brahmananda Rao, C. V. S., & Sivaramakrishna, A. (2023). Recent advances in biodegradable polymers – Properties, applications and future prospects. *European Polymer Journal*, 192, 112068. <https://doi.org/10.1016/J.EURPOLYMJ.2023.112068>

Nazareth, M., Marques, M. R. C., Leite, M. C. A., & Castro, I. B. (2019). Commercial plastics claiming biodegradable status: Is this also accurate for marine environments? *Journal of Hazardous Materials*, 366, 714–722. <https://doi.org/10.1016/j.jhazmat.2018.12.052>

Nutrien. (2012). *SAFETY DATA SHEET Product Name: ESN Polymer Coated Urea 44-0-0*
Section 1-Identification of The Material and Supplier ESN Polymer Coated Urea 44-0-0
Section 2-Hazards Identification Statement of Hazardous Nature Emergency Overview Long Term Exposure: No data for health effects associated with long term inhalation. Long Term Exposure: No data for health effects associated with long term skin exposure.

Nutrien. (2018a). *ESN® Polymer Coated Urea 44-0-0 Product identifier Other means of identification Product type Emergency telephone number (with hours of operation) Section 1. Identification ESN® Polymer Coated Urea 44-0-0.*

Nutrien. (2018b). *ESN® Polymer Coated Urea 44-0-0 Product identifier Other means of identification Product type Emergency telephone number (with hours of operation) Section 1. Identification ESN® Polymer Coated Urea 44-0-0.*

Pan, Y., Gao, S. H., Ge, C., Gao, Q., Huang, S., Kang, Y., Luo, G., Zhang, Z., Fan, L., Zhu, Y., & Wang, A. J. (2023). Removing microplastics from aquatic environments: A critical review.

In *Environmental Science and Ecotechnology* (Vol. 13). Editorial Board, Research of Environmental Sciences. <https://doi.org/10.1016/j.ese.2022.100222>

Panthe, G., Bajagain, R., Chaudhary, D. K., Kim, P. G., Kwon, J. H., & Hong, Y. (2024). The release, degradation, and distribution of PVC microplastic-originated phthalate and non-phthalate plasticizers in sediments. *Journal of Hazardous Materials*, 470, 134167.
<https://doi.org/10.1016/J.JHAZMAT.2024.134167>

Peng, Q., Liu, B., Hu, Y., Wang, A., Guo, Q., Yin, B., Cao, Q., & He, L. (2023). The role of conventional tillage in agricultural soil erosion. *Agriculture, Ecosystems & Environment*, 348, 108407. <https://doi.org/10.1016/J.AGEE.2023.108407>

Poursat, B. A. J., Langenhoff, A. A. M., Feng, J., Goense, J., Peters, R. J. B., & Sutton, N. B. (2024). Effect of ultra-high-density polyethylene microplastic on the sorption and biodegradation of organic micropollutants. *Ecotoxicology and Environmental Safety*, 279, 116510. <https://doi.org/10.1016/J.ECOENV.2024.116510>

Qi, Y., Ossowicki, A., Yang, X., Huerta Lwanga, E., Dini-Andreote, F., Geissen, V., & Garbeva, P. (2020). Effects of plastic mulch film residues on wheat rhizosphere and soil properties. *Journal of Hazardous Materials*, 387, 121711.
<https://doi.org/10.1016/J.JHAZMAT.2019.121711>

Qi, Y., Yang, X., Pelaez, A. M., Huerta Lwanga, E., Beriot, N., Gertsen, H., Garbeva, P., & Geissen, V. (2018). Macro- and micro- plastics in soil-plant system: Effects of plastic mulch film residues on wheat (*Triticum aestivum*) growth. *Science of The Total Environment*, 645, 1048–1056. <https://doi.org/10.1016/J.SCITOTENV.2018.07.229>

- Qiu, Y., Zhou, S., Qin, W., Zhang, C., Lv, C., & Zou, M. (2023). Effects of land use on the distribution of soil microplastics in the Lihe River watershed, China. *Chemosphere*, 324, 138292. <https://doi.org/10.1016/J.CHEMOSPHERE.2023.138292>
- Ransom, C. J., Jolley, V. D., Blair, T. A., Sutton, L. E., & Hopkins, B. G. (2020). Nitrogen release rates from slow- And controlled-release fertilizers influenced by placement and temperature. *PLoS ONE*, 15(6 June). <https://doi.org/10.1371/journal.pone.0234544>
- Rezaei, M., Abbasi, S., Pourmahmood, H., Oleszczuk, P., Ritsema, C., & Turner, A. (2022). Microplastics in agricultural soils from a semi-arid region and their transport by wind erosion. *Environmental Research*, 212, 113213.
<https://doi.org/10.1016/J.ENVRES.2022.113213>
- Rillig, M. C., Ingraffia, R., & De Souza Machado, A. A. (2017). Microplastic incorporation into soil in agroecosystems. *Frontiers in Plant Science*, 8.
<https://doi.org/10.3389/fpls.2017.01805>
- Ruggero, F., Gori, R., & Lubello, C. (2019). Methodologies to assess biodegradation of bioplastics during aerobic composting and anaerobic digestion: A review. In *Waste Management and Research* (Vol. 37, Issue 10, pp. 959–975). SAGE Publications Ltd.
<https://doi.org/10.1177/0734242X19854127>
- Sashiwa, H., Fukuda, R., Okura, T., Sato, S., & Nakayama, A. (2018). Microbial degradation behavior in seawater of polyester blends containing poly(3-hydroxybutyrate-co-3-hydroxyhexanoate) (PHBHHx). *Marine Drugs*, 16(1). <https://doi.org/10.3390/md16010034>
- Schell, T., Hurley, R., Buenaventura, N. T., Mauri, P. V., Nizzetto, L., Rico, A., & Vighi, M. (2022). Fate of microplastics in agricultural soils amended with sewage sludge: Is surface

water runoff a relevant environmental pathway? *Environmental Pollution*, 293, 118520.

<https://doi.org/10.1016/J.ENVPOL.2021.118520>

Seo, Y., Zhou, Z., Lai, Y., Chen, G., Pembleton, K., Wang, S., He, J. zheng, & Song, P. (2024).

Micro- and nanoplastics in agricultural soils: Assessing impacts and navigating mitigation.

Science of The Total Environment, 931, 172951.

<https://doi.org/10.1016/J.SCITOTENV.2024.172951>

Šerá, J., Serbruyns, L., De Wilde, B., & Koutný, M. (2020). Accelerated biodegradation testing

of slowly degradable polyesters in soil. *Polymer Degradation and Stability*, 171, 109031.

<https://doi.org/10.1016/J.POLYMDERADSTAB.2019.109031>

Shen, M., Song, B., Zeng, G., Zhang, Y., Huang, W., Wen, X., & Tang, W. (2020). Are

biodegradable plastics a promising solution to solve the global plastic pollution?

Environmental Pollution, 263, 114469. <https://doi.org/10.1016/J.ENVPOL.2020.114469>

Shen, M., Zhang, Y., Zhu, Y., Song, B., Zeng, G., Hu, D., Wen, X., & Ren, X. (2019). Recent

advances in toxicological research of nanoplastics in the environment: A review. In

Environmental Pollution (Vol. 252, pp. 511–521). Elsevier Ltd.

<https://doi.org/10.1016/j.envpol.2019.05.102>

Shruti, V. C., & Kutralam-Muniasamy, G. (2024). Migration testing of microplastics in plastic

food-contact materials: Release, characterization, pollution level, and influencing factors.

TrAC Trends in Analytical Chemistry, 170, 117421.

<https://doi.org/10.1016/j.trac.2023.117421>

Sintim, H. Y., Bary, A. I., Hayes, D. G., Wadsworth, L. C., Anunciado, M. B., English, M. E.,

Bandopadhyay, S., Schaeffer, S. M., DeBruyn, J. M., Miles, C. A., Reganold, J. P., & Flury,

M. (2020). In situ degradation of biodegradable plastic mulch films in compost and agricultural soils. *Science of The Total Environment*, 727, 138668.
<https://doi.org/10.1016/J.SCITOTENV.2020.138668>

Sintim, H. Y., & Flury, M. (2017). Is Biodegradable Plastic Mulch the Solution to Agriculture's Plastic Problem? *Environmental Science and Technology*, 51(3), 1068–1069.
<https://doi.org/10.1021/ACS.EST.6B06042>

Sofyane, A., Atlas, S., Lahcini, M., Vidović, E., Ameduri, B., & Raihane, M. (2024). Insights into hydrophobic (meth)acrylate polymers as coating for slow-release fertilizers to reduce nutrient leaching. *Polymer Chemistry*, 15(33), 3327–3340.
<https://doi.org/10.1039/D4PY00573B>

Straub, S., Hirsch, P. E., & Burkhardt-Holm, P. (2017). Biodegradable and petroleum-based microplastics do not differ in their ingestion and excretion but in their biological effects in a freshwater invertebrate Gammarus fossarum. *International Journal of Environmental Research and Public Health*, 14(7). <https://doi.org/10.3390/ijerph14070774>

Strungaru, S. A., Jijie, R., Nicoara, M., Plavan, G., & Faggio, C. (2019). Micro- (nano) plastics in freshwater ecosystems: Abundance, toxicological impact and quantification methodology. In *TrAC - Trends in Analytical Chemistry* (Vol. 110, pp. 116–128). Elsevier B.V.
<https://doi.org/10.1016/j.trac.2018.10.025>

Su, P., Wang, J., Zhang, D., Chu, K., Yao, Y., Sun, Q., Luo, Y., Zhang, R., Su, X., Wang, Z., Bu, N., & Li, Z. (2022). Hierarchical and cascading changes in the functional traits of soil animals induced by microplastics: A meta-analysis. *Journal of Hazardous Materials*, 440, 129854. <https://doi.org/10.1016/J.JHAZMAT.2022.129854>

- Sun, H., Lei, C., Xu, J., & Li, R. (2021). Foliar uptake and leaf-to-root translocation of nanoplastics with different coating charge in maize plants. *Journal of Hazardous Materials*, 416, 125854. <https://doi.org/10.1016/J.JHAZMAT.2021.125854>
- Taysom, T. W., LeMonte, J. J., Ransom, C. J., Stark, J. C., Hopkins, A. P., & Hopkins, B. G. (2023). Polymer Coated Urea in ‘Russet Burbank’ Potato: Yield and Tuber Quality. *American Journal of Potato Research*, 100(6), 451–463. <https://doi.org/10.1007/s12230-023-09931-5>
- Tian, L., Jinjin, C., Ji, R., Ma, Y., & Yu, X. (2022). Microplastics in agricultural soils: sources, effects, and their fate. In *Current Opinion in Environmental Science and Health* (Vol. 25). Elsevier B.V. <https://doi.org/10.1016/j.coesh.2021.100311>
- Tokiwa, Y., Calabia, B. P., Ugwu, C. U., & Aiba, S. (2009a). Biodegradability of plastics. In *International Journal of Molecular Sciences* (Vol. 10, Issue 9, pp. 3722–3742). <https://doi.org/10.3390/ijms10093722>
- Tokiwa, Y., Calabia, B. P., Ugwu, C. U., & Aiba, S. (2009b). Biodegradability of plastics. In *International Journal of Molecular Sciences* (Vol. 10, Issue 9, pp. 3722–3742). <https://doi.org/10.3390/ijms10093722>
- Trenkel, M. E., & Impr. Point 44). (2010). *Slow- and controlled-release and stabilized fertilizers : an option for enhancing nutrient use efficiency in agriculture*. IFA, International fertilizer industry Association.
- USDA. (2022). *Soil Quality Indicators Soil Structure & Macropores*.

Wahyuningtyas, N., & Suryanto, H. (2017). Analysis of Biodegradation of Bioplastics Made of Cassava Starch. *Journal of Mechanical Engineering Science and Technology*, 1(1), 24–31.
<https://doi.org/10.17977/um016v1i12017p024>

Wang, W., Yuan, W., Xu, E. G., Li, L., Zhang, H., & Yang, Y. (2022). Uptake, translocation, and biological impacts of micro(nano)plastics in terrestrial plants: Progress and prospects. *Environmental Research*, 203, 111867. <https://doi.org/10.1016/J.ENVRES.2021.111867>

Wang, Y., Zhang, J. H., Zhang, Z. H., & Jia, L. Z. (2016). Impact of tillage erosion on water erosion in a hilly landscape. *Science of The Total Environment*, 551–552, 522–532.
<https://doi.org/10.1016/J.SCITOTENV.2016.02.045>

Wang, Y., Zhang, Z., Zhang, J., Liang, X., Liu, X., & Zeng, Y. (2021). Effect of surface rills on soil redistribution by tillage erosion on a steep hillslope. *Geomorphology*, 380, 107637.
<https://doi.org/10.1016/J.GEOMORPH.2021.107637>

Xu, J., Zuo, R., Shang, J., Wu, G., Dong, Y., Zheng, S., Xu, Z., Liu, J., Xu, Y., Wu, Z., & Huang, C. (2023). Nano- and micro-plastic transport in soil and groundwater environments: Sources, behaviors, theories, and models. *Science of The Total Environment*, 904, 166641.
<https://doi.org/10.1016/J.SCITOTENV.2023.166641>

Yang, C., & Gao, X. (2022). Impact of microplastics from polyethylene and biodegradable mulch films on rice (*Oryza sativa* L.). *Science of The Total Environment*, 828, 154579.
<https://doi.org/10.1016/J.SCITOTENV.2022.154579>

Yang, J., Tu, C., Li, L., Li, R., Feng, Y., & Luo, Y. (2023). The fate of micro(nano)plastics in soil–plant systems: Current progress and future directions. *Current Opinion in Environmental Science and Health*, 32. <https://doi.org/10.1016/j.coesh.2022.100438>

Yin, L., Wen, X., Huang, D., Du, C., Deng, R., Zhou, Z., Tao, J., Li, R., Zhou, W., Wang, Z., & Chen, H. (2021). Interactions between microplastics/nanoplastics and vascular plants.

Environmental Pollution, 290. <https://doi.org/10.1016/j.envpol.2021.117999>

Yousif, E., & Haddad, R. (2013). *Photodegradation and photostabilization of polymers, especially polystyrene: review*. <http://www.springerplus.com/content/2/1/398>

Yu, H., Qi, W., Cao, X., Hu, J., Li, Y., Peng, J., Hu, C., & Qu, J. (2021). Microplastic residues in wetland ecosystems: Do they truly threaten the plant-microbe-soil system? *Environment International*, 156, 106708. <https://doi.org/10.1016/J.ENVINT.2021.106708>

Yu, Y., Griffin-LaHue, D. E., Miles, C. A., Hayes, D. G., & Flury, M. (2021). Are micro- and nanoplastics from soil-biodegradable plastic mulches an environmental concern? *Journal of Hazardous Materials Advances*, 4, 100024.
<https://doi.org/10.1016/J.HAZADV.2021.100024>

Yu, Z. fu, Song, S., Xu, X. lu, Ma, Q., & Lu, Y. (2021). Sources, migration, accumulation and influence of microplastics in terrestrial plant communities. *Environmental and Experimental Botany*, 192, 104635. <https://doi.org/10.1016/J.ENVEXPBOT.2021.104635>

Yuan, W., Hibi, Y., Tamura, R., Sumita, M., Nakamura, Y., Naito, M., & Tsuda, K. (2023). Revealing factors influencing polymer degradation with rank-based machine learning. *Patterns*, 4(12), 100846. <https://doi.org/10.1016/J.PATTER.2023.100846>

Zemke, J. J., Enderling, M., Klein, A., & Skubski, M. (2019). The influence of soil compaction on runoff formation. A case study focusing on skid trails at forested andosol sites. *Geosciences (Switzerland)*, 9(5). <https://doi.org/10.3390/geosciences9050204>

Zhang, J., Ren, S., Xu, W., Liang, C., Li, J., Zhang, H., Li, Y., Liu, X., Jones, D. L., Chadwick, D. R., Zhang, F., & Wang, K. (2022a). Effects of plastic residues and microplastics on soil ecosystems: A global meta-analysis. *Journal of Hazardous Materials*, 435.
<https://doi.org/10.1016/j.jhazmat.2022.129065>

Zhang, J., Ren, S., Xu, W., Liang, C., Li, J., Zhang, H., Li, Y., Liu, X., Jones, D. L., Chadwick, D. R., Zhang, F., & Wang, K. (2022b). Effects of plastic residues and microplastics on soil ecosystems: A global meta-analysis. *Journal of Hazardous Materials*, 435.
<https://doi.org/10.1016/j.jhazmat.2022.129065>

Zhang, M. (1994). *Polymer coated urea N release rate and n uptake by barley*.

Zhao, L., Qin, Q., Geng, H., Zheng, F., Zhang, X. J., Li, G., Xu, X., & Zhang, J. (2023). Effects of upslope inflow rate, tillage depth, and slope gradients on hillslope erosion processes and hydrodynamic mechanisms. *CATENA*, 228, 107189.
<https://doi.org/10.1016/J.CATENA.2023.107189>

Zhao, X., Song, X., Li, L., Wang, D., Meng, P., & Li, H. (2023). Effect of microrelief features of tillage methods under different rainfall intensities on runoff and soil erosion in slopes. *International Soil and Water Conservation Research*.

<https://doi.org/10.1016/J.ISWCR.2023.10.001>

Zhao, Z. Y., Li, W. B., Wang, P. Y., Tao, H. Y., Zhou, R., Cui, J. Y., Zhang, J., Tian, T., Zhao, X. Z., Wang, Y. B., & Xiong, Y. C. (2023). Farmers' participation into the recovery of waste agricultural plastic film: An application of the Theory of Planned Behavior. *Waste Management*, 169, 253–266. <https://doi.org/10.1016/J.WASMAN.2023.06.036>

Zhou, Y., Jing, J., Yu, R., Zhao, Y., Gou, Y., Zhang, Z., Tang, H., Zhang, H., & Huang, Y. (2023).

Microplastics in plateau agricultural areas: Spatial changes reveal their source and distribution characteristics. *Environmental Pollution*, 319.

<https://doi.org/10.1016/j.envpol.2023.121006>

Zielinski, J. M. (2001). Block Copolymers, Transport Through. *Encyclopedia of Materials:*

Science and Technology, 739–743. <https://doi.org/10.1016/B0-08-043152-6/00142-X>

Zuo, X., Zhang, C., Zhang, X., Wang, R., Zhao, J., & Li, W. (2023). Wind tunnel simulation of

wind erosion and dust emission processes, and the influences of soil texture. *International*

Soil and Water Conservation Research. <https://doi.org/10.1016/J.ISWCR.2023.08.005>

7 Appendix A: Assessment of soil sampling methods for the quantification of polymer coatings

7.1 Sampling Methodologies

7.1.1 Bulk Density Sampling Methodology

A 50 cm x 50 cm square was placed surrounding the coordinates for each sampling position. A bulk density sample with a surface area of 20 cm² was taken within the 2500 cm² square. Two bulk density samples were taken before the surface area monolith sample. Each bulk density sample was excavated to a depth of 5 cm (100 cm³). Bulk density rings were pressed into the soil until its rim was aligned with the topsoil. The surrounding soil was carved away to collect the bulk density sample (Figure 7-1). Samples were placed within individual tinfoil wrapping with labeled coordinates. The bulk density areas were filled and leveled post collection.



Figure 7-1: Polymer capsules recovered using the bulk density methodology.

7.1.2 Surface Area Monolith Sampling Methodology

An excavated monolith sample with a surface area of 625 cm² was extracted from the 2500 cm² sampling area previously described in 7.1.1. Each surface area monolith was excavated to a depth of 5 cm (3125 cm³ volume). A quarter of the initial 50 cm x 50 cm sampling square was vertically indented with a spade and soil was pulled away from the soil sample (Figure 7-2) to reduce soil compression and maintain stability. A measuring tape was used to mark the 5 cm below the monolith's surface. Soil was extracted in blocks shown in and placed into containers with labeled coordinates using the spade. The excavated area was filled and leveled post collection.



Figure 7-2: Carved excavated surface area monolith.

7.2 Assessment of Sampling Methodologies

7.2.1 Recovery Rate of Polymer Coatings

Two sampling methodologies were assessed to determine whether the cost and time-effective bulk density sampling methodology was sufficient in describing polymer coating concentration. The bulk density sampling method is quick, contains a non-intensive extraction process, and provides detailed data suggesting the placement of the polymer coatings within the soil. The

limitation of the bulk density sampling method is that it may not be fully representative of polymer concentration across a field site. The surface area monolith sampling method involves extracting a larger volume of soil using a spade. A larger soil volume extraction from the surface area monolith sampling should provide representative data to analyze polymer concentration. Surface area monolith sample may be more complete in its ability to characterize the landscape, but the sampling method is more labor intensive, has an increased extraction period, and takes longer to process within the laboratory.

7.2.2 Visual Assessment of Methodologies

Concentration was calculated per unit area and directly compared the polymer coating concentration across sampling methodologies (Figure 7-3). Soil samples were collected in a pairwise fashion within the same 0.25 m^2 quadrate to reduce spatial variability.

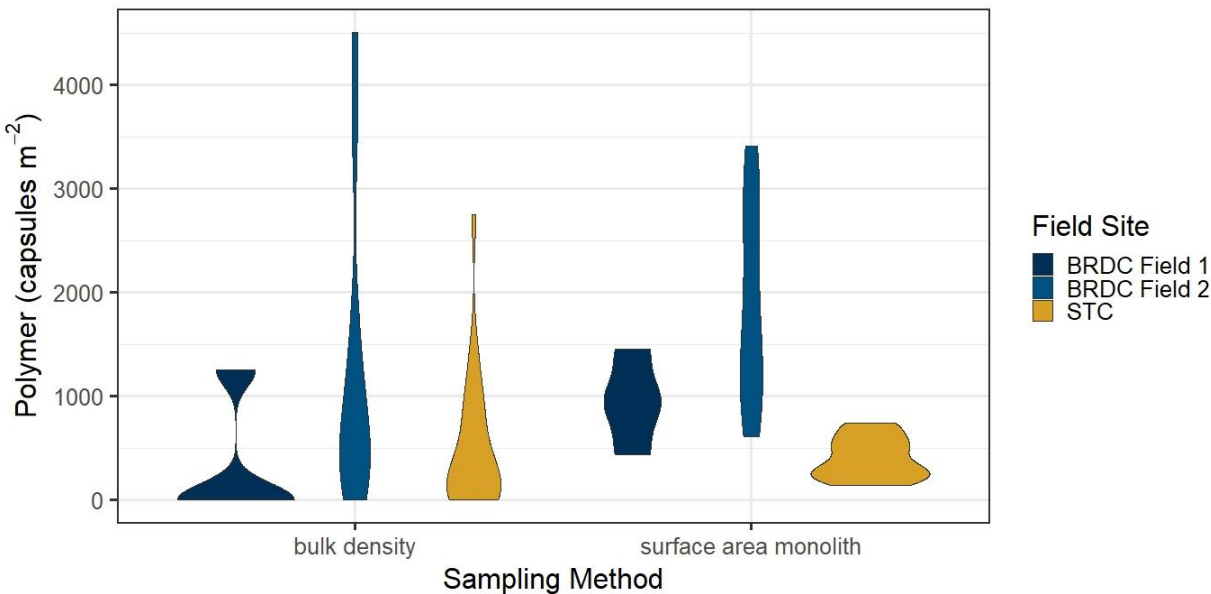
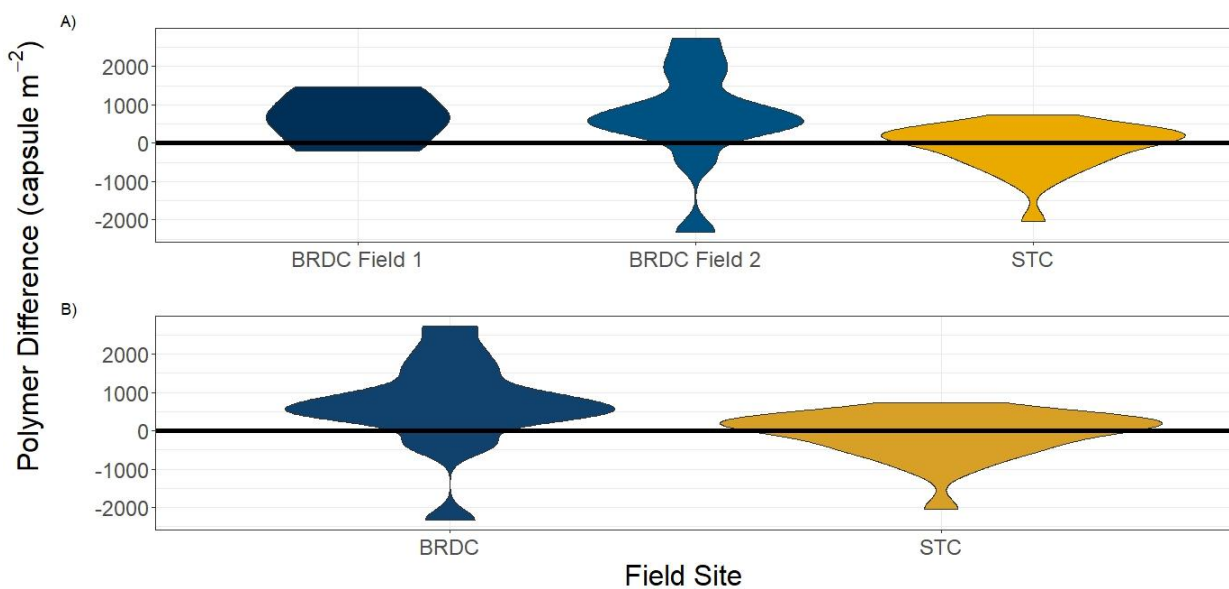


Figure 7-3: Polymer coating concentration was bimodal using bulk density and was normal using surface area monolith methodologies. Statistics are performed by Wilcoxon Rank sum, comparing the polymer coating concentration between methodologies at BRDC Field 1, BRDC Field 2, and STC *** $p = 0.09158$, $p = 0.02642$, $p = 0.25710$.

Concentration distribution varied between sampling methodologies (Figure 7-3). The bulk density method resulted in a positively skewed or a bimodal distribution. The surface area monolith method resulted in a normal distribution. Polymer coating concentration within the bulk density method was more variable due to the small sample area. The smaller surface area had varying results surrounding bands of fertilizer at BRDC. The bulk density sampling method also resulted in a skewed data set across the broadcast application of ESN at STC.

A qualitative pairwise comparison of polymer concentration differences was conducted to determine the shift in polymer coating concentration between sampling methods (Figure 7-4). The Bulk density method was negated from the surface area monolith method to visualize concentration differences. Symmetry across zero defines no difference between sampling methods.



*Figure 7-4: Banded fertilizer application resulted in a difference between bulk density and surface area monolith sampling methodologies and broadcast fertilizer application resulted in no difference between methodologies. The difference in polymer coating concentration was normal for BRDC and STC. Statistics are performed by Wilcoxon Rank sum, comparing the polymer coating concentration between methodologies ***p = 0.00065.*

Polymer concentration at BRDC was not symmetric across zero for banded fertilizer applications. Polymer concentration at STC was symmetric across zero for broadcast fertilizer applications. The lack of symmetry across zero at BRDC suggests that the sampling methods are different. Polymer concentration at BRDC demonstrates the significance of sample placement of the bulk density ring in contrast to the fertilizer band(s). A statistical test is required to determine whether the methods were statistically different. A bimodal distribution of polymer concentration was measured using the bulk density sampling methodology, and a non-normalized statistical test was used.

7.2.3 Wilcoxon Rank Sum

The Wilcoxon rank sum tests if two variables have the same continuous distribution and whether a significant difference between the two variables occurs. Assumption requirements of the Wilcoxon rank sum test include that the data is paired, and randomly and independently selected. The Wilcoxon rank sum is the nonparametric equivalent to the paired t-test and is applicable when the data do not follow a normal distribution. The two variables that were measured across the field sites were the recovery rate of the two methodologies. The Wilcoxon test compares if a significant difference occurs in the polymer coating concentration across the field sites. The Wilcoxon test would demonstrate the applicability of the two methodologies based on if a statistical difference was measurable between the data sets. The Wilcoxon rank sum test was calculated for each of the field sites and the collective difference between the field sites. The difference between field sites resulted in statistically different sampling methodologies (Table 10).

Table 10: Comparison of mean polymer coatings between bulk density and surface area monolith sampling methods using Wilcoxon Rank-Sum analysis. A statistical difference between bulk density and surface area monolith sampling methods occurred at BRDC Field 2.

Field Site	Wilcoxon statistic	P-value	Sample difference	N
BRDC	191	0.00916	835	16
BRDC Field 1	13	0.09158	848	4
BRDC Field 2	106	0.02642	869	12
STC	320	0.25710	70	24
BRDC - STC	316	0.00065	687	40

Fertilizer application history affects the recovery rate of polymer coatings. The two methodologies under broadcast ESN fertilizer applications were not statistically different in polymer coating concentration. However, the two methodologies under banded ESN fertilizer applications were statistically different.

7.2.4 Methodology Selection

Selection of the best sampling methodology was instrumental in achieving the necessary standard for polymer coating quantification and assessing the polymer's biodegradability. Data across field site categories such as landscape elevation should be normalized to accurately measure polymer coating concentration. The surface area monolith sampling method was sufficient in providing normalized data across fertilizer application methods. A difference in polymer coating concentration was measured between soil sampling methods across application history. There were unanswerable questions about the applicability of the bulk density sampling method. What is a properly defined result for sampling along bands and between bands to assess polymer concentration across the field site? What is the definable area between banded and non-banded fertilizer application if polymers moved laterally over time? The bulk density sampling method lacked the ability to address spatial variance under banded fertilizer practices. Based on

the sampling methodology results, subsequent soil samples were collected using the surface area monolith method.

8 Appendix B: Soil Temperature and Water Content in the Field and Greenhouse Studies

Soil temperature and moisture content influence microbial activity. These two factors can indicate whether the soil is under ideal conditions for microbial activity. Polymer decomposition and surface degradation rate is reliant on microbial activity. Microorganisms have distinct temperature and moisture ranges that are optimal for microbial activity. Determining polymer coating degradation rate within Manitoban soils was necessary to evaluate temporal significance in various environmental conditions.

Optimization of both soil temperature and moisture levels within specific ranges was essential to promote optimal microbial activity. The optimal microbial activity resulted in achieving optimal polymer coating degradation rates. These two soil conditions were closely watched in the incubation study to maintain aerobic conditions such that they may be compared with the field study. Maintaining a stable soil temperature was needed to provide favorable conditions for polymer degradation, as it directly influences physiological and biochemical processes within microbial communities. Consistent aerobic conditions were needed to accurately compare polymer degradation rates between incubation and field studies.

Two environmental factors that were evaluated (soil temperature and moisture content) to compare polymer degradation across different climates. The continental climate in Manitoba compared to a greenhouse tropical climate can demonstrate the significance of environmental conditions on polymer coating degradation. The environmental conditions between the two studies can influence microbial activity. For example, the expansion of microorganisms on the polymer coatings surface relies on stable soil temperatures. Additionally, mesophiles' activity is

optimal at temperatures greater than 20 °C. Soil temperature can also influence soil moisture content by affecting water infiltration through the soil matrix. Water applied to the soil replicates infiltrates to the polymer coatings surface providing moisture needed to support the growth of microbial communities.

Solar radiation dynamically drives soil temperature and is a necessary energy source for microbial activity. Intensity and duration of sunlight vary throughout the day and across seasons. These factors changes seasonally, which affects the total amount of solar radiation the soil receives. Solar angles affect the magnitude of solar radiation which changes seasonally, reducing the heat-energy acquired from the sun. Water can affect soil temperatures through evaporation and heat transportation by conduction, convection, and radiation between the soil and air. Airflow can also affect the heat transportation between the air and soil. Soil temperature was maintained in optimal conditions (Figure 8-1).

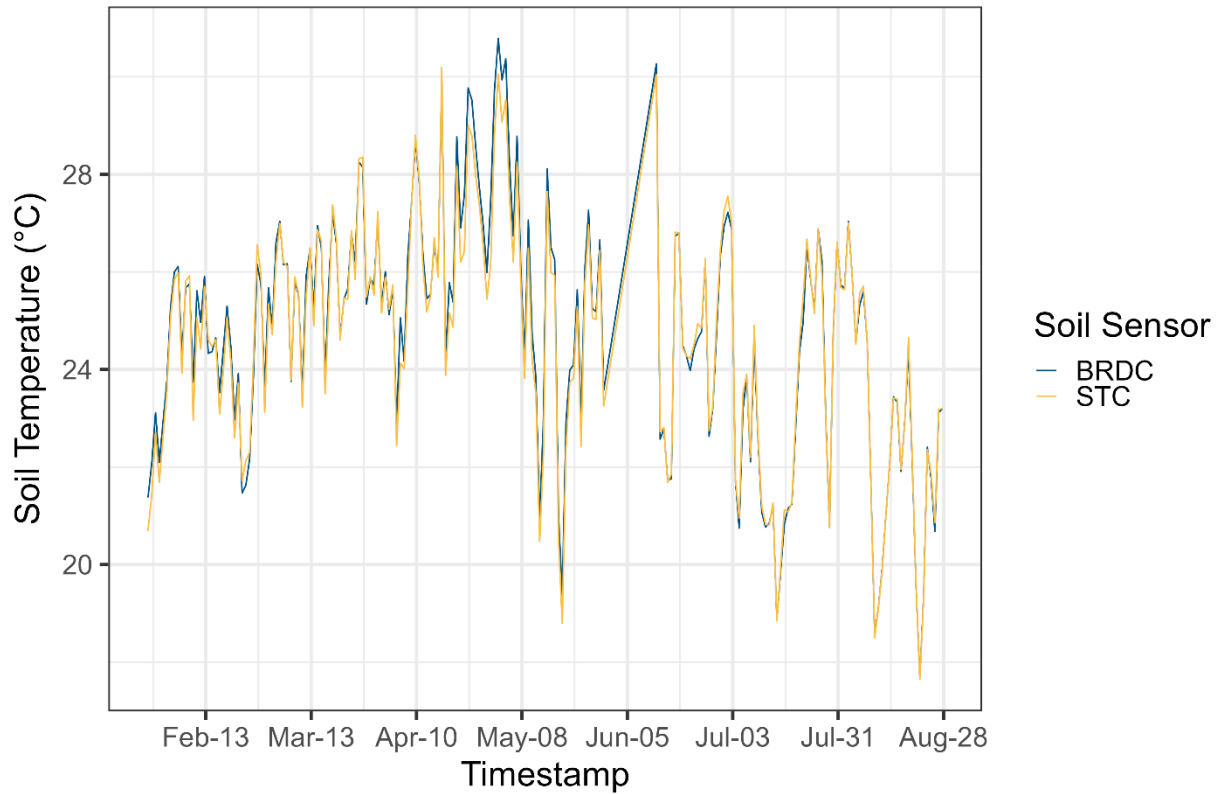


Figure 8-1: Mean soil temperature of soil replicates were equivalent between BRDC and STC soils during the incubation study.

Soil moisture content affects the metabolic rate of microorganisms. Moisture content may affect cellular hydration, oxygen availability, and the amount of microorganisms within the soil. Adequate soil moisture conditions promote metabolic activity in microorganisms and growth rate of the biofilm. The amount of water within the soil matrix reduces the presence and availability of oxygen. Both water and oxygen are present within the macropore and micropore space in the soil matrix, and the macropore's domain within the soil is a component in infiltration and retention of water within the soil. The 2-mm aggregates minimize differences in porous space under uniform conditions within the respective soil matrices.

Stable soil moisture content within a specific range was necessary to stimulate optimal aerobic polymer degradation. A dynamic relationship between soil moisture and microbial communities

exists. Stable moisture content is needed for both nutrient cycling and polymer degradation. Microorganisms require water for the enzymatic reaction to breakdown the polymer chain to simpler forms that may be absorbed. Extremes in soil moisture content can impede polymer degradation. Lower moisture content may impede microbial activity, while excessive soil moisture content may change the degradation process. Within Fairbairn et al., 2023, anaerobic greenhouse gas fluxes deviated from zero above thirty percent soil moisture content. Excessive soil moisture conditions limit the amount of O₂ available and promote anaerobic conditions.

The degradation rate of polymer coatings was affected by soil moisture changes. The incubation study reflected aerobic soil conditions, which occur primarily within Manitoban. Soil probe (Model 5TM, Decagon Devices, Inc.) were used to measure soil moisture. However, the soil probe measured the soil moisture in a 5 cm radius surrounding the probe. The planting pots used within the incubation study did not encase a 5 cm radius surrounding the soil probe. This resulted in an unknown volume of air outside the pots being used to calculate the soil moisture. Lower soil moisture will be measured in this case due to the probes zone of influence (Decagon Devices, 2010). The soil moisture data recorded in the greenhouse did not accurately reflect the true volumetric water content but was used to determine and optimize watering schedules for the two soil types. The optimized watering schedule was used to maintain a constant moisture content near field capacity. Therefore, soil moisture was monitored and maintained on a regular schedule to ensure optimal soil moisture in aerobic conditions (Figure 8-2).

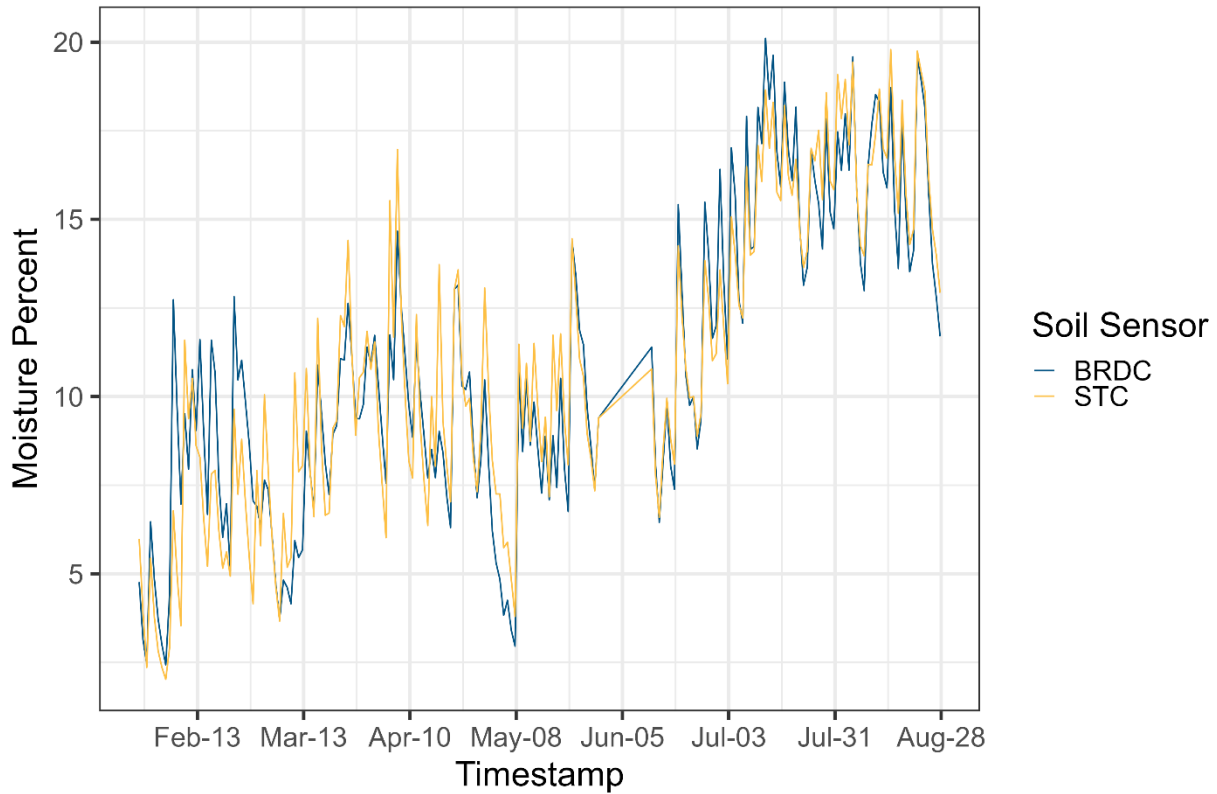


Figure 8-2: Mean soil moisture of soil replicates were equivalent between BRDC and STC soils during the incubation study.

Climate conditions affect the moisture content within the field. The valleys within the soil moisture data occurred within the months that frozen soil can be observed. The initial peak spike following the valley indicates the snowmelt period in which a portion of water leaves the field site as surface runoff (3.2.2). However, soil moisture levels may vary between field sites yearly (Figure 8-3). Low soil moisture throughout the non-frozen soil could reduce polymer degradation observed within the field site.

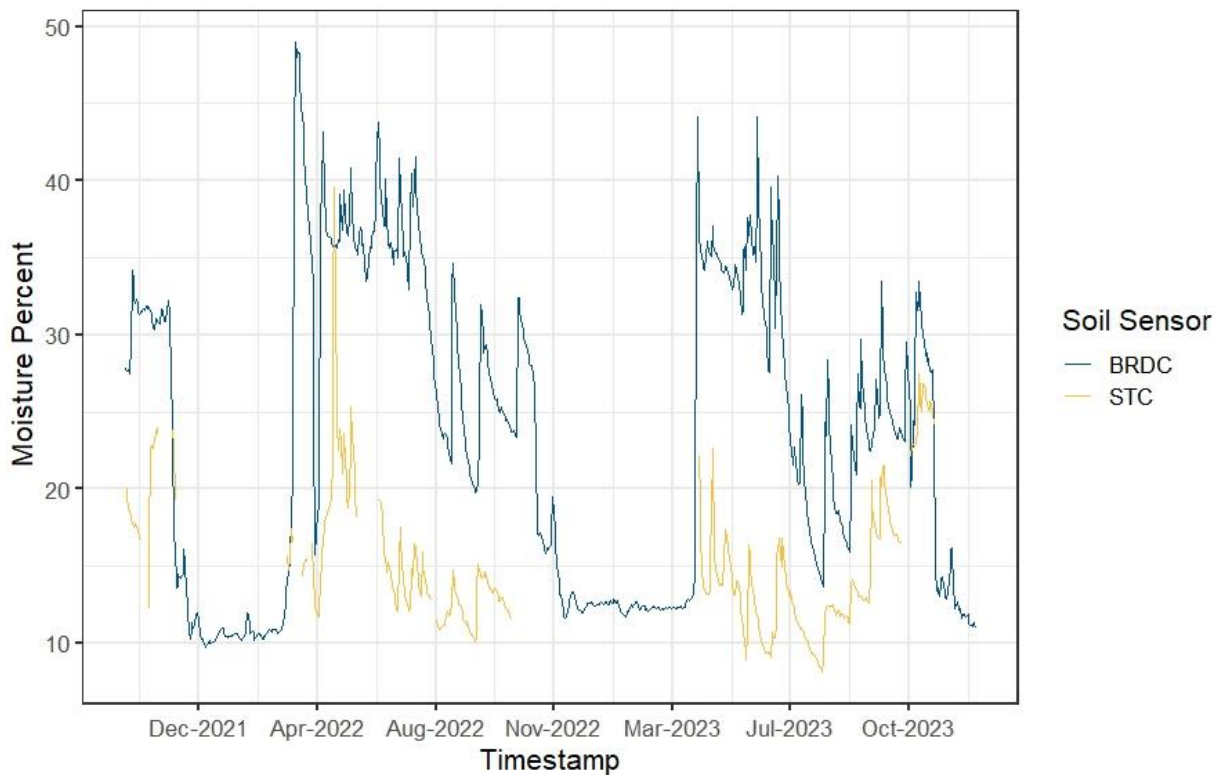


Figure 8-3: Seasonal variability in soil moisture visualized across BRDC and STC field sites during the thesis. Frozen soil in Manitoba resulted in lowered soil moisture readings between 2022 and 2024.

Microorganisms use heat-energy as a resource to degrade polymer coatings. For example, a prominent range of soil temperature for mesophiles' microbial activity ranges between 20-45 °C. Through thermodynamic processes, heat within the soil is used as an energy resource for the microorganism's productivity. However, soil temperatures under environmental conditions fluctuate during the year. Polymer coating degradation could be negligible throughout the year within frozen soil. This would reduce polymer degradation throughout the year that would be expected to occur compared to other climates. The soil temperatures fluctuate at 20 °C within the summer month (Figure 8-4).

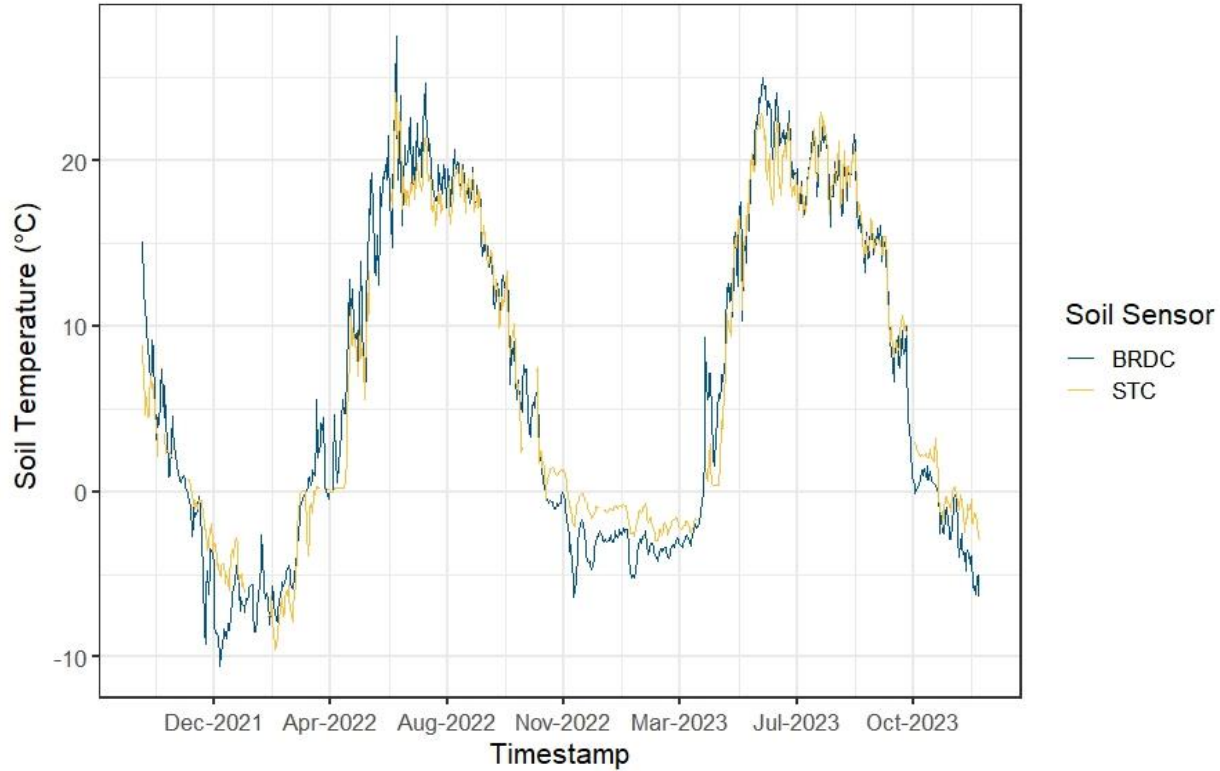


Figure 8-4: Seasonal variability in soil temperature visualized across BRDC and STC field sites during the thesis. The mean soil temperature of BRDC and STC was 5° between 2022 and 2024.

Soil temperature is a factor of the incubation study and field study that may affect the rate of degradation. Soil probes (Model 5TM, Decagon Devices, Inc.) were installed at 5 cm depths at both field sites. The summation of heat energy is acquired across both systems to determine whether soil temperature is a driving factor for polymer degradation at BRDC and STC. A mean daily temperature above 20 °C would indicate that the day received ample heat energy to be considered a growing day with the ability for sufficient polymer coating degradation. A comparison between the number of days with soil temperature above 20 °C and linear degradation slope of the polymer coating was used to compare the heat-energy effectivity on polymer degradation. To account for the difference in heat acquisition, the sum of daily soil temperatures above 20 °C was compared with linear degradation rates.

Table 11: Comparison of polymer coating degradation using linear regression between field and incubation for soil temperature above 20 °C.

Field Site	Study	Days Above 20	Linear Degradation ($\mu\text{g day}^{-1}$)
BRDC	Field	31	0.155
STC	Field	43	0.237
Combined	Incubation	190	77.4

The field data ratio of linear degradation per daily 20 °C reading resulted in 1.39:1.53 relationship between BRDC: STC (Table 11). The close ratio between the field study suggests that the two-soil type's degradation is not statistically different for days above 20 °C. The degradation between Wheatland/Stockton and Dezwood soils were not statistically different within 3.1.2. Additionally, BRDC was expected to have a lower degradation since it was applied 6 years before the STC field site. The lower value obtained in the ratio could be accounted for since polymer degradation is reduced over time using the spherical shell model. Therefore, soil temperature above 20 °C could be essential for polymer degradation. Additionally, polymer degradation by daily soil temperature above 20 °C indicates which type of microorganism group dominates polymer coating degradation (i.e., Mesophiles). However, the incubation degradation rate was statistically higher than the field degradation rate under optimal soil temperature and moisture conditions (3.1.2). Therefore, the difference in polymer degradation between studies highlights the impact of optimal conditions compared to natural environmental conditions.

9 Appendix C: Model Comparison

A negative exponential curve is often used to model the decay and degradation of biodegradable products. The degradation curve contains an initial degradation rate, which reduces over time, which defines the negative curvature. Linear regression is another form of a line tangent to the negative exponential curve. Linear regressions are commonly used for statistical models to evaluate a simple relationship between variables and a normal residual plot must occur.

9.1 Negative Exponential Function Derivation

A few corrections were made to the spherical model for mass deterioration since the polymer coating is a thin shell structure and not a sphere. The density is assumed constant across the shell of the polymer coating. The volume of the shell is the calculated difference between the outer edge subtracting the inner edge since the volume is a shell and not a sphere. The mass within the density function is the initial polymer coating mass that is degrading. These adaptations were applied to convert the spherical model into a shell model (Equation 2-6). Derivation of the negative exponential function starting with the specific surface degradation rate constant and creating the mass loss as a function of time using (Chamas et al., 2020):

$$k_d = -\frac{1}{\rho * SA} * \frac{dm}{dt}$$

$$k_d = -\frac{1}{4\pi R^2 m} * \frac{dm}{dt}$$

$$-\frac{4\pi R^2 k_d}{V_o} dt = \frac{1}{m} dm$$

$$\int_0^t -\frac{4\pi R^2 k_d}{V_o} dt = \int_{m_0}^{m_t} \frac{1}{m} dm$$

$$-\frac{4\pi R^2 k_d t}{V_o} = \ln(m_t - m_o)$$

$$e^{\frac{-4\pi R^2 k_d t}{V_o}} = |m_t - m_o|$$

When the mass of polymer coating capsule at some point in time (m_t) goes to zero, the negative exponential model can be modeled by the following equation:

$$m_t = e^{\frac{-4\pi R^2 k_d t}{V_o}} - m_0$$

The variables derived within the applied fit were compared to a negative exponential equation to relate the degradation of the polymer coating.

$$A(t) = A_o e^{(-sx)} - K$$

Based on the derivation of the negative exponential using a spherical shell, the variables could explain the amount of polymer present in the system at time 0 (A_o), the decay rate (S) based on polymer type/composition/molecular weight, temperature, moisture, size and shape, the mean polymer coating capsule mass (K), and time (x). A vertical shift based on the mean polymer coating capsule mass was implemented to determine the intersection of zero mass at a point in time based on the previous derivation.

9.2 Mass as a Function of Time

Adaptations in 9.1 Negative Exponential Function Derivation were also applied to convert the spherical model into a shell model (Equation 2-7).

Equation 9-1: Spherical degradation Model.

$$m_t = \left[(m_o)^{\frac{1}{3}} - \frac{\frac{2}{3}}{3} k_d (\pi \rho)^{\frac{1}{3}} t \right]^3 \quad (9-1)$$

9.3 Complete Degradation Time

The complete degradation time is a result of the mass as a function of time (Equation 9-1). The complete degradation time has a final mass of zero, which simplifies the expression. Density of the polymer coating is a function of the initial mass divided by the initial volume.

$$m_t = \left[(m_o)^{\frac{1}{3}} - \frac{6^{\frac{2}{3}}}{3} * k_d (\pi \rho)^{\frac{1}{3}} * t \right]^3$$

$$0 = \left[(m_o)^{\frac{1}{3}} - \frac{6^{\frac{2}{3}}}{3} * k_d (\pi \rho)^{\frac{1}{3}} * t_d \right]^3$$

$$\sqrt[3]{0} = \sqrt[3]{\left[(m_o)^{\frac{1}{3}} - \frac{6^{\frac{2}{3}}}{3} * k_d (\pi \rho)^{\frac{1}{3}} * t_d \right]^3}$$

$$0 = (m_o)^{\frac{1}{3}} - \frac{6^{\frac{2}{3}}}{3} * k_d (\pi \rho)^{\frac{1}{3}} * t_d$$

$$(m_o)^{\frac{1}{3}} = \frac{6^{\frac{2}{3}}}{3} * k_d \left(\frac{\pi m_o}{V_o} \right)^{\frac{1}{3}} * t_d$$

$$t_d = \frac{3}{6^{\frac{2}{3}} * k_d} \left(\frac{m_o}{\frac{\pi m_o}{V_o}} \right)^{\frac{1}{3}}$$

Equation 9-2: Complete Degradation for decreasing radii and surface area of a sphere.

$$t_d = \frac{3}{6^{\frac{2}{3}} * k_d} \sqrt[3]{\frac{V_0}{\pi}} \quad (9-2)$$

The complete degradation that is modeled by a sphere is given by (Equation 9-2). Similarly, degradation occurs over the shell rather than the volume of a sphere. Adaptations in 9.1 Negative

Exponential Function Derivation were also applied to convert the spherical model into a shell model (Equation 2-8). The difference in these volumes' accounts for the degradation of the polymer coating. This assumes that the polymer coating is not broken and does not degrade from both the inner and outer surface area.

10 Appendix D: Release Rate of Urea

The incubation study contained two phases of polymer coating deterioration with the application of fresh ESN. A linear least square regression curve was applied over the full duration of the incubation study to visualize the loss of urea in the first 105 days (Figure 10-1). The initial phase comprised of ESN that had polymer coatings that contained urea and was characterized by higher mass percentage loss over time (Figure 10-2). The secondary phase of the incubation study was absent of observable and measurable urea and was characterized by a lower mass percentage loss over time. The incubation study received elevated soil moisture compared to the field study. An enhanced rate of urea release should occur within the incubation study compared to the natural environment. The characteristic release of slow-release fertilizer follows an elongated ‘s’ shape from a single coated urea granule (Trenkel, 2010). Therefore, the mass reduction should follow an inverted elongated ‘s’ shape. The inverted elongated ‘s’ shape was measured within the greenhouse incubation study (Figure 10-1). The N release from the PCU in the greenhouse incubation study followed the expected slow-release pattern.

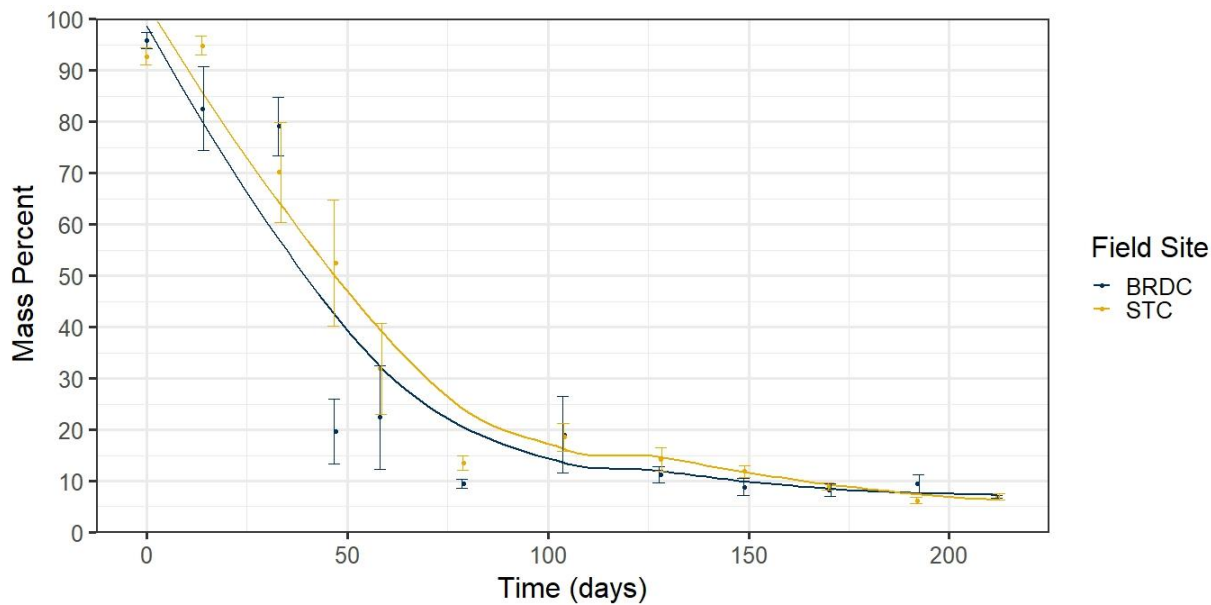


Figure 10-1: The incubation data is characterized by two phases that include the present of urea and the absence of urea. The first 104 days represent PCU fertilizer containing urea and subsequent days represent the absence of urea.

An absolute value bell curve could describe the rate of urea release during the initial phase of the incubation study. An accelerated polymer coating degradation could have occurred during the early phases as the biofilm expands. The mass lost by urea removal and polymer coating degradation during this phase could overshadow the contribution of the biofilm expansion during the early phases of the greenhouse incubation study. The majority of urea was released between 20-60 days. Following the exponential release, the rate of urea released plateaued, and then decreased until day 105.

Release timing of urea is significant to the vegetation and producers. ESN was developed to release urea during the presence of sufficient soil moisture and temperature. The polymer coating protects the urea from losing substance during suboptimal soil conditions. Natural soil conditions may vary across the growing season and not have adequate levels of soil temperature and moisture, which would release urea slower. The majority of the urea release occurred before the 80th-day mark under optimal soil conditions. Soil temperature in Manitoban soils are

substantially less than the incubation study (Appendix B: Soil Temperature and Water Content in the Field and Greenhouse Studies). The release of urea under natural soil conditions should be at most equal or slower release than the release during the incubation study. STC soil had a slower urea release rate than that of the BRDC Field site (Figure 10-2).

The range of urea release from ESN varies based on environmental conditions. Polymer coating would fully release urea between 50-80 days (ESN, 2023). For incubated ESN, a near complete release of N was achieved in 40 days with temperatures ≥ 20 °C in sandy loam soils and clayey soils (Golden et al., 2011). The observance of urea was present until day 105 under optimal aerobic soil conditions (Figure 10-2). Slow release PCU fertilizer incorporated into the soil was slower to release nitrogen under static environmental conditions, and nitrogen release occurred between 54-118 days (Ransom et al., 2020). Therefore, the urea release within the incubation study is consistent with other literature.

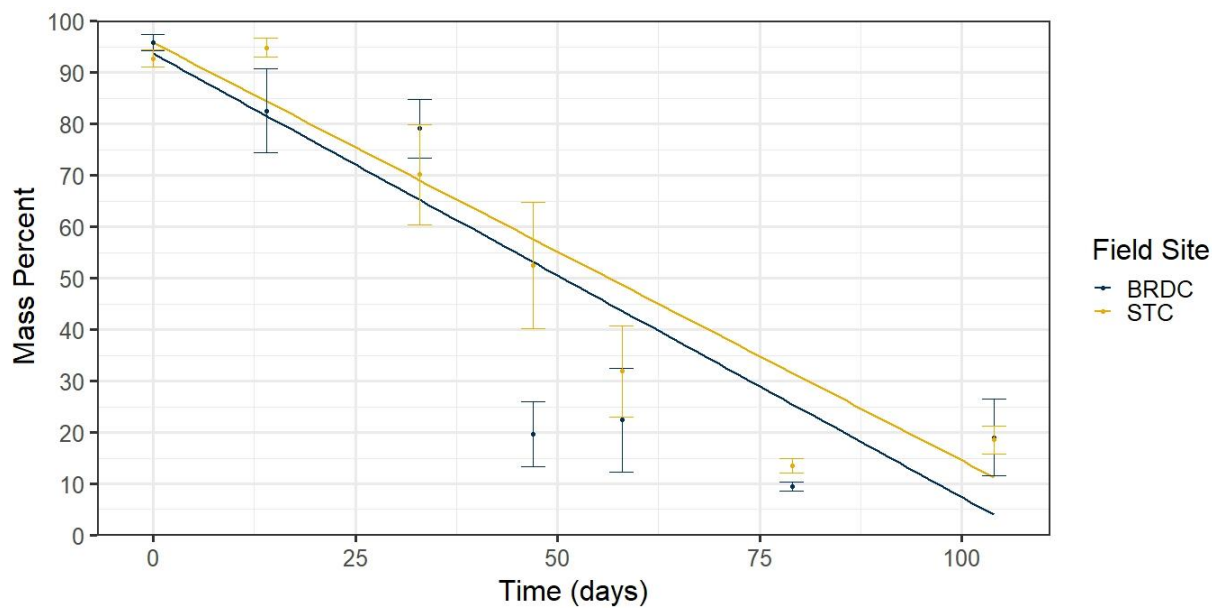


Figure 10-2: The first phase of the incubation data is primarily characterized by the loss of urea. The mass of the first 104 days is represented by polymer coatings with urea and the mass of urea is much larger than the mass of the polymer coating.

11 Appendix E: Soil Organic Carbon and Nitrogen

Table 12: Soil organic carbon and nitrogen percentage across BRDC Field 1, BRDC Field 2, and STC field sites and elevations.

Field Site	Elevation	Nitrogen %	Carbon %
BRDC Field 1	Combined	0.303 ± 0.018	3.211 ± 0.202
BRDC Field 2	Combined	0.284 ± 0.009	3.126 ± 0.096
STC	Combined	0.284 ± 0.007	3.566 ± 0.097
STC	Upper	0.277 ± 0.009	3.504 ± 0.140
STC	Middle	0.314 ± 0.017	3.962 ± 0.196
STC	Lower	0.262 ± 0.007	3.233 ± 0.113